5-1976

Photosynthesis, Dark Respiration, and Growth of Rumex Patientia L. Exposed to UV-B (280-315 nm) Irradiance Corresponding to Reduced Atmospheric Ozone Concentrations

William B. Sisson

PHOTOSYNTHESIS, DARK RESPIRATION AND GROWTH OF *RUMEX PATIENTIA* L. EXPOSED TO UV-B (280-315 NM) IRRADIANCE CORRESPONDING TO REDUCED ATMOSPHERIC OZONE CONCENTRATIONS

by

William B. Sisson

A dissertation submitted in partial fulfillment
of the requirements for the degree

of

DOCTOR OF PHILOSOPHY

in

Range Ecology

Approved:

UTAH STATE UNIVERSITY
Logan, Utah

1976

ACKNOWLEDGMENTS

I would like to extend a most sincere thanks to Dr. Martyn M. Caldwell for sharing his expertise and friendship during the course of this study. In addition, I would like to acknowledge the many insights and constructive criticisms provided me as a result of a critical review of the thesis manuscript by Dr. Caldwell.

Special acknowledgement is due Dr. Don D. Dwyer, Range Science Department Head and member of my graduate committee, for the financial support he provided during the initial three months of my graduate program and for his review of this thesis. I would also like to extend a sincere thanks to Drs. William F. Campbell, James MacMahon and Herman Wiebe for serving on my graduate committee, reviewing the thesis and for providing many helpful suggestions.

With no intended purpose of slighting other members of the genus Rumex, this thesis is dedicated to Rumex patientia L.

William B. Sisson

TABLE OF CONTENTS

Page

ACKNOWLEDGMENTS ii

LIST OF TABLES. v

LIST OF FIGURES vi

ABSTRACT. xiii

Chapter

I. INTRODUCTION. 1

II. METHODOLOGY 9

UV-B Radiation Enhancement Methodology 10

III. PHOTOSYNTHESIS, DARK RESPIRATION AND GROWTH OF RUMEX PATIENTIA L. EXPOSED TO UV-B IRRADIANCE (280-315 nm) SIMULATING A REDUCED ATMOSPHERIC OZONE COLUMN. 26

Introduction 26
Methods. 27
Results. 32

Controlled-environment studies. 32
Field study 44

Discussion 44

IV. THE RECIPROCITY RELATIONSHIP IN THE RESPONSE OF RUMEX PATIENTIA L. EXPOSED TO UV RADIATION. 54

Introduction 54
Methods. 55
Results. 62

TABLE OF CONTENTS (Continued)

Page

Ontogeny and photosynthesis of Rumex patientia L. leaves exposed to four levels of UV irradiance 62

The reciprocity relationship for depression of photosynthesis and leaf growth of Rumex patientia L. exposed to UV irradiation 65

Simulation model of photosynthesis and leaf growth of Rumex patientia L. exposed to solar UV radiation corresponding to reduced atmospheric ozone concentrations. 76

Discussion. 109

V. CONCLUSIONS. 114

LITERATURE CITED 123

LIST OF TABLES

Table — Page

1. Mean dry and fresh weight for aboveground biomass, total leaf area, and fresh and dry weight to leaf area ratios of Rumex patientia after 22 days of UV irradiation (simulating a 0.18 atm·cm ozone column; angle of 30° from the zenith) and control treatments in controlled-environment studies. Irradiation between 400 and 700 nm was 800 μeinsteins·m^{-2}·s^{-1}. Each value represents the mean of 4 to 6 replicates 43

2. Total chlorophyll, chlorophyll a and chlorophyll b for leaf 1 through 7 of Rumex patientia after 28 days of UV radiation enhanced (simulating a 0.18 atm·cm ozone column at an angle of 30° from the zenith) and control treatments in controlled-environment studies. Irradiation between 400-700 nm was 800 μeinsteins·m^{-2}·s^{-1}. Chlorophyll concentrations are expressed as mg/g fresh or dry weight. Each value represents the mean of 4 to 6 replicates. 45

3. Treatments employed in the evaluation of photosynthesis and growth of Rumex patientia L. under irradiation regimes simulating stratospheric ozone decreases 60

4. Percent reduction in photosynthesis of UV irradiance treatments 1, 2 and 3 relative to treatment 4 and their associated biologically effective UV irradiance 73

LIST OF FIGURES

Figure — Page

1. Curves A and B represent spectral irradiance of a simulated 0.18 atm·cm ozone column and a 0.29 atm·cm ozone column which is the mean base level of ozone during August in northern Utah (latitude 42°N, 112°W longitude), respectively. Measurements taken during a cloudless day in August with the sun at 30° from the zenith. Curve C represents the relative energy effectiveness as defined by Caldwell (1971). 6

2. Spectral irradiance of (A) two Westinghouse FS-40 'sun lamps' each filtered by one layer of Kodacel TA401 (5 mil; 0.13 mm) plastic film, (B) two Westinghouse FS-40 'sun lamps' each filtered by two layers of Kodacel TA 401 (5 mil; 0.13 mm) plastic film, (C) two Westinghouse FS-40 'sun lamps' each filtered by one layer of Mylar Type A (10 mil; 0.25 mm) plastic film, (D) one unfiltered Westinghouse FS-40 'sun lamps' at 9.2 cm. The dashed line (E) is the spectral irradiance predicted by equation 4 for 0.18 atm·cm ozone with the sun at 30° from the zenith using the UV radiation flux values of Bener (1972). Spectroradiometric measurements of A, B and C were made with the lamps in configuration illustrated in Figure 3. All measurements were made in the absence of global irradiation. 14

3. End view of the FS-40 lamp configuration used in field and controlled-environment UV radiation supplementation studies. 16

4. Cosine corrected spectroradiometric measurements of global solar irradiance with the sun at an angle of 30° from the zenith, supplemented with two FS-40 'sun lamps' each filtered with (A) Mylar Type A (10 mil; 0.25 mm) yielding the control ozone concentration of 0.29 atm·cm, and (B) Kodacel TA-401 (5 mil; 0.13 mm), simulating a 0.18 atm·cm ozone concentration. Curve C represents the predicted spectral irradiance at 0.18 atm·cm ozone from a base level of 0.29 atm·cm, according to equation 4. 18

LIST OF FIGURES (Continued)

Figure Page

5. Cosine-corrected spectroradiometric measurements of global solar irradiance with the sun at an angle of 30° from the zenith, supplemented with two FS-40 'sun lamps' each filtered with (A) one layer Mylar Type A (10 mil; 0.25 mm), yielding the control ozone concentration of 0.29 atm·cm, and (B) two layers Kodacel TA-401 (5 mil; 0.13 mm) simulating a 0.22 atm·cm stratospheric ozone concentration. Curve C represents the predicted spectral irradiance at 0.07 atm·cm ozone decrease from 0.29 atm·cm by equation 4. 21

6. Simulated ozone reduction (atm·cm) resulting from global solar irradiance supplemented with two FS-40 'sun lamps' each filtered with one layer of Kodacel TA-401 (5 mil; 0.13 mm) plastic film for a cloudless day in August at latitude 42°N. 24

7. Spectroradiometric measurements in a controlled-environment for (A) two FS-40 lamps each filtered with one layer of Kodacel TA-401 (5 mil) plastic film plus a 6000-W xenon arc filtered with one layer Mylar Type A (10 mil) plastic film simulating a 0.18 atm·cm ozone column when the sun is at 30° from the zenith and (B) two FS-40 lamps and a 6000-W xenon arc each filtered with one layer Mylar Type A (10 mil) plastic film. The FS-40 lamps in each treatment were in the configuration illustrated by Figure 3. Irradiance between 400 and 700 nm was 800 μeinsteins·m^{-2}·s^{-1}. 31

8. Net photosynthesis and the associated CO_2 resistances (r'_r = residual resistance; $r'_s + r'_a$ = leaf resistance) of the third leaf of Rumex patientia L. for 7 hours of UV irradiance (●----●) (simulating a 0.18 atm·cm stratospheric ozone level at an angle of 30° from the zenith) and control (o——o) treatment. Irradiance between 400 and 700 was 400 μeinsteins·m^{-2}·s^{-1}. Vertical bars represent ± one standard error and each point is the mean of 5 replicates. . . . 34

LIST OF FIGURES (Continued)

Figure Page

9. Net photosynthesis and CO_2 resistances (r'_r = residual resistance; r'_s and r'_a = leaf resistances) of Rumex patientia L. during 7 days of UV irradiance (●----●) (simulating a 0.18 atm·cm stratospheric ozone level at an angle of 30° from the zenith) and control (o——o) treatment in controlled-environment studies. Irradiance between 400 and 700 nm was 400 μeinsteins·m^{-2}·s^{-1}. Vertical bars represent ± one standard error and each value is the mean of 4 or 5 replicates. 37

10. Net photosynthesis and dark respiration of Rumex patientia L. during 7 days of UV irradiance (●----●) (simulating a 0.18 atm·cm stratospheric ozone level at an angle of 30° from the zenith) and control (o——o) treatment in controlled-environment studies. Irradiance between 400 and 700 nm was 800 μeinsteins·m^{-2}·s^{-1}. Vertical bars represent ± one standard error and each point is the mean of 4 to 6 replicates. 39

11. Leaf length for leaves 1 through 6 of Rumex patientia L. during 23 days of UV irradiance (---)(simulating a 0.18 atm·cm stratospheric ozone level at an angle of 30° from the zenith) and control (——) treatment in controlled-environment studies. Irradiance between 400 and 700 nm was 800 μeinsteins·m^{-2}·s^{-1}. Each point represents the mean of 6 replicates. 42

12. Net photosynthesis and CO_2 resistances (r'_r = residual resistance; $r'_s + r'_a$ = leaf resistance) of Rumex patientia L. during 8 days of UV irradiance (●----●) (simulating a 0.18 atm·cm stratospheric ozone level at an angle of 30° from the zenith) and control (o——o) treatment in field studies. Irradiance between 400 and 700 nm was 800 μeinsteins·m^{-2}·s^{-1} during photosynthetic determinations. Vertical bars represent ± one standard error and each point is the mean of 4 to 6 replicates. 47

LIST OF FIGURES (Continued)

Figure Page

13. Leaf elongation rates ($mm \cdot day^{-1}$) of the first leaf of Rumex patientia L. during 18 days of UV irradiance (●) (simulating a 0.18 atm·cm ozone column) and control (o) treatment in controlled environment studies. The curves represent least square fits of the UV irradiance (—— ——) and control treatment (——) elongation rates. The dashed line (---) represents the expected leaf elongation rate of the UV irradiated leaf if the reduction in elongation rate were solely a function of the depressed photosynthetic rates of that leaf. Each point represents the mean of 6 replicates. See text for details. 52

14. Spectroradiometric measurements in a controlled-environment for spectral irradiance (A) simulating a 0.18 atm·cm stratospheric ozone column when the sun is at 30° from the zenith, (B) simulating a 0.22 atm·cm ozone column when the sun is at 30° from the zenith, (C) simulating a 0.29 atm·cm ozone column when the sun is at 15° from the zenith, and (D) with all biologically effective UV radiation as defined by equation 2 removed. See text and Table 3 for lamp/filter systems used to achieve the spectral irradiance levels shown. Irradiance between 400 and 700 nm was 800 $\mu einsteins \cdot m^{-2} \cdot s^{-1}$. 57

15. Mean net photosynthesis for the third leaf of Rumex patientia L. exposed to four levels of UV irradiance (Figure 14) (A) simulating a 0.18 atm·cm ozone column when the sun is at 30° from the zenith, (B) simulating a 0.22 atm·cm ozone column when the sun is at 30° from the zenith, (C) simulating a 0.29 atm·cm ozone column when the sun is at 15° from the zenith and (D) with no biologically effective UV irradiation as defined by equation 2 above 1.0×10^{-3} $W \cdot m^{-2} \cdot nm^{-1}$. This controlled-environment study was conducted at 800 $\mu einsteins \cdot m^{-2} \cdot s^{-1}$ during the middle 8 hr of an 11-hr photoperiod with the remaining 3 hr irradiance at 680 $\mu einsteins \cdot m^{-2} \cdot s^{-1}$. The vertical bars represent ± one standard deviation and each point represents the mean of 4 to 6 replicates 64

LIST OF FIGURES (Continued)

Figure Page

16. Leaf area measurements of the third leaf of Rumex patientia L. exposed to four UV spectral irradiance (Figure 14) (A) simulating a 0.18 atm·cm ozone column when the sun is at 30° from the zenith, (B) simulating a 0.22 atm·cm ozone column when the sun is at 30° from the zenith, (C) simulating a 0.29 atm·cm ozone column when the sun is 15° from the zenith and (D) with no biologically effective UV radiation as defined by equation 2 above 1×10^{-3} $W \cdot m^{-2} \cdot nm^{-1}$. The controlled-environment study was conducted at 800 μeinsteins·$m^{-2} \cdot s^{-1}$ during the middle 8 hr of an 11 hr photoperiod with the remaining 3 hr irradiance at 680 μeinsteins·$m^{-2} \cdot s^{-1}$. The vertical bars represent ± one standard deviation and each point is the mean of 4 to 6 replicates. 67

17. Least squares fit to the net photosynthetic data determined for the third leaf of Rumex patientia L. exposed to four levels of UV irradiance (treatment 1 ▲——▲; treatment 2 Δ—— ——Δ; treatment 3 o——o); treatment 4 ●——●). Each point represents the mean of 4 to 6 replicates. 69

18. Plot of the percent reduction in net photosynthesis determined for treatments 1 (▲), 2 (Δ) and 3 (o) relative to treatment 4 as a function of biologically effective UV irradiance as defined by equation 2. The curve represents a least squares fit to the data . . 71

19. Plot of the logarithm of net photosynthetic reduction of treatments 1 (▲), 2 (o) and 3 (Δ) relative to treatment 4 (no biologically effective UV radiation above 1.0×10^{-3} $W \cdot m^{-2} \cdot nm^{-1}$ as defined by equation 2) as a function of biologically effective UV irradiation. The line represents a least squares fit to the data. 75

20. Leaf area of the third leaf of Rumex patientia L. exposed to four levels of UV irradiance in a controlled environment study. The curves represent least squares fits to the data (treatment 1 (▲), 2 (Δ), 3 (o) and 4 (●)). Each point represents the mean of 4 to 6 replicates. 78

LIST OF FIGURES (Continued)

Figure Page

21. Leaf expansion rates of the third leaf of Rumex patientia L. exposed to four levels of UV irradiance determined from the least squares fits to the data of Figure 20 (treatment 1 (——••——), 2 (----), 3 (—— ——) and 4 (———)) . . . 80

22. A least squares fit to the ozone concentration data (●) of Hering and Borden (1967) from March 1 to September 21, 1965. 83

23. Predicted daily biologically effective UV irradiation ($J \cdot m^{-2} \cdot day^{-1}$) for cloudless days between April 1 and September 21 for ozone concentration reductions of 5 (B), 15 (C) and 40 percent (D) from a least squares fit (Figure 22) to the ozone data of Hering and Borden (1967) 86

24. Predicted net photosynthetic rates of the third leaf of Rumex patientia L. exposed to UV-B radiation simulating a 5 percent atmospheric ozone reduction for the April 1 to May 5 (----) and June 1 to July 5 (—— ——) periods. Predicted photosynthetic rates are expressed as a reduction from a least squares fit (———) to the photosynthetic data of treatment 4 . 89

25. Predicted net photosynthetic rates of the third leaf of Rumex patientia L. exposed to UV-B radiation simulating a 15 percent atmospheric ozone reduction for the April 1 to May 5 (----) and June 1 to July 5 (—— ——) periods. Predicted photosynthetic rates are expressed as a reduction from a least squares fit (———) to the photosynthetic data of treatment 4 . . . 92

26. Predicted net photosynthetic rates of the third leaf of Rumex patientia L. exposed to UV-B radiation simulating a 40 percent atmospheric ozone reduction for the April 1 to May 5 (----) and June 1 to July 5 (—— ——) periods. Predicted photosynthetic rates are expressed as a reduction from a least squares fit (———) to the photosynthetic data of treatment 4 . 94

27. Predicted total leaf area of Rumex patientia L. exposed to UV-B radiation corresponding to normal ozone concentrations (A), and reductions of 5 (B), 15 (C) and 40 percent (D) during the period April 1 to May 5. For these simulations, a new leaf was initiated every 7 days 97

LIST OF FIGURES (Continued)

Figure Page

28. Predicted total leaf area of Rumex patientia L. exposed to UV-B radiation corresponding to normal ozone concentrations (A), and reductions of 5 (B), 15 (C) and 40 percent (D) during the period June 1 to July 5. For these simulations, a new leaf was initiated every 7 days 99

29. Predicted total carbon dioxide uptake ($mgCO_2 \cdot hr^{-1}$) for Rumex patientia L. exposed to UV-B radiation corresponding to normal ozone concentrations (A), and reductions of 5 (B), 15 (C) and 40 percent (D) during the period April 1 to May 5. For these simulations, a new leaf was initiated every 7 days and irradiance within the 400 to 700 nm waveband was 800 $\mu einsteins \cdot m^{-2} \cdot s^{-1}$ 101

30. Predicted total carbon dioxide uptake ($mgCO_2 \cdot hr^{-1}$) for Rumex patientia L. exposed to UV-B radiation corresponding to normal ozone concentrations (A), and the reductions of 5 (B), 15 (C) and 40 percent (D) during the period June 1 to July 5. For these simulations, a new leaf was initiated every 7 days and irradiance within the 400 to 700 nm waveband was 800 $\mu einsteins \cdot m^{-2} \cdot s^{-1}$ 103

31. Net photosynthesis of the third leaf of Rumex patientia L. during 8 days of UV irradiance (Δ——Δ) (simulating a 0.18 atm·cm stratospheric ozone level at an angle of 30° from the zenith) and control (o——o) treatment in field studies, and those predicted (▫——▫). Irradiance between 400 and 700 nm for both the measured and predicted rates was 800 $\mu einsteins \cdot m^{-2} \cdot s^{-1}$ 106

32. Total global irradiation ($cal \cdot cm^{-2} \cdot min^{-1}$) for July 12, 13, 15, 16 and 17, 1974. Total global irradiation for July 10, 11 and 14 were cloudless days and the same as July 12. (I. Dirmhirn, personal communication) 108

ABSTRACT

Photosynthesis, Dark Respiration, and Growth of

Rumex patientia L. Exposed to UV-B (280–315 nm)

Irradiance Corresponding to Reduced

Atmospheric Ozone Concentrations

by

William B. Sisson, Doctor of Philosophy

Utah State University, 1976

Major Professor: Dr. Martyn M. Caldwell
Department: Range Science

Net photosynthesis, dark respiration, chlorophyll concentrations and growth were determined for Rumex patientia L. exposed to UV-B radiation corresponding to reduced atmospheric ozone concentrations. The hypothesis of whether reciprocity is maintained in the response of R. patientia to polychromatic UV-B radiation was tested. On the basis of the relationships derived from these studies, a simulation model was developed for the prediction of photosynthesis and growth of R. patientia exposed to UV-B radiation corresponding to any atmospheric ozone reduction.

Photosynthetic rates were found to be depressed after two hours exposure to UV-B irradiance simulating a 0.18 atm·cm ozone column when the sun is at 30° from the zenith. During this initial exposure period, partial stomatal closure was implicated in the suppression of photosynthesis. However, after one day exposure,

substantial increases in photosynthetic resistances apart from stomatal diffusion resistance occurred in the UV-irradiated plants and no differences in stomatal diffusion resistance were apparent between UV-irradiated and control plants. Dark respiration rates were slightly higher in those plants exposed to UV radiation.

Leaf expansion of R. patientia was substantially repressed but only during the initial few days of exposure. Thereafter, leaf expansion was similar in the UV-irradiated and control plants. A reduction in total plant dry weight and leaf area of approximately 50 percent occurred after 22 days treatment while chlorophyll concentrations remained unaltered. Time of leaf initiation was shown to be delayed in those plants exposed to UV-B radiation. Leaf longevity was decreased with increased UV radiation but accelerated whole-plant senescence and death was not observed.

Photosynthetic rates determined through the ontogeny of the third leaf of R. patientia exposed to four levels of UV irradiance were found to be depressed as a function of the accumulated biologically effective UV irradiation. Thus, reciprocity was demonstrated between 6350 and 3175 J biologically effective UV irradiation.

Results of the simultion model showed that under reduced atmospheric ozone concentrations, suppression of photosynthesis and leaf growth would be more severe during mid-summer (i.e. June) than would occur during the March to early May period. This

results from smaller solar angles from the zenith and lower prevailing ozone concentrations prevalent during June.

A validation test of the model was made with photosynthetic data obtained during a field study with R. patientia exposed to UV-B radiation corresponding to a 38 percent atmospheric ozone reduction (0.18 atm·cm when the sun was at 30° from the zenith). This validation test showed a reasonable correspondence between the measured and predicted photosynthetic rates.

R. patientia was selected as the test species for this study because (1) it is reasonably sensitive to UV radiation as determined in preliminary studies evaluating approximately 20 native and agricultural plant species, (2) it is normally exposed to full sunlight in its natural habitat, and (3) individual leaves are relatively long-lived (about 60 days) and are not normally shaded by other leaves of the same plant. Although this species probably represents one of the more sensitive plants to UV radiation, it would be this group of sensitive plants that would be initially affected under conditions of reduced atmospheric ozone. If more resistant plants with long-lived plant parts also accumulate UV radiation damage as was shown to occur in R. patientia, over sufficient periods of time even these species might be significantly impacted under conditions of reduced atmospheric ozone.

(142 pages)

CHAPTER I

INTRODUCTION

Global ultraviolet (UV) radiation fluctuates both in quality and intensity with the angle of the sun above the horizon, cloudiness, stratospheric ozone concentration and particulates in the air. No appreciable UV-B (280-315 nm; Meyer and Seitz, 1942) radiation below 295 nm is received on the earth's surface due to absorption of UV radiation by the stratospheric ozone layer. Ozone, concentrated primarily in the upper atmosphere above 12 km, displays an annual cyclic pattern. At 42°N latitude, a maximum of approximately 0.40 atm·cm occurs in February with a low of about 0.27 atm·cm in October and November (Hering and Borden, 1967). A reduction of the stratospheric ozone concentration would result in a predictable shift in the terrestrial global spectrum to include the shorter UV-B radiation wavelenths below 295 nm (Green, Sawada and Shettle, 1974). Such a reduction could result from catalytic interactions of ozone with oxides of nitrogen released in the stratosphere by aircraft (Grobecker, Coroniti and Cannon, 1974; Johnston, 1971), halomethanes diffusing from the troposphere (Cicerone, Stolarski and Walters, 1974; Molina and Rowland, 1974; Hammond, 1975) or other man-induced perturbations of the stratosphere. Although a shift in the global UV-B radiation spectrum resulting from partial ozone depletion would be small (Bener, 1972; Green et al., 1974), any added increment of shorter wavelength UV-B radiation might prove significant since it is effectively absorbed by nucleic acids and proteins (Giese, 1964).

Physiological investigations with UV radiation have, in the past, dealt principally with monochromatic 254 nm radiation. From these studies, an array of deleterious effects on plants have been demonstrated. These include such responses as reduced growth (Reynolds, 1935), inhibition of several component reactions of photosynthesis (Arnold, 1933; Jones and Kok, 1966; Mantai and Bishop, 1967; Shavit and Avron, 1963) and stimulated dark respiration (Owen, 1957). Extrapolation of known responses to 254 nm radiation in assessing the ramifications of a UV-B radiation enhanced global spectral irradiance does not at the present time appear plausible for three reasons. First, biological responses to UV-B radiation tend to be highly wavelength specific with respect to efficiency of photobiological action (Caldwell, 1971; Giese, 1964). Secondly, the biologically potent wavelengths shorter than 280 nm would not be transmitted to the earth's surface by a reduction of the ozone layer to even 40 percent of its present thickness (Green et al., 1974). Finally there may be qualitative as well as quantitative differences in the response to 254-nm radiation and radiation in the 280 to 315 nm waveband as has been reported for Chlamydomonus reinhardi (Nachtwey, 1975). Although a concerted effort has been directed toward elucidation of the deleterious effects of the 254 nm wavelength on plant metabolism, little is presently known in regard to the 280 to 315 nm waveband and its effect on whole-plant growth and metabolism. This is particularly true regarding photobiological information on plant responses to a UV-B enhanced

global spectral irradiance as would occur under reduced atmospheric ozone concentrations. To date, no studies have been completed on the effects of UV-B radiation corresponding to a quantifiable reduction in atmospheric ozone and its effect on plant growth and metabolism.

Several UV radiation action spectra have been published and many of the plant responses to UV irradiation are believed to involve protein and nucleic acid chromatophores (Bell and Merinova, 1961; Caldwell, 1971; Hollaender and Emmons, 1941; Knapp et al., 1939; Van Baalen and O'Donnell, 1972). Based on these studies, Caldwell (1971) proposed a generalized curve representing the relative photon effectiveness of UV-B radiation to induce a biological response when protein and nucleic acid chromatophores are involved. Green et al. (1974) formulated this generalized action spectrum for each UV-B wavelength on an energy basis in the form:

$$\Sigma\ (\lambda) = 2.618\ [1 - (\lambda/313.3)^2]e^{-(\lambda-300)/31.08} \qquad (1)$$

This generalized action spectrum provides a reasonable approximation for a number of biological responses to monochromatic UV-B irradiation including the inhibition of photosynthesis in Chlorella pyrenoidosa (Bell and Merinova, 1961). For polychromatic UV-B irradiation, it could be hypothesized that the biologically effective UV-B irradiation ($W \cdot m^{-2}$) integrated over the 280-315 nm waveband and time according to this generalized action spectrum might provide a quantitative measure for the determination of a dose-response relationship in higher plants. Quantitatively, the biologically

effective UV-B irradiation is characterized on an energy basis in the form:

$$\Sigma(I) = \int_{280}^{315} E_\lambda \, I_\lambda \, d\lambda \qquad (2)$$

where I_λ represents the irradiation intensity in $W \cdot m^{-2} \cdot nm^{-1}$ and E_λ represents the relative energy effectiveness as defined by equation 1 for each wavelength (Caldwell, 1971). For global irradiation, the area defined by this formula is represented in Figure 1 as the sum of the areas a_1 plus a_2 for the spectral irradiance represented by Curve A. Curves A and B (Figure 1) are field measurements of global spectral irradiance of a simulated 0.18 atm·cm ozone column and a 0.29 atm·cm ozone column, which is the average base level in August in northern Utah, at an angle of 30° from the zenith, respectively. Curve C represents the generalized action spectrum of UV-B radiation as defined by Caldwell (1971) expressed here on a relative energy basis. Since the present study is concerned with UV-B irradiance corresponding to certain decreases in stratospheric ozone, the area defined by a_1 for the particular situation depicted in Figure 1 would then define the quantitative measure of the additional biologically effective UV-B irradiance of concern in this study.

On an energy basis, the additional biologically effective UV-B irradiance occurring as a result of decreased atmospheric ozone concentrations would then be:

$$\Sigma(I) = \int_{280}^{315} E_\lambda \, I_{\lambda \, a_1} \, d\lambda - \int_{280}^{315} E_\lambda \, I_{\lambda a_2} \, d\lambda \qquad (3)$$

where $I_{\lambda a_2}$ and $I_{\lambda a_1}$ represent UV-B irradiances under normal (eg.

Figure 1. Curves A and B represent spectral irradiance of a simulated 0.18 atm·cm ozone column and a 0.29 atm·cm ozone colum which is the mean base level of ozone during August in northern Utah (latitude 42°N, 112°W longitude), respectively. Measurements taken during a cloudless day in August with the sun at 30° from the zenith. Curve C represents the relative energy effectiveness as defined by Caldwell (1971).

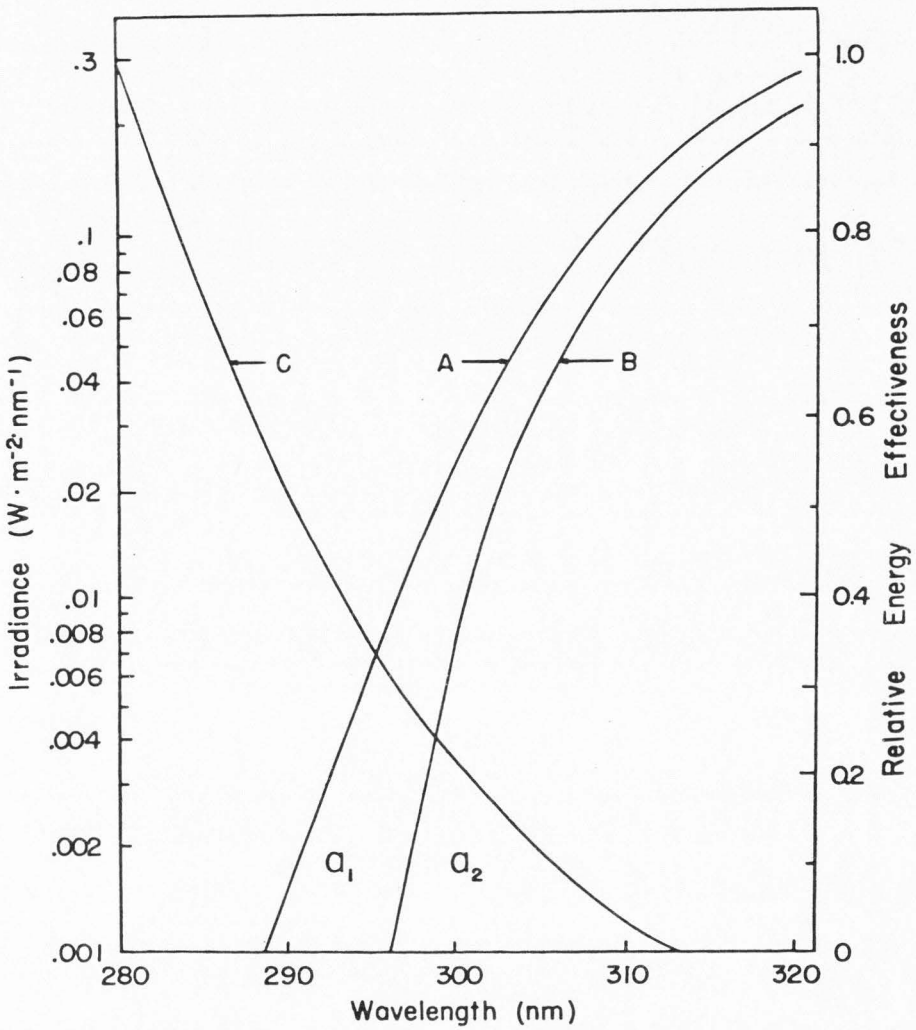
.3
.1
.08
.06
.04
.02
.01
.008
.006
.004
.002
.001
Irradiance (W · m⁻² · nm⁻¹)
280
290
300
310
320
Wavelength (nm)
1.0
0.8
0.6
0.4
0.2
0
Relative Energy Effectiveness
C
A
B
a1
a2

0.29 atm·cm) and reduced ozone concentrations, respectively. The term E_λ represents the relative biological effectiveness as defined by equation 1 at each wavelength.

The initial objective of this study was to quantify changes in photosynthesis and growth of Rumex patientia L. exposed to a UV-B irradiance corresponding to a specific decrease in stratospheric ozone. Both field and controlled-environment studies were employed in the testing of the hypothesis that UV-B irradiance corresponding to a 38 percent ozone decrease will adversely affect plant processes. Additional parameters assayed in the testing of this hypothesis included dark respiration, chlorophyll concentrations, dry and fresh weights, and time of leaf exertion.

If plants are adversely affected when exposed to a UV-B enhanced irradiance, the degree of metabolic suppression might follow some dose-response relationship. The Bunsen-Roscoe reciprocity law of photochemistry states that when the product of intensity and exposure time is constant, a constant photochemical reaction results. This relationship was shown as early as 1916 by Verhoeff and Bell for UV radiation, and with some modifications, holds for most photochemical reactions driven by monochromatic UV radiation (Bucholtz, 1931). Although whole-plant responses to polychromatic UV-B irradiance entails a very complex situation, it could be hypothesized that the Bunsen-Roscoe reciprocity law of photochemistry holds within certain limits. The test of this hypothesis involved a controlled-environment study in which photosynthesis and leaf growth rates were determined through the ontogeny

of single leaves subjected to four levels of UV-B irradiance. For these experiments, dose was defined by equation 3 in terms of biologically effective energy.

Perhaps the limiting factors in the evaluation of a UV-B enhanced global irradiance are the technical aspects of UV-B radiation supplementation and the quantitative characterization of relatively subtle responses of plants to small increases in UV-B irradiance. Thus, a major aim of this study was to extrapolate plant responses under relatively large simulated ozone reductions (eg. 38 percent) to predict responses under more subtle stratospheric ozone reductions (less than 15 percent). Predictive equations for photosynthesis and growth were generated from dose-response relationships derived during the test for reciprocity. A computer simulation model was developed with these equations and the analytic equations of Green et al. (1974) for predicting global UV-B irradiance corresponding to any stratospheric ozone level and altitude of the sun. A validation test of the simulation model was made by correlating data from a field experiment to data generated from the simulation model.

R. patientia was selected as the test species for this study because (1) it is reasonably sensitive to UV radiation as determined in preliminary studies evaluating approximately 20 native and agricultural plant species, (2) it is normally exposed to full sunlight in its natural habitat, and (3) individual leaves are relatively long-lived (about 60 days) and are not normally shaded by other leaves of the same plant.

CHAPTER II

METHODOLOGY

Net photosynthetic rates of single leaves were determined with a Siemen's Corp. gas exchange systems (Koch, Lange and Schulze, 1971). A Beckman Model 215 infrared gas analyzer measured CO_2 differences of incoming and outgoing air streams. Leaf diffusive resistances were measured and calculated by a modification of the technique of Gaastra (1959). A multiplier (1.594) which relates the diffusion coefficients of CO_2 and H_2O (McPherson and Slatyer, 1973) was used to calculate CO_2 diffusive resistances from the H_2O diffusive resistances. In this study, the CO_2 mesophyll resistance originally defined by Gaastra is replaced by the residual resistance term since this includes all diffusive and metabolic components of the total CO_2 resistance apart from stomatal and boundary layer resistances (Gifford and Musgrave, 1972).

Artificial irradiation above 315 nm for net photosynthetic rate determinations was provided by four incandescent Sylvania 300-watt lamps. Total quanta in the 400-700 nm waveband were monitored in the cuvette by a Lambda Co., Model LI-190SR quantum sensor (Biggs et al., 1971). Irradiation intensity was adjusted to simulate the total quanta in the 400-700 nm waveband used in each controlled-environment experiment. Photosynthetic determinations for the plants irradiated in the field were made at 800 μeinsteins$\cdot m^{-2} \cdot s^{-1}$ (400-700 nm).

Air and leaf temperatures within the curvette were measured with platinum wire resistance thermometers and fine-wire thermocouples, respectively. A Cambridge Model 800 dew point hygrometer measured water vapor concentrations. Specific water vapor concentrations of the incoming cuvette air stream was achieved by mixing two air streams of different water vapor concentrations.

Leaf areas were measured with a Lambda Model II-3000 portable area meter. Photosynthesis is expressed on a leaf area (one side) basis. Dry weight determinations were made after oven drying at 42C for two days.

Chlorophyll analysis was completed by homogenizing leaves in 80 percent acetone and centrifuging the homogenate at 1500 xg for 7 minutes. Chlorophyll concentrations were determined by the method of Arnon (1949).

UV-B Radiation Enhancement Methodology

Methodology pertaining to UV-B radiation supplementation within this section presents only the basic approach employed in the various studies reported in subsequent chapters. A more detailed description of specific spectral irradiance assayed and the associated methodology is presented in appropriate chapters.

Stratospheric ozone, the principal atmospheric absorber of UV radiation, varies considerably with latitude and season (Hering and Borden, 1967). Analysis of spectroradiometric measurements of global irradiance in Logan, Utah, when compared with expected

spectral irradiance for various ozone concentrations according to analytic equations of Green et al. (1974) and data of Bener (1972) suggests a mean level of 0.29 atm·cm ozone in the month of August at latitude 42°N and 112°W longitude. This level of ozone is used as base level for calculations of various degrees of stratospheric ozone depletion and resultant UV-B radiation increases employed in the studies described in following chapters.

The predicted UV-B spectral irradiance, I_λ, corresponding to different levels of atmospheric ozone depletion was determined by the formula of Sisson and Caldwell (1975):

$$I_\lambda = \frac{I_{m,\lambda}}{e^{10(1/\cos\theta)e^{(300-\lambda)/8}(O_{z_2} - O_{z_1})}} \qquad (4)$$

The global irradiance supplemented by the control lamp system (described below) in the field is represented by $I_{m,\lambda}$ ($W \cdot m^{-2} \cdot nm^{-1}$), O_{z_1} is the base ozone level (0.29 atm·cm) and O_{z_2} is the reduced level of ozone being simulated. Theta, θ, represents the angle of the sun from the zenith. This equation was derived from the analytic formulations of Green et al. (1974). With a mean error of less than 5 percent, this equation can predict global (diffusive + direct beam) irradiance changes as a function of ozone depletion, as given by Bener (1972). This equation is, however, not as satisfactory for wavelengths shorter than 292 nm or for situations where the angle from the zenith is greater than 50° or base ozone concentrations are less than 0.15 atm·cm.

Appropriately filtered Westinghouse Corp. FS-40 'sun lamps' provided UV radiation supplementation to simulate irradiance within the 280-320 nm waveband for various levels of stratospheric ozone depletion. The spectral irradiance of one unfiltered FS-40 lamp measured at a distance of 9.2 cm is shown in Figure 2. The spectral composition as well as intensity of these lamps changes rapidly over the first 100 hr so that prior burning of the lamps before experimental use was necessary to obtain a relatively constant UV radiation regime.

To test plant response to a 0.11 atm·cm stratospheric ozone decrease (from a base level of 0.29 atm·cm; 30° angle from the zenith), a lamp/filter system was developed for use in both field and controlled environment applications. The filter employed with the FS-40 lamps to produce this UV radiation enhancement was a polyester film marketed as Kodacel TA 401 (5 mil, 0.13 nm) (Kodak Co.). The spectral irradiance provided by two FS-40 lamps filtered with this polyester film in the configuration shown in Figure 3, in the absence of global irradiation, is presented in Figure 2. Similar measurements taken in the field with the sun at 30° from the zenith during a cloudless day with the Kodacel-filtered lamp supplementation (simulating a 0.11 atm·cm ozone reduction) are presented in Figure 4. The spectral irradiance of the filtered lamps and the global irradiance was corrected for cosine response errors of the Gamma Scientific Co. spectroradiometer. These corrections were made by dividing the sky hemisphere into 5° radial segments (from 0° to 90°) and applying a cosine error correction

Figure 2. Spectral irradiance of (A) two Westinghouse FS-40 'sun lamps' each filtered by one layer of Kodacel TA401 (5 mil; 0.13 mm) plastic film, (B) two Westinghouse FS-40 'sun lamps' each filtered by two layers of Kodacel TA 401 (5 mil; 0.13 mm) plastic film, (C) two Westinghouse FS-40 'sun lamps' each filtered by one layer of Mylar Type A (10 mil, 0.25 mm) plastic film, (D) one unfiltered Westinghouse FS-40 'sun lamp' at 9.2 cm. The dashed line (E) is the spectral irradiance predicted by equation 4 for 0.18 atm·cm ozone with the sun at 30° from the zenith using the UV radiation flux values of Bener (1972). Spectroradiometric measurements of A, B and C were made with the lamps in configuration illustrated in Figure 3. All measurements were made in the absence of global radiation.

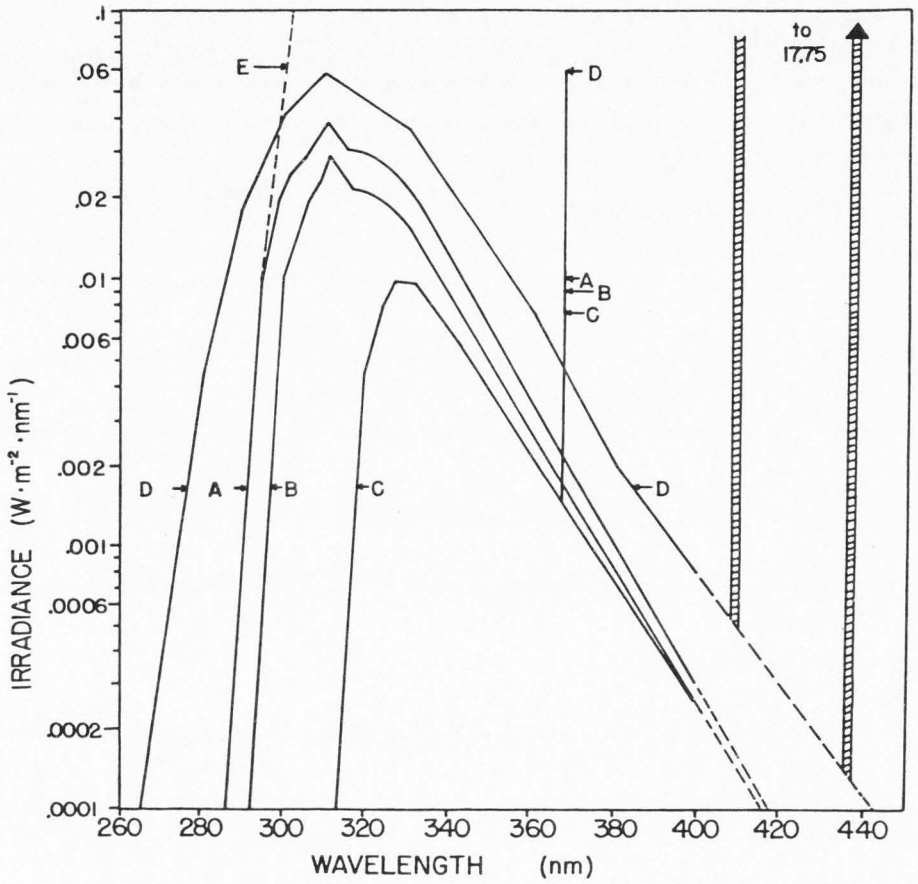
IRRADIANCE (W·m⁻²·nm⁻¹)
.1
.06
.02
.01
.006
.002
.001
.0006
.0002
.0001
260
280
300
320
340
360
380
400
420
440
WAVELENGTH (nm)
E
D
A
B
C
D
A
B
C
D
to
17.75

Figure 3. End view of the FS-40 lamp configuration used in field and controlled-environment UV radiation supplementation studies.

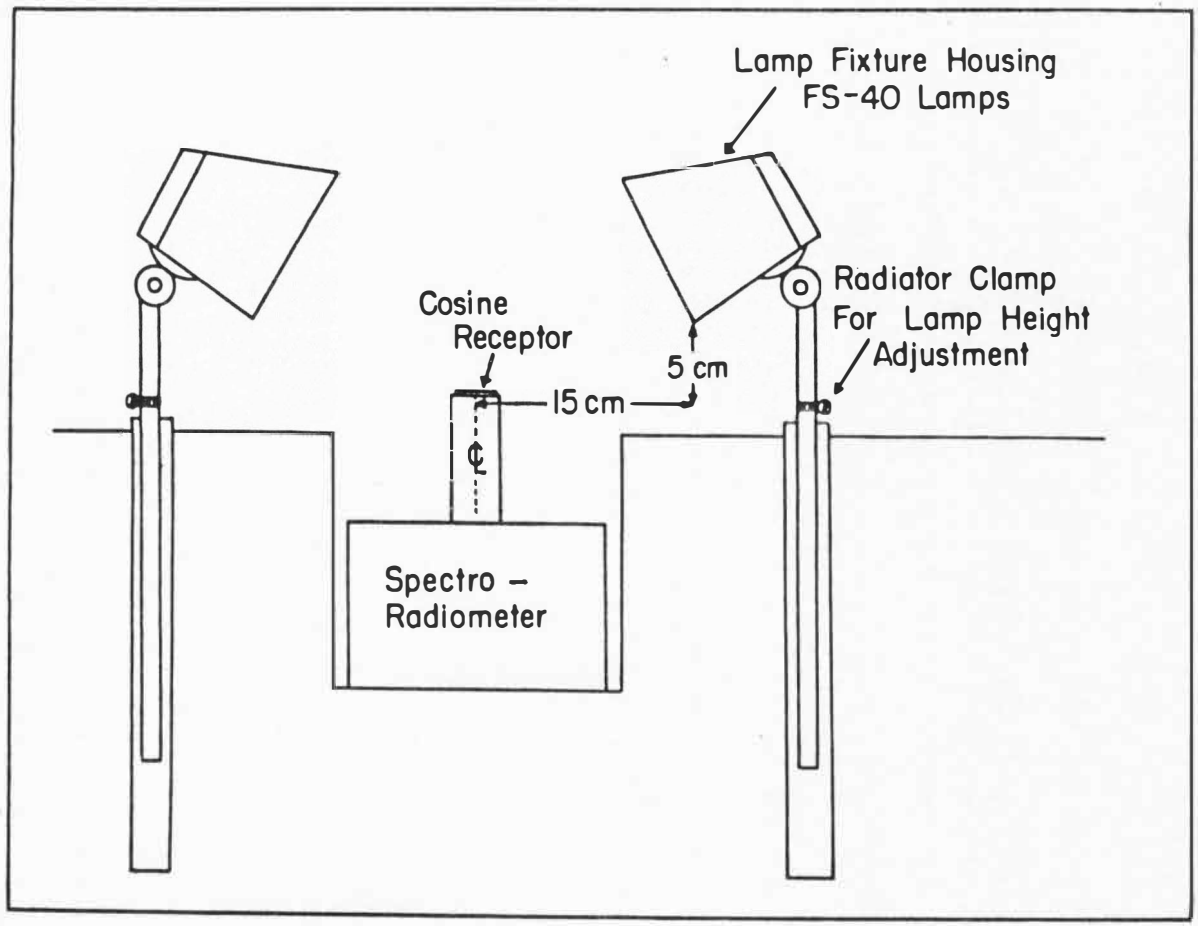
Lamp Fixture Housing
FS-40 Lamps
Radiator Clamp
For Lamp Height
Adjustment
Cosine
Receptor
5 cm
15 cm
Spectro –
Radiometer

Figure 4. Cosine corrected spectroradiometric measurements of global solar irradiance with the sun at an angle of 30° from the zenith, supplemented with two FS-40 'sun lamps' each filtered with (A) Mylar Type A (10 mil; 0.25 mm) yielding the control ozone concentration of 0.29 atm.cm, and (B) Kodacel TA-401 (5 mil; 0.13 mm), simulating a 0.18 atm·cm ozone concentration. Curve C represents the predicted spectral irradiance at 0.18 atm·cm ozone from a base level of 0.29 atm·cm, according to equation 4.

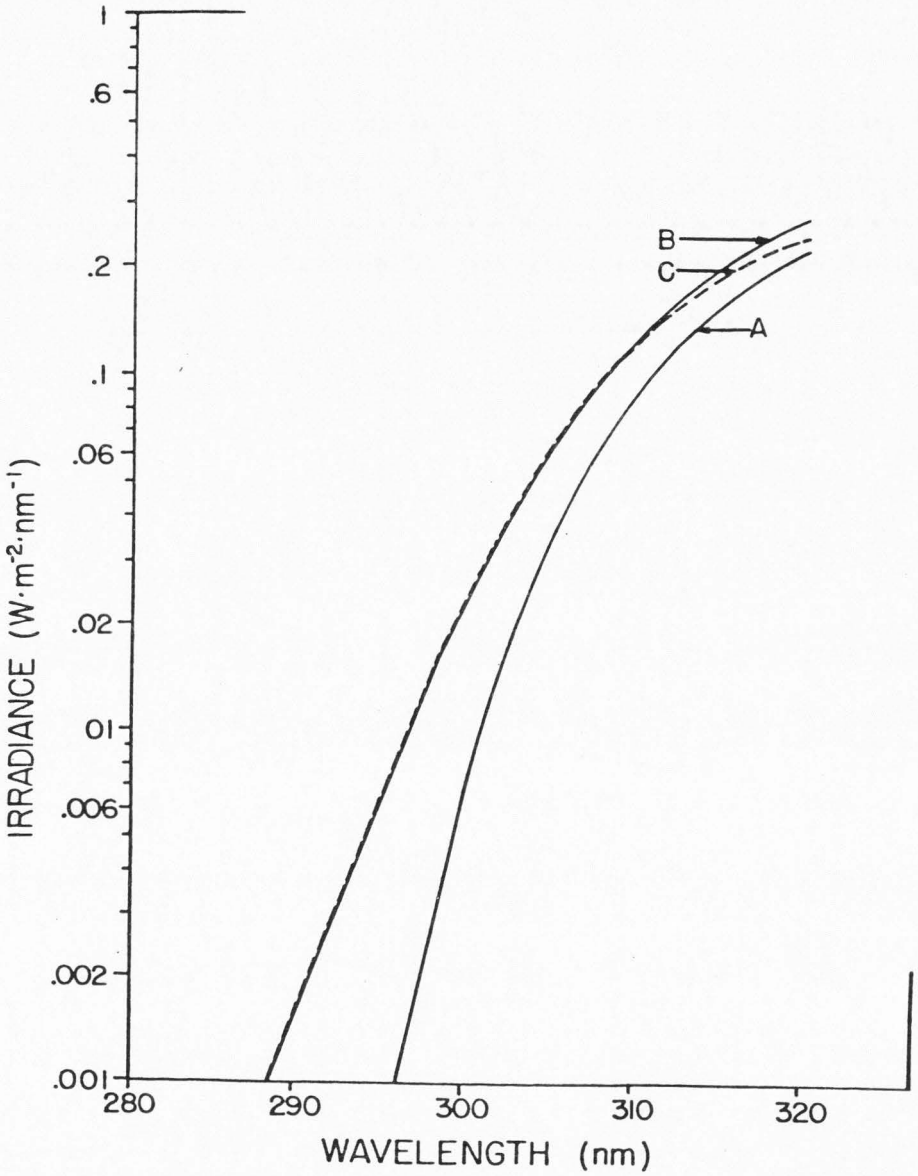
1
.6
.2
.1
.06
.02
.01
.006
.002
.001
IRRADIANCE (W·m⁻²·nm⁻¹)
B
C
A
280
290
300
310
320
WAVELENGTH (nm)

factor for each sky segment for diffusive irradiance and incorporating a cosine error correction factor for direct solar irradiance and the irradiance provided by the lamp system.

For UV irradiance supplementation in the field designed to simulate a 0.07 atm·cm ozone reduction (from a base 0.29 atm·cm), two layers of Kodacel TA 401 (5 mil; 0.13 mm) were used with each FS-40 lamp in the configuration illustrated in Figure 3. Spectroradiometric measurements taken in the absence of global irradiance and in the field during a cloudless day with the sun at 30° from the zenith (cosine-corrected) are presented in Figures 2 and 5, respectively.

As shown in Figure 2, three principal lines of radiant energy corresponding to the mercury-vapor emission spectrum (365, 404.6 and 435.8 mm) are observed in the radiant emission of this lamp at wavelengths greater than 320 nm. The 365 nm wavelength has been shown to repress growth of Ginkgo pollen (Klein and Edsall, 1967) and suppress vegetative growth of higher plants (Klein, Edsall and Gentile, 1965). Although the 365 nm wavelength is evident in the spectral irradiance of the FS-40 lamp (0.06 $W \cdot m^{-2}$ at 9.2 cm distance), when this lamp is used to supplement solar UV irradiation, the FS-40 lamps provide a comparative small addition of 365 nm radiation to the 360-370 nm waveband already present in irradiation from the sun (approximately 5 $W \cdot m^{-2}$; angle from the zenith 30°) or the xenon arc (approximately 2.2 $W \cdot m^{-2}$; when the lamp is operating at 800 $\mu einsteins \cdot m^{-2} \cdot s^{-1}$ between 400-700 nm). Nevertheless, so that differences in plant response to the UV

Figure 5. Cosine-corrected spectroradiometric measurements of global solar irradiance with the sun at an angle of 30° from the zenith, supplemented with two FS-40 'sun lamps' each filtered with (A) one layer Mylar type A (10 mil; 0.25 mm), yielding the control ozone concentration of 0.29 atm·cm , and (B) two layers Kodacel TA-401 (5 mil; 0.13 mm), simulating a 0.22 atm·cm stratospheric ozone concentration. Curve C represents the predicted spectral irradiance at 0.07 atm·cm ozone decrease from 0.29 atm·cm by equation 4.

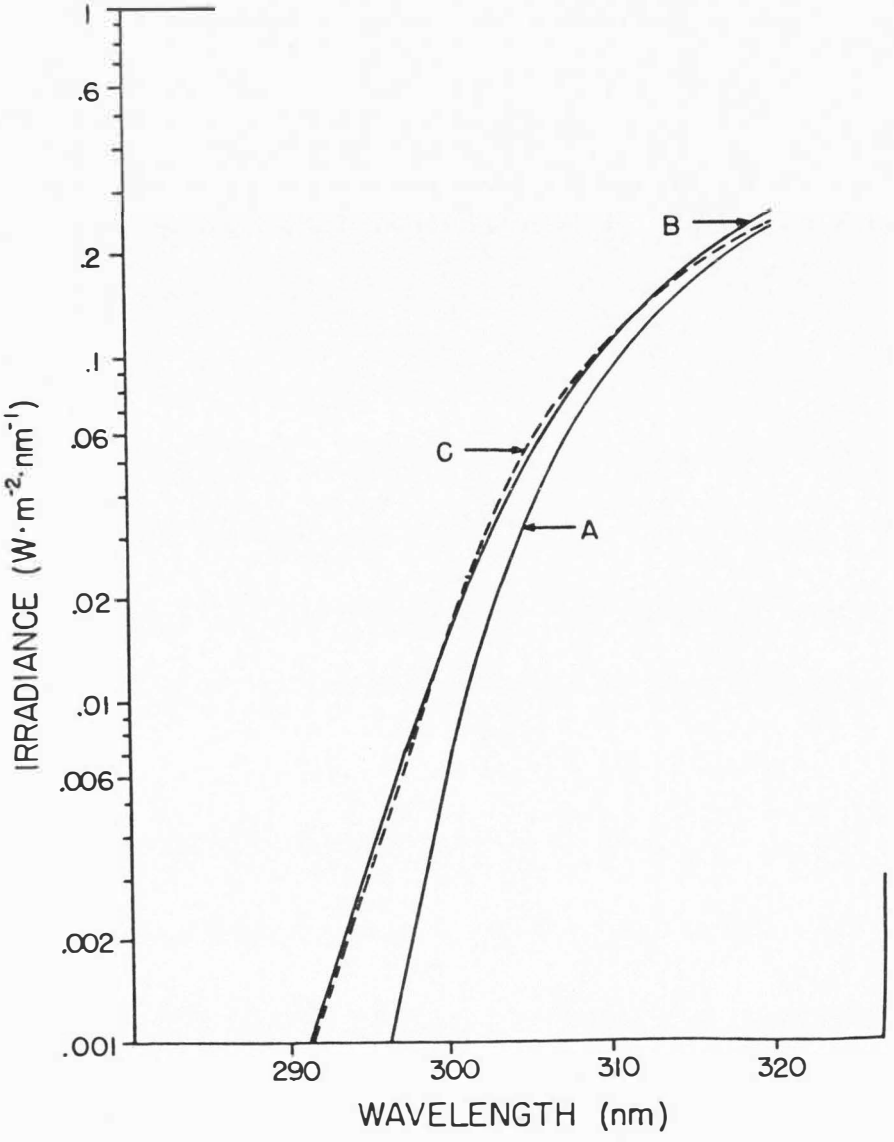
1
.6
.2
.1
.06
.02
.01
.006
.002
.001
IRRADIANCE (W·m⁻²·nm⁻¹)
B
C
A
290
300
310
320
WAVELENGTH (nm)

radiation and control treatments can be attributed solely to the 280-315 nm waveband, the control treatment also consisted of two FS-40 'sun lamps', each filtered with one layer of Mylar Type A (10 mil) plastic film. This filter effectively absorbs all UV radiation below 315 nm but has transmission characteristics similar to Kodacel film above 315 nm. Spectroradiometric measurements of two FS-40 'sun lamps' each filtered by Mylar Type A (10 mil) plastic film in the absence of global radiation in the configuration illustrated in Figure 3 are shown in Figure 2.

In field experiments, the lamp/filter systems were utilized to supplement UV-B radiation during the time period when the angle of the sun from the zenith was less than 50°. Since normal global irradiance fluctuates within this time interval as a function of the angle from the zenith, it is not possible to simulate a constant ozone reduction irradiation regime with a constant UV-B enhancement spectral irradiance from the Kodacel-filtered lamp system. As is apparent in Figure 6, which depicts the simulated ozone depletion for a day in August, for angles from the zenith between 35° and 50°, the simulated ozone reduction increases. The UV radiation supplement provided by the Kodacel-filtered lamp system is equivalent to 0.11 atm·cm stratospheric ozone decrease for angles from the zenith between 35° and 30°. For periods during the day when the angle from the zenith is greater than 50°, the lamp/filter systems were not used.

The lamp/filter systems described for use in field experiments were similarly employed in controlled-environment studies. A plastic

Figure 6. Simulated ozone reduction (atm·cm) resulting from global solar irradiance supplemented with two FS-40 'sun lamps' each filtered with one layer of Kodacel TA 401 (5 mil; 0.13 mm) plastic film for a cloudless day in August at latitude 42°N.

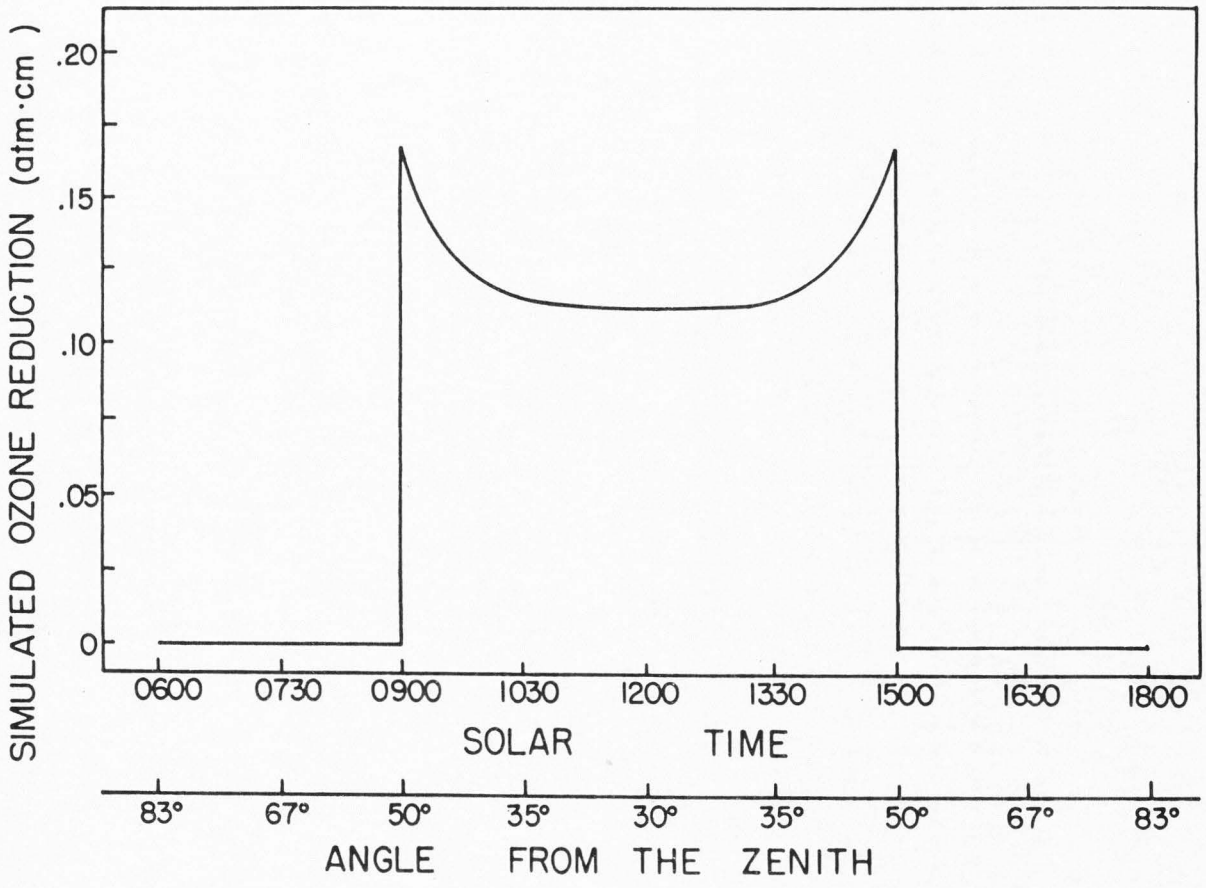
SIMULATED OZONE REDUCTION (atm·cm)
.20
.15
.10
.05
0
0600
0730
0900
1030
1200
1330
1500
1630
1800
SOLAR TIME
83°
67°
50°
35°
30°
35°
50°
67°
83°
ANGLE FROM THE ZENITH

film or glass-filtered 6000-watt xenon arc (Osram Co.) provided irradiation above 315 nm and is described in applicable chapters. In all controlled-environment studies, the temperature was programmed to simulate a July day in Logan, Utah (13 to 37C).

The plastic film filters were routinely replaced approximately every 3, 11-hr days or equivalent time period due to photochemical degradation and the resultant change in transmission.

CHAPTER III

PHOTOSYNTHESIS, DARK RESPIRATION AND GROWTH OF *RUMEX PATENTIA* L. EXPOSED TO UV-B IRRADIANCE (280-315 nm) SIMULATING A REDUCED ATMOSPHERIC OZONE COLUMN

Introduction

Photosynthetic inhibition by 254 nm UV radiation was first observed by Arnold (1933) in *Chlorella pyrenoidosa*. Since this initial study, the effects of 254 nm radiation on the photosynthetic process has been investigated in some detail, primarily with alga as the test organism (Bell and Merinova, 1961; Black, 1973; Halldal, 1964; Lockhart and Brodführer, 1961; Mantai and Bishop, 1967; Trebst, 1974; Van Baalen, 1968). Components of the photosynthetic process suggested as being directly affected by 254 nm radiation include inhibition of electron transport (Arnold, 1933; Erixon and Butler, 1972), the Hill reaction (Jones and Kok, 1966; Mantai and Bishop, 1967; Shavit and Avron, 1963) and non-cyclic photophosphorylation (Jones and Kok, 1966). A utilization of these studies in assessing an enhanced UV global spectral irradiance resulting from reduced atmospheric ozone concentrations could result in a misrepresentation in predicted higher-plant responses. These studies often utilized intense 254 nm radiation in the absence of concomitant longer wavelength radiation similar to global irradiance.

In addition, biological responses are highly wavelength specific with respect to efficiency of photobiological action (Caldwell, 1971; Giese, 1964) and the 254 nm wavelength would not be transmitted even under severe ozone reductions to 40 percent of its present concentration (Green et al., 1974).

An evaluation of the response of higher-plants exposed to a UV radiation enhanced global spectral irradiance correlated with specific atmospheric ozone reductions is presently nonexistent. Thus, this chapter reports an evaluation of net photosynthesis, dark respiration and growth of Rumex patientia L. exposed to UV irradiation corresponding to the global UV spectral irradiance which would occur with partial ozone reduction. The level of ozone reduction simulated was an approximate 38 percent decrease from normal.

Methods

Germination of R. patientia L. seeds was carried out in petri dishes and the seedlings were transplanted individually into peat pots and then into 10-cm pots at initiation of the first leaf. The plants remained in a greenhouse until full expansion of the third leaf. Temperatures in the greenhouse fluctuated between 20C during the night and 35C during the day. From these plants, the most uniform-appearing plants were selected for each controlled-environment experiment. For field studies, the plants were transferred to field plots for approximately a week of equilibration under normal global irradiation prior to treatment. Again, only the most uniform-appearing plants were selected for the experiment. In

all experiments, the third leaf was used in photosynthetic determinations and upon initiation of treatment, the plants were approximately five weeks old from the time of germination. At initiation of each experiment, the third leaf was approximately 15 days old.

Net photosynthetic rate determinations were made on the third leaf of all plants initially selected for experimentation. Those plants expressing the most uniform net photosynthetic rates were randomly selected for subsequent control and UV radiation treatments. To achieve uniform irradiation over the entire surface of the third leaf, and thereby reduce variability, the third leaf was maintained horizontal to the light sources by white string looped over the petiole.

Net photosynthetic rates of plants from both field and controlled-environment studies were determined in the Siemens cuvette with a UV-enhanced spectral irradiance corresponding to that used in the respective experiments. For the UV-irradiated plants, the normal cuvette cover was replaced with one layer of Kodacel TA-401 (5 mil) plastic film filter and two Westinghouse FS-20 'sun lamps' provided the desired UV radiation enhancement to simulate a 0.18 atm·cm ozone column.

The light source in the controlled-environment experiments was a 6000-watt Osram Co. xenon arc mounted below a parabolic reflector. The UV radiation enhanced treatment consisted of (1) one layer of Mylar Type A (10 mil) plastic film which enclosed the lamp and removed all UV radiation produced by the xenon arc below 315 nm and (2) two Westinghouse FS-40 'sun lamps' each filtered

by one layer of Kodacel TA-401 (5 mil) plastic film provided supplemental UV irradiation corresponding to a 0.18 atm·cm stratospheric ozone column at an angle from the zenith of 30° (Figure 7). The normal level of ozone in August in northern Utah (42°N latitude, 112°W longitude) where this population of Rumex was collected, is approximately 0.29 atm·cm. The control irradiation treatment consisted of the same lamps as used in the UV radiation enhanced treatment. All lamps (two FS-40 'sun lamps'; a 6000-W xenon arc) in the control treatment were filtered with one layer of Mylar Type A (10 mil) plastic film (Figure 7).

An 11-hr photoperiod was used in all controlled-environment studies with temperature programmed to simulate a July day in Logan, Utah (37 to 13C).

In field studies, a simulated 0.18 atm·cm ozone column was also evaluated. As previously described for the controlled-environment studies, two FS-40 'sun lamps' each filtered by Kodacel TA 401 (5 mil) or Mylar Type A (10 mil) plastic film filters were used for the UV radiation and control treatments, respectively. Spectral irradiances resulting from global irradiance with (Kodacel-filtered FS-40 'sun lamps'; 0.18 atm·cm ozone simulation) and without (Mylar-filtered FS-40 'sun lamps'; 0.29 atm·cm ozone) supplemented UV radiation below 315 nm are shown in Figure 4. These measurements were made when the angle from the zenith was 30° during a cloudless day with a Gamma Scientific Co. spectroradiometer. The lamp/filter systems were used daily when the angle from the zenith was less than 50°.

Figure 7. Spectroradiometric measurements in a controlled-environment for (A) two FS-40 lamps each filtered with one layer of Kodacel TA-401 (5 mil) plastic film plus a 6000-W xenon arc filtered with one layer Mylar Type A (10 mil) plastic film simulating a 0.18 atm·cm ozone column when the sun is at 30° from the zenith and (B) two FS-40 lamps and a 6000-W xenon arc each filtered with one layer Mylar Type A (10 mil) plastic film. The FS-40 lamps in each treatment were in the configuration illustrated by Figure 3. Irradiance between 400 and 700 mm was 800 μeinsteins·m^{-2}·s^{-1}.

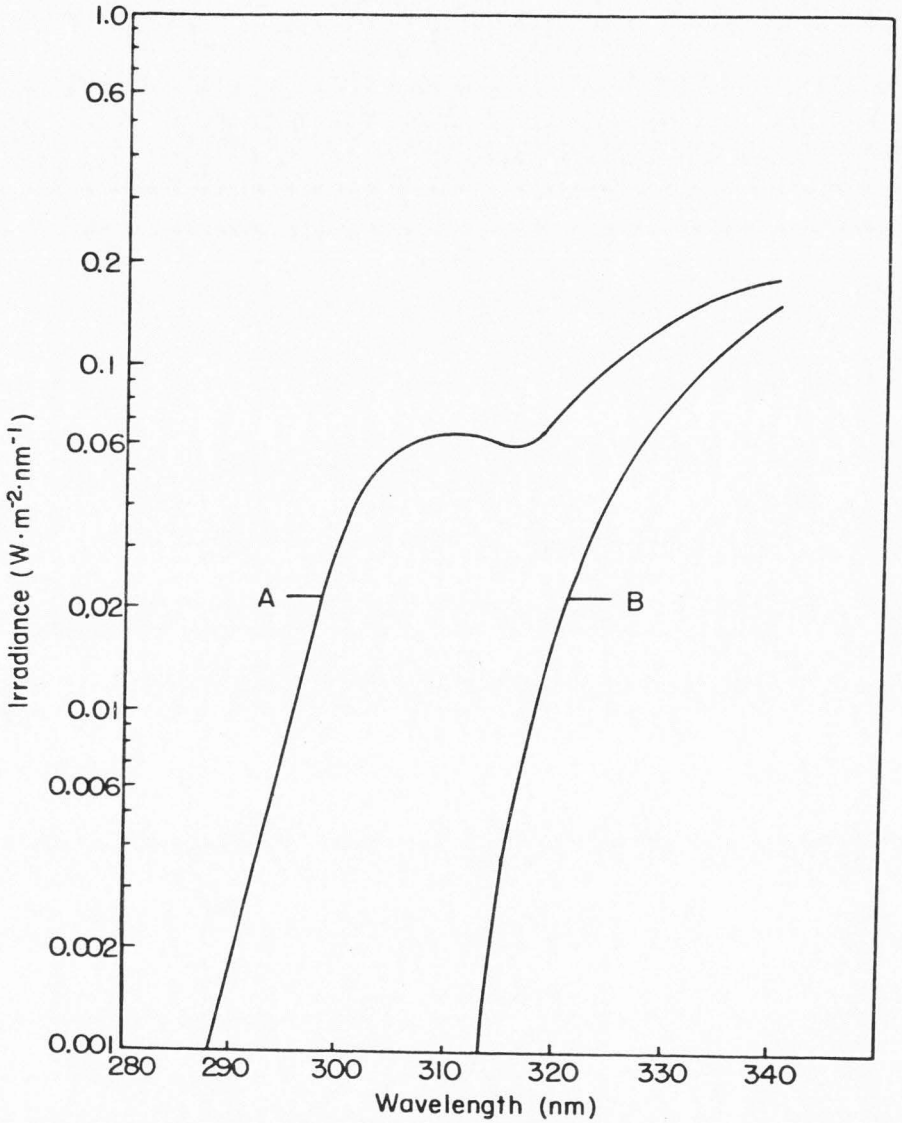
1.0
0.6
0.2
0.1
0.06
0.02
0.01
0.006
0.002
0.001
Irradiance (W·m⁻²·nm⁻¹)
A
B
280
290
300
310
320
330
340
Wavelength (nm)

Results

Controlled-environment studies

Net photosynthetic rates of R. patientia over a 7-hr period were determined to measure the initial short-term effects of a UV-enhanced irradiance simulating a 0.18 atm·cm ozone column with the sun at 30° from the zenith. The visible part of the spectrum (400-700 nm) was maintained at 400 μeinsteins·m^{-2}·s^{-1}. Consistent, significant differences ($P<.05$) between the UV radiation and control treatments were found after 2 hr exposure (Figure 8). Mean net photosynthetic rates of the UV radiation treated plants were depressed about 15 percent below the control plants after 7-hr treatment. This difference was still apparent after a 10-hr dark period. Although total CO_2 resistance was significantly greater for the plants exposed to UV irradiance, the variability exhibited by the components of the total CO_2 resistance between treatments eliminated statistically significant differences ($P<.05$) (Figure 8). The leaf resistance component ($r'_a + r'_s$), however, appeared to be more responsible for the significant increase in total CO_2 resistance than did the residual component (r'_r). This would suggest an effect on stomatal aperture. Zill and Tolbert (1958) similarly observed a 30 to 50 percent stomatal closure in Thatcher wheat after 30 minutes of intense 254-nm radiation (3.5 W·m^{-2}).

Net photosynthetic rate determinations over a 7-day period under the same UV-enhanced irradiance and visible irradiance as used in the previous short-term study (400 μeinsteins·m^{-2}·s^{-1}

Figure 8. Net photosynthesis and the associated CO_2 resistances (r'_r = residual resistance; $r'_s + r'_a$ = leaf resistance) of the third leaf of Rumex patientiaL. for 7 hours of UV irradiance (●----●) (simulating a 0.18 atm·cm stratospheric ozone level at an angle of 30° from the zenith) and control (o——o) treatment. Irradiance between 400 and 700 nm was 400 μeinsteins·$m^{-2}·s^{-1}$. Vertical bars represent ± one standard error and each point is the mean of 5 replicates.

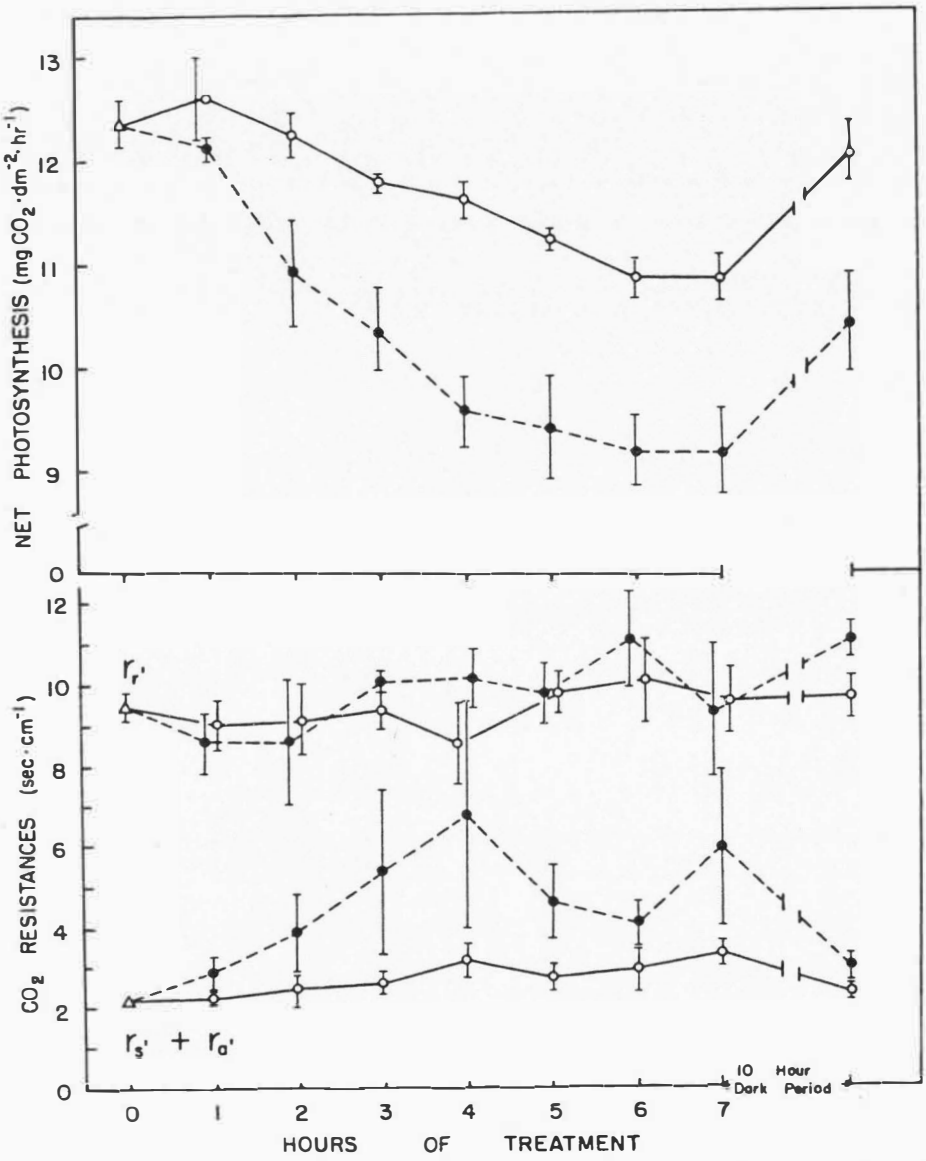
NET PHOTOSYNTHESIS (mg $CO_2 \cdot dm^{-2} \cdot hr^{-1}$)
13
12
11
10
9
0
CO_2 RESISTANCES (sec · cm^{-1})
12
10
8
6
4
2
0
r_r'
$r_s' + r_a'$
10 Hour Dark Period
0
1
2
3
4
5
6
7
HOURS OF TREATMENT

between 400-700 nm) are presented in Figure 9. Net photosynthetic rates of the UV-radiation-treated plants were significantly ($P<.05$) reduced after one, 11-hr day of treatment. Leaf resistances ($r'_a + r'_s$) did not differ significantly ($P<.05$) between treatments, whereas the residual resistances (r'_r) were found significantly ($P<.05$) different after one day of UV radiation exposure (Figure 9). The decreasing photosynthetic rates and increasing r'_r observed in the control plants over time is probably due to increasing leaf age since the same leaves (third leaf) were used for photosynthetic determinations throughout the study.

Photosynthetic rates of R. patientia under the same UV-enhanced irradiance, temperatures and photoperiod as the previous experiment but with 800 μeinsteins$\cdot m^{-2} \cdot s^{-1}$ (400-700 nm) yielded essentially the same results (Figure 10). These experiments were conducted at two levels of visible irradiance (400 and 800 μeinsteins$\cdot m^{-2} \cdot s^{-1}$ for the waveband between 400 and 700 nm) to determine if the effects of UV irradiation would be more severe at a lower visible irradiance when light for photosynthesis and photorepair processes might be more limiting. However, comparable accumulative UV-B radiation repression of photosynthesis is suggested for both visible irradiance experiments through 7 days of exposure. In addition, an almost identical response was noted for the calculated r'_r and $r'_a + r'_s$ resistances in both the 400 and 800 μeinsteins$\cdot m^{-2} \cdot s^{-1}$ (400-700 nm) experiments. That is, no statistically significant ($P<.05$) differences were found between the UV-irradiated and control plants for $r'_a + r'_s$ although r'_r differed statistically after one day of

Figure 9. Net photosynthesis and CO_2 resistances (r_r' = residual resistance; r_s' and r_a' = leaf resistances) of Rumex patientia L. during 7 days of UV irradiance (●----●) (simulating a 0.18 atm·cm stratospheric ozone level at an angle of 30° from the zenith) and control (o——o) treatment in controlled-environment studies. Irradiance between 400 and 700 nm was 400 μeinsteins·$m^{-2}·s^{-1}$. Vertical bars represent ± one standard error and each value is the mean of 4 or 5 replicates.

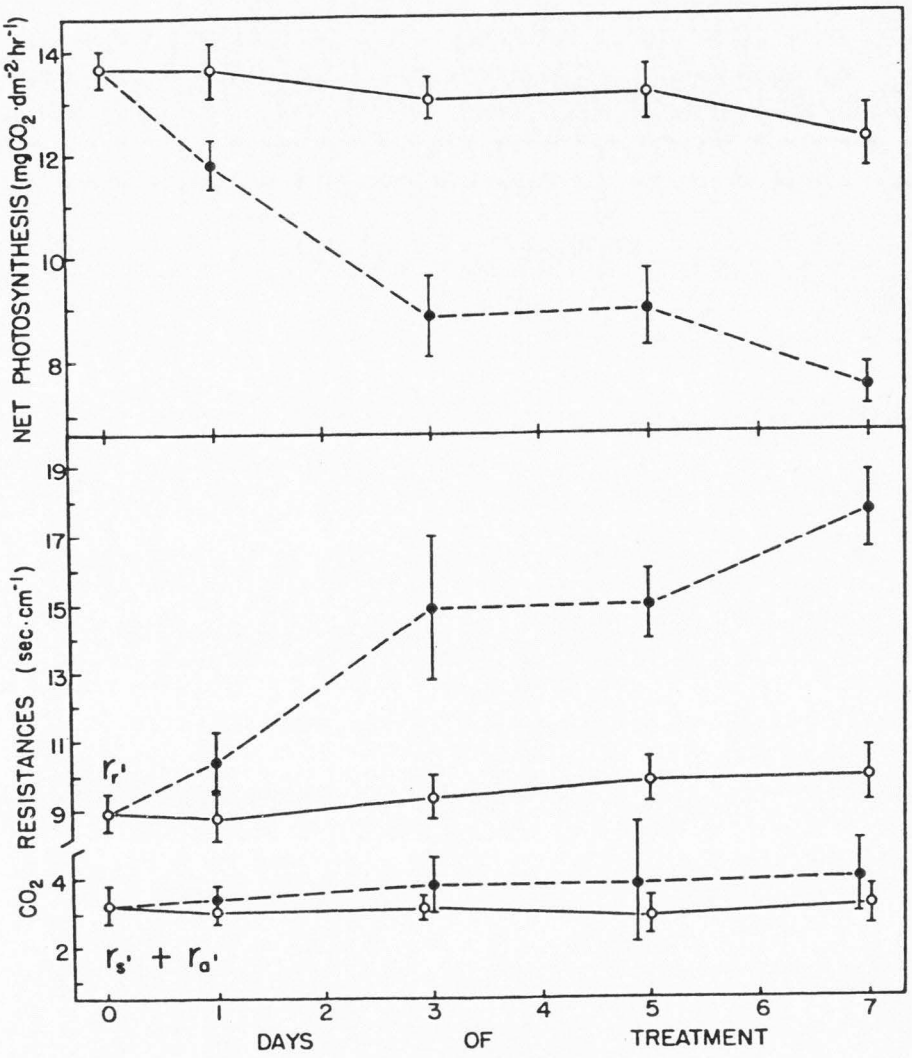
NET PHOTOSYNTHESIS (mg CO_2 · dm^{-2} · hr^{-1})
14
12
10
8
CO_2 RESISTANCES (sec · cm^{-1})
19
17
15
13
11
9
4
2
r_r'
$r_s' + r_a'$
0
1
2
3
4
5
6
7
DAYS OF TREATMENT

Figure 10. Net photosynthesis and dark respiration of Rumex patientia L. during 7 days of UV irradiance (●----●) (simulating a 0.18 atm·cm stratospheric ozone level at an angle of 30° from the zenith) and control (o——o) treatment in controlled-environment studies. Irradiance between 400 and 700 nm was 800 μeinsteins·$m^{-2}.s^{-1}$. Vertical bars represent ± one standard error and each point is the mean of 4 to 6 replicates.

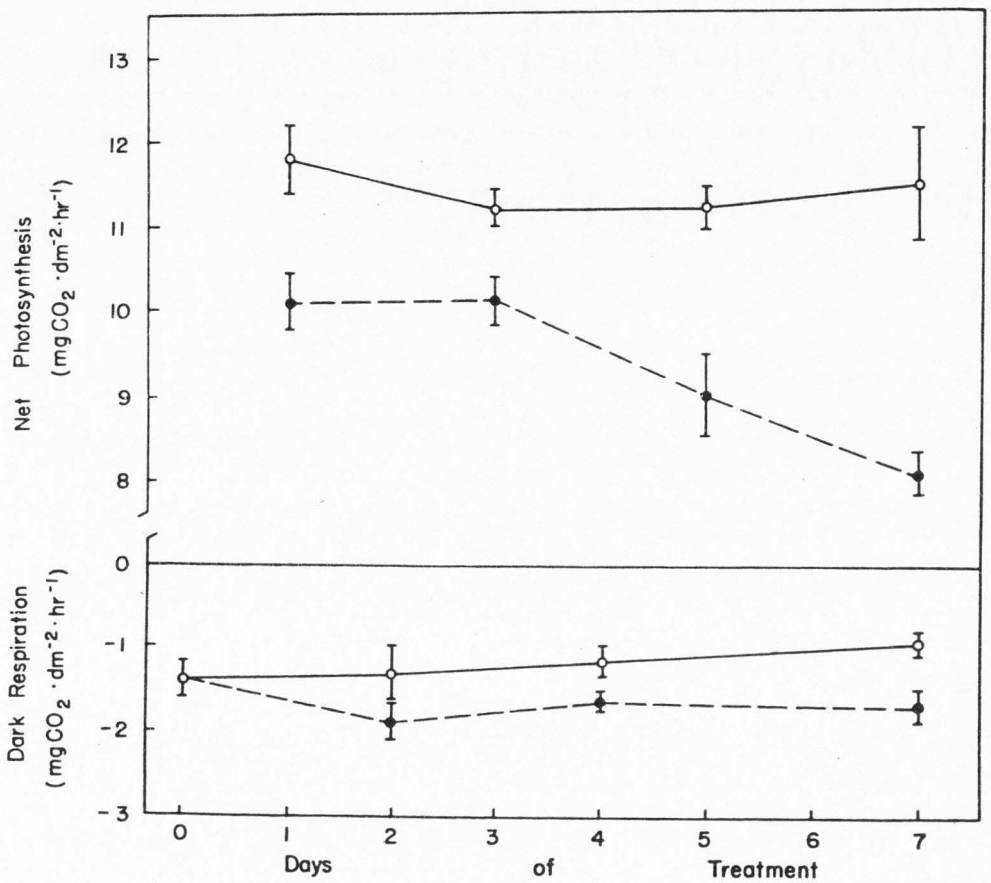
Net Photosynthesis
(mg CO2 · dm-2 · hr-1)
13
12
11
10
9
8
Dark Respiration
(mg CO2 · dm-2 · hr-1)
0
-1
-2
-3
0
1
2
3
4
5
6
7
Days of Treatment

treatment. Stomatal aperature did not appear to be affected in the longer-term UV-radiation-enhanced treatments (400 or 800 μeinsteins·m^{-2}·s^{-1} between 400 and 700 nm) as was suggested to occur in the short-term (7-hr) exposure period.

Dark respiration rates determined in this experiment (800 μeinsteins·m^{-2}·s^{-1} between 400 and 700 nm treatment) were significantly ($P<.05$) higher in the UV-radiation-enhanced treatment (Figure 10). Owen (1957) reported that short-term exposure of tobacco plants to 254-nm radiation (8.7 W·m^{-2}) also resulted in increased dark respiration rates and furthermore, that longer UV radiation exposure caused continued increases in respiration rates. In the present study, however, a relatively stable elevated dark respiration rate was maintained through 7 days of UV radiation exposure.

Leaf length measurements for the 800 μeinsteins·m^{-2}·s^{-1} (400-700 nm) experiment are shown in Figure 11. Leaf lengths for each leaf were compared between treatments for each day beginning at leaf initiation. Consistent, significant ($P<.05$) differences were found after 3 days treatment in leaf number 1, and 2 days for leaves 2-6. As shown in Figure 11, leaf length and time of leaf exertion are retarded for leaves 2 through 6 when plants were exposed to the enhanced UV irradiance. Upon termination of this study, dry and fresh weights for aboveground biomass and total leaf area were determined (Table 1). Mean values of the UV-radiation treated plants were less than 50 percent of the control plants and all parameters differed significantly ($P<.01$) between

Figure 11. Leaf length for leaves 1 through 6 of Rumex patientia L. during 23 days of UV irradiance (-----) (simulating a 0.18 atm·cm stratospheric ozone level at an angle of 30° from the zenith) and control (———) treatment in controlled-environment studies. Irradiance between 400 and 700 nm was 800 μeinsteins·m^{-2}·s^{-1}. Each point represents the mean of 6 replicates.

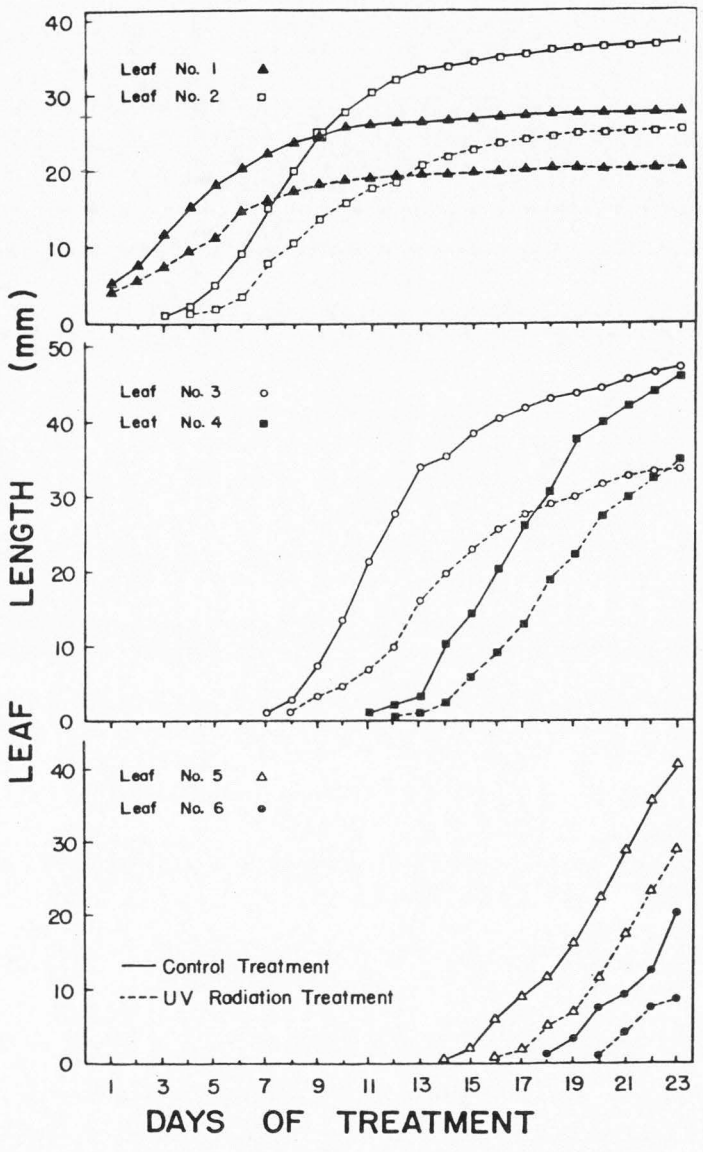
Leaf No. 1
Leaf No. 2
Leaf No. 3
Leaf No. 4
Leaf No. 5
Leaf No. 6
Control Treatment
UV Radiation Treatment
LEAF LENGTH (mm)
DAYS OF TREATMENT
0
10
20
30
40
50
1
3
5
7
9
11
13
15
17
19
21
23

Table 1. Mean dry and fresh weight for aboveground biomass, total leaf area, and fresh and dry weight to leaf area ratios of Rumex patientia after 22 days of UV irradiation (simulating a 0.18 atm·cm ozone column; angle of 30° from the zenith) and control treatments in controlled-environment studies. Irradiation between 400 and 700 nm was 800 μeinsteins·m^{-2}·s^{-1}. Each value represents the mean of 4 to 6 replicates.

	UV radiation treatment	Control treatment
Leaf Area (cm^2)	44.79	89.67**
Fresh weight (g)	1.37	2.99**
Fresh weight: Leaf area	0.030	0.033
Dry weight (g)	0.13	0.29**
Dry weight: Leaf area	0.003	0.003

**Represents significant differences at $P<.01$.

treatment and control. Fresh and dry weight to leaf area ratios were similar between treatments (Table 1). Total chlorophyll, chlorophyll a and chlorophyll b concentrations were also determined on a fresh and dry weight basis. As shown in Table 2, no consistent differences were found between treatments.

Field study

Net photosynthesis was determined for R. patientia in a field experiment under a UV-enhanced global spectral irradiance corresponding to a 0.18 atm·cm ozone column when the sun was 30° from the zenith (Figure 12). Under these conditions, significantly ($P<.05$) depressed photosynthetic rates were found for the UV-enhanced treatment plants after 3 days. The calculated CO_2 resistances (Figure 12) followed similar trends as those of plants treated similarly in controlled-environment experiments.

Discussion

The UV-enhanced irradiance corresponding to a 0.18 atm·cm ozone column resulted in an almost immediate suppression of photosynthesis and leaf expansion of R. patientia. Decreased photosynthesis could be detected after only two hours of exposure to the UV irradiance. Partial stomatal closure is implicated in the suppression of photosynthesis during the initial exposure to radiation. However, after one day of exposure, leaf resistances ($r'_a + r'_s$) did not differ between UV-irradiated and control plants, indicating that stomatal diffusion resistance was not involved in the lower photosynthetic

Table 2. Total chlorophyll, chlorophyll a and chlorophyll b for leaf 1 through 7 of Rumex patientia after 28 days of UV radiation enhanced (simulating a 0.18 atm·cm ozone column at an angle of 30° from the zenith) and control treatments in controlled-environment studies. Irradiation between 400-700 nm was 800 μeinsteins·m^{-2}·s^{-1}. Chlorophyll concentrations are expressed as mg/g fresh or dry weight. Each value represents the mean of 4 to 6 replicates.

	Control treatment			UV radiation treatment		
Leaf No.	Total	a	b	Total	a	b
(A) Fresh weight						
1	1.02	0.65	0.36	0.95	0.62	0.33
2	1.31	0.88	0.43	1.31	0.87	0.44
3	1.46	0.99	0.47	1.54	1.05	0.49
4	1.58	1.11	0.47	1.79	1.22	0.58
5	1.78	1.22	0.56	1.70	1.19	0.51
6	1.79	1.27	0.53	1.73	1.18	0.55
7	1.76	1.17	0.59			
(B) Dry weight						
1	10.83	6.94	3.89	9.84	6.41	3.43
2	11.95	8.06	3.09	13.56	8.99*	4.58
3	14.22	9.69	4.53	14.66	10.52	4.67
4	15.36	10.77	4.59	18.58*	12.60*	5.97*
5	17.16	11.78	5.38	16.59	11.59	5.01
6	17.35	12.01	5.09	16.64	11.36	5.29
7	16.16	11.37	5.80			

* Represents significant ($P<.05$) differences between control and UV radiation treatments for the particular parameter and leaf number.

Figure 12. Net photosynthesis and CO_2 resistances (r'_r = residual resistance; $r'_s + r'_a$ = leaf resistance) of Rumex patientia L. during 8 days of UV irradiance (●———●) (simulating a 0.18 atm·cm stratospheric ozone level at an angle of 30° from the zenith) and control (o——o) treatment in field studies. Irradiance between 400 and 700 nm was 800 μeinsteins·$m^{-2}·s^{-1}$ during photosynthetic determinations. Vertical bars represent ± one standard error and each point is the mean of 4 to 6 replicates.

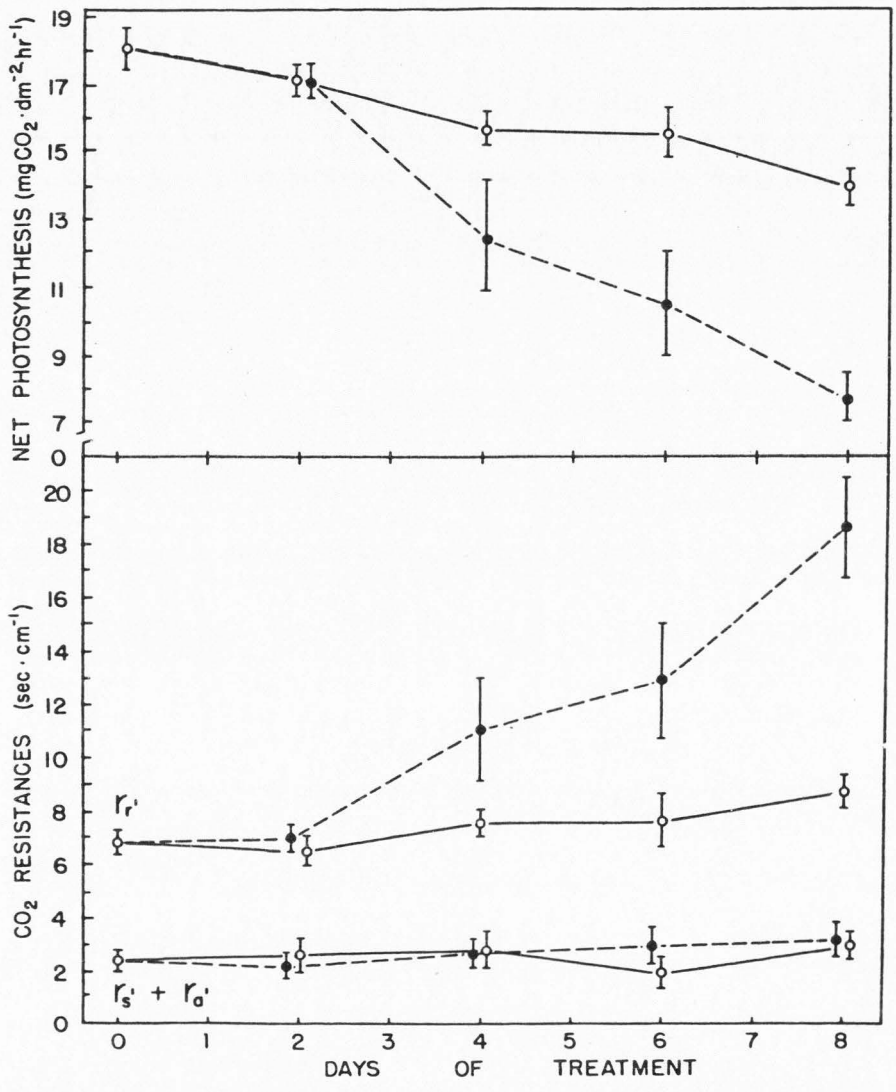
NET PHOTOSYNTHESIS (mg CO2 · dm-2 hr-1)
19
17
15
13
11
9
7
0
CO2 RESISTANCES (sec · cm-1)
20
18
16
14
12
10
8
6
4
2
0
rr'
rs' + ra'
0
1
2
3
4
5
6
7
8
DAYS OF TREATMENT

rates of the UV-irradiated plants. The effects of the UV irradiation must therefore involve other components of the photosynthetic apparatus apart from stomatal diffusion as indicated by the increased residual resistance term.

Unlike earlier reports of chlorophyll destruction by intense 254-nm radiation (Cline and Salisbury, 1966; El-Mansey and Salisbury, 1971), chlorophyll concentrations were not depressed by irradiance in the 288 to 315-nm waveband. If UV irradiance in this waveband has the potential to destroy chlorophyll similar to 254-nm radiation, the intensities, exposure periods, or both were insufficient to cause destruction in this study. Thus, the repressed photosynthetic rates of the UV irradiated plants were not a secondary effect of chlorophyll destruction.

Photoreactivation involves a partial or complete repair of molecular damage induced by UV irradiation. This repair is dependent on radiation of longer wavelengths (315 to 550 nm). A variety of deleterious physiological manifestations of UV irradiation (primarily 254-nm) in higher plants has been shown to be photoreactivable (Caldwell, 1971; Owen, 1957). However, conclusive evidence that impairment of photosynthesis by UV radiation is photoreactivable has not been found although this is suggested by Van Baalen (1968) in his experiments with blue-green alga. Apart from photoreactivation, visible radiation may also contribute to the repair or replacement of damaged organelles or tissues. Thus, experiments involving an enhanced UV irradiance were conducted at two levels of visible irradiance (400 and 800 μeinsteins$\cdot m^{-2} \cdot s^{-1}$; 400-700 nm)

to determine if the effects of UV irradiation would be more severe under conditions of low visible light. After three days exposure, photosynthesis in the UV-irradiated plants of the low-visible-light experiment was depressed to 68 percent of control plant photosynthesis while rates of the UV-irradiated plants in the high-visible-light experiment were still 90 percent of rates of control plants. However, after seven days of UV radiation exposure, photosynthesis of UV-irradiated plants in the high-visible-light experiment was depressed almost as much as in the low-visible-light experiment (70 and 62 percent of the control plants, respectively). Although UV radiation does appear to be more effective in depressing photosynthesis when visible light intensities are low, this effect appears to be pronounced only during the early stages of treatment.

Under conditions of either high or low visible light, the depressive effects of UV irradiation on photosynthesis appear to accumulate with continued exposure. Although plants in these experiments were exposed to UV radiation corresponding to a sizeable depletion of atmospheric ozone (38 percent reduction), even with only a 5 or 10 percent reduction, the effects of this increased ultraviolet irradiance could be significant for plants with reasonably long-lived leaves if the damage accumulates in a manner similar to that demonstrated in these experiments.

Although UV radiation damage to photosynthesis appeared to accumulate over longer exposure, depression of leaf expansion did not. The reduction of leaf expansion rates was most severe in the very early stages of leaf elongation and apparently involves an effect of UV radiation apart from simply limiting the supply of

photosynthates for growth. When daily elongation rates of the first leaf are plotted from initiation of the UV radiation treatment (Figure 13), it is apparent that leaf expansion rates were depressed below those of the control plant leaf only during the first few days. In this figure is also a plot of the expected expansion rate of the first leaf exposed to UV radiation if growth rates of that leaf were dependent solely on its own photosynthesis for growth and there was no appreciable delay between production of photosynthates and their utilization in the growth process. This hypothetical situation would represent the most pronounced possible case of growth reduction as a consequence of suppressed photosynthetic rates by UV radiation. In this situation, depression of leaf expansion rates would show an accumulative response as does the depression of photosynthesis. Instead, the reduction in expansion rates during the first two days of ontogeny suggests that UV irradiation is acting directly on leaf expansion processes. The suppressive effect of UV radiation on the expansion rates of subsequent leaves are similar to the first leaf (see Figure 11), although time of leaf exertion is delayed in the plants exposed to UV irradiation. The effects of UV irradiation on development and growth of other leaves later in the treatment may reflect both the direct effects of UV irradiance on leaf expansion processes as well as photosynthate limitation.

The potential of increased solar ultraviolet radiation resulting from partial ozone destruction to decrease the growth and productivity of sensitive higher plants is apparent in this study. The direct effects of UV irradiance on depressed photosynthetic rates,

Figure 13. Leaf elongation rates ($mm \cdot day^{-1}$) of the first leaf of Rumex patientia L. during 18 days of UV irradiance (•) (simulating a 0.18 atm·cm ozone column) and control (o) treatment in controlled-environment studies. The curves represent least square fits of the UV irradiance (—— ——) and control treatment (——) elongation rates. The dashed line (---) represents the expected leaf elongation rate of the UV irradiated leaf if the reduction in elongation rate were solely a function of the depressed photosynthetic rates of that leaf. Each point represents the mean of 6 replicates. See text for details.

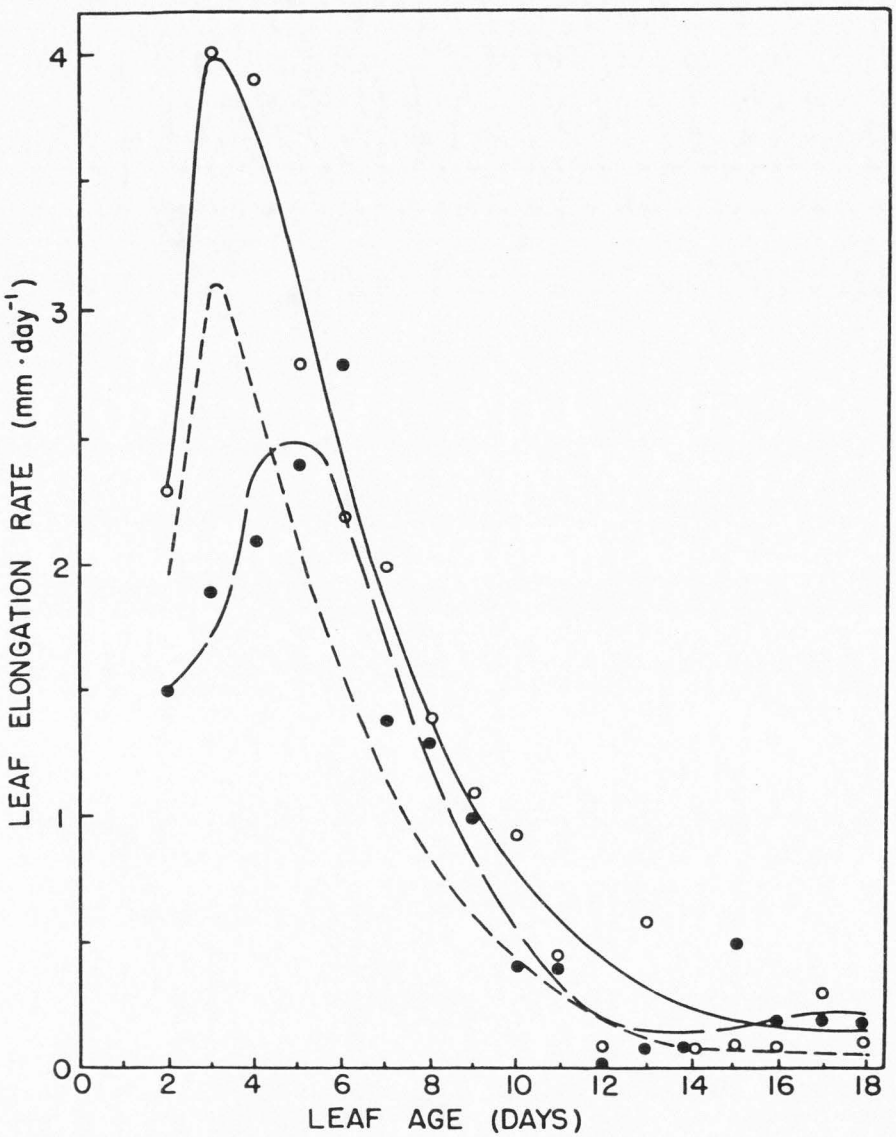
LEAF ELONGATION RATE (mm · day⁻¹)
LEAF AGE (DAYS)
0
1
2
3
4
0
2
4
6
8
10
12
14
16
18

decreased leaf expansion processes, and also the apparent stimulation of dark respiration would all contribute to reducing the carbon economy of the plant.

CHAPTER IV

THE RECIPROCITY RELATIONSHIP IN THE RESPONSE OF RUMEX PATIENTIA L. EXPOSED TO UV RADIATION

Introduction

The objective of this study was to test the hypothesis that reciprocity is maintained in the response of R. patientia L. to polychromatic UV-B irradiance simulating reduced atmospheric ozone concentrations. Quantitatively, the measure of biologically effective UV-B irradiance utilized in this test can be expressed in the form:

$$\Sigma\ (I) = \int_{280}^{315} E_\lambda\ I_{\lambda a_1}\ d\lambda\ - \int_{280}^{315} E_\lambda\ I_{\lambda a_2}\ d\lambda \qquad (5)$$

where $I_{\lambda a_2}$ and $I_{\lambda a_1}$ represent UV-B irradiance under normal (eg. 0.29 atm·cm) and reduced ozone concentrations, respectively. The term E_λ represents the relative biologically effectiveness as defined by equation 1 at each wavelength. Thus, $\Sigma(I)$ represents the additional biologically effective UV irradiation of concern in the test of reciprocity.

If recriprocity is maintained, then R. patientia L. leaves should accumulate damage produced by exposure to biologically effective UV irradiance over time. This tendency to accumulate detrimental effects of UV radiation on plant physiological processes

would be important for long-lived plant parts even under relatively small (eg. less than 15 percent) ozone reductions. The functional value of these relationships is the predictability of plant responses to additional fluxes of biologically effective UV irradiation that would occur under reduced atmospheric ozone concentrations.

The second aim of this study was to develop a simulation model for the prediction of plant response (ie. photosynthesis and growth) to any level of atmospheric ozone and its resultant UV-B irradiation. The basis of this simulation model is the biologically effective UV irradiation as defined by equation 5 and its relationship with plant growth and photosynthesis derived during the experiments testing for reciprocity. A validation test of the simulation model was made with a field study conducted under a UV irradiation supplement simulating a 0.18 atm·cm ozone column when the sun was at 30° from the zenith.

Methods

Net photosynthetic rates were determined as previously described in Chapter II. Artificial irradiation was provided by four, 300-watt Sylvania 'cool-beam' spotlights adjusted to 800 μeinsteins$\cdot m^{-2} \cdot s^{-1}$. Plexiglass cuvette covers were used during all photosynthetic rate determinations.

Four levels of UV spectral irradiance were employed in the controlled-environment experiments (Figure 14). Treatment 1 (curve A, Figure 14) simulated a 0.18 atm·cm ozone column with the

Figure 14. Spectroradiometric measurements in a controlled-environment for spectral irradiance (A) simulating a 0.18 atm·cm atmospheric ozone column when the sun is at 30° from the zenith, (B) simulating a 0.22 atm·cm ozone column when the sun is at 30° from the zenith, (C) simulating a 0.29 atm·cm ozone column when the sun is at 15° from the zenith, and (D) with all biologically effective UV radiation as defined by equation 1 removed. See text and Table 3 for lamp/filter systems used to achieve the spectral irradiance levels shown. Irradiance between 400 and 700 nm was 800 μeinsteins·m^{-2}·s^{-1}.

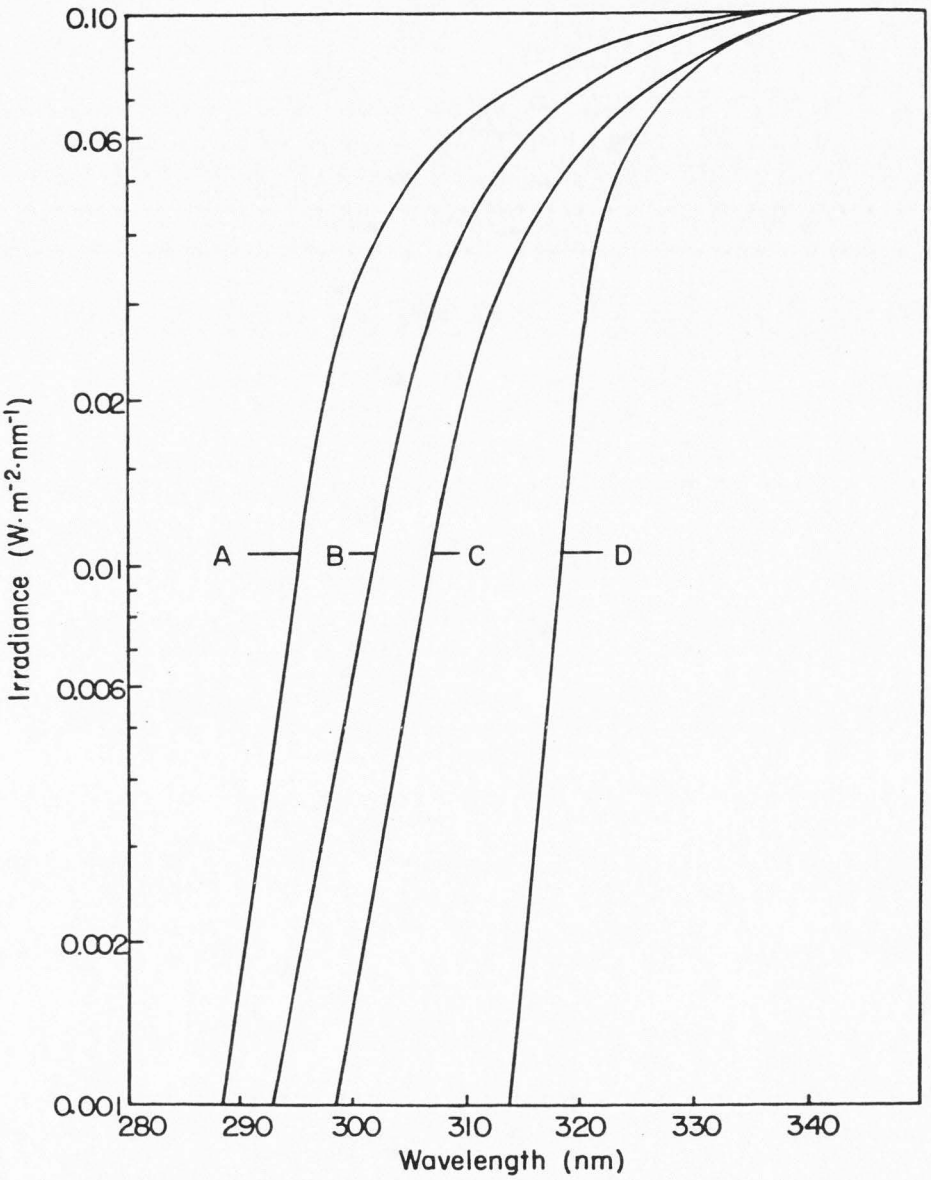
0.10
0.06
0.02
0.01
0.006
0.002
0.001
Irradiance (W·m⁻²·nm⁻¹)
A
B
C
D
280
290
300
310
320
330
340
Wavelength (nm)

sun at 30° from the zenith. The mean level of ozone in northern Utah in August is approximately 0.29 atm·cm. The radiation sources used to produce this spectral irradiance consisted of (1) a 6000-W xenon arc filtered with three layers of Kodacel TA-401 (5 mil) plastic film filters and (2) two Westinghouse FS-40 'sun lamps', each filtered by one layer of Kodacel TA-401 (5 mil) plastic film filter in the configuration illustrated in Figure 3.

Treatment 2 (curve B, Figure 14) simulated a 0.22 atm·cm ozone column with the sun at 30° from the zenith. The radiation sources used for this treatment consisted of (1) a 6000-W xenon arc filtered with 2-mm, WG-320 glass filters (Schott Co.) and (2) two Westinghouse FS-40 'sun lamps' each filtered by two layers of Kodacel TA-401 (5 mil) plastic film filters in the configuration illustrated in Figure 3.

Treatment 3 (curve C, Figure 14) simulated a 0.29 atm·cm ozone column with the sun at 15° from the zenith. The lamp/filter combinations used to produce this spectral irradiance were (1) a 6000-W xenon arc filtered by 2-mm, WG 320 glass filters (Schott Co.) and (2) two Westinghouse FS-40 'sun lamps' each filtered by Mylar type 'A' (10 mil) polyester film in the configuration illustrated in Figure 3.

Treatment 4 (curve D, Figure 14) was produced by a 6000-W xenon arc and 2 Westinghouse FS-40 'sun lamps', each filtered by one layer of Mylar type 'A' (10 mil) polyester film. As shown in Figure 14, the spectral irradiance produced by this lamp/filter combination did not include wavelengths shorter than 313 nm above

1.0×10^{-3} $W \cdot m^{-2} \cdot nm^{-1}$. The biologically effective UV radiation action spectrum shown in Figure 1 does not include wavelengths above 313.3 nm as defined in equation 1. Thus, this treatment represents no biologically effective UV-B irradiation if integrated by equation 2 when irradiance above 1.0×10^{-3} $W \cdot m^{-2} \cdot nm^{-1}$ is considered. Therefore, this treatment provided growing conditions with no biologically effective UV-B radiation which could be compared to other treatments (1, 2, and 3) consisting of various levels of biologically effective UV-B radiation. The biologically effective UV-B irradiance according to equation 1 was 0.0986, 0.0296, and 0.0087 $W \cdot m^{-2}$ for treatments 1, 2 and 3, respectively. A summary of the four UV irradiance treatments and their respective lamp/filter systems is given in Table 3.

The ozone concentration simulated in treatments 1 and 2 were predicted by equation 4 from a base ozone level of 0.29 atm·cm with the sun at 30° from the zenith. This predicted spectral irradiance was then compared to the data of Bener (1972) and the spectral irradiance predicted by the analytic equations of Green et al. (1974) as a further verification of the simulated ozone level. Treatment 3 ozone concentration was determined by direct comparison to the predicted spectral irradiance of the analytic equations of Green et al. (1974).

An 11-hour photoperiod was employed with temperature programmed to simulate a July day in northern Utah (13 to 37C). The spectral irradiance levels shown in Figure 14 for treatments 1, 2 and 3 were used during the middle 8 hours of the 11-hour photoperiod.

Table 3. Treatments employed in the evaluation of photosynthesis and growth of Rumex patientia L. under irradiation regimes simulating stratospheric ozone decreases.

Treatment number	Biologically effective UV-irradiance ($W \cdot m^{-2}$)	Atmospheric ozone level corresponding to UV-B irradiance (atm·cm)	Angle from the zenith	Lamp/filter system
1	0.0986	0.18	30°	(a) xenon arc with 3 layers of Kodacel TA-401 (5 mil) plastic film (b) two FS-40 'sun lamps' with 1 layer Kodacel (5 mil).
2	0.0296	0.22	30°	(a) xenon arc with 2 mm Schott Co., WG-320 glass filters (b) two FS-40 lamps with 2 layers Kodacel (5 mil)
3	0.0087	0.29	15°	(a) xenon arc with 2 mm Schott Co., WG-320 glass filters (b) two FS-40 lamps with 1 layer Mylar (10 mil)
4	0	--	--	(a) xenon arc with 1 layer Mylar (10 mil) (b) two FS-40 lamps with 1 layer Mylar (10 mil)

Intensity of irradiation within the 400 to 700 nm waveband was maintained at 800 μeinsteins·m^{-2}·s^{-1} (400-700 nm) during this 8-hour period for all treatments. During the remaining 3 hours, the spectral irradiance of all treatments corresponded with curve D of Figure 14. This was accomplished by turning off the FS-40 'sun lamps' and placing a sheet of Mylar Type 'A' (10 mil) plastic film filter between the plant bed and the filtered 6000-W xenon arc for all treatments. In addition to excluding all irradiation below approximately 315 nm, total quanta in the 400 to 700 waveband was reduced from 800 μeinsteins·m^{-2}·s^{-1}, to approximately 680 μeinsteins·m^{-2}·s^{-1}.

Rumex patientia L. seeds were germinated in petri dishes and the seedlings transplanted into 10 cm pots at the time of initiation of the first leaf. The plants were grown in a greenhouse until the third leaf was initiated. The plants were approximately 25 days old at this time. From these plants, 24 of the most uniform-appearing plants were selected for subsequent treatment. Of these 24 plants, 6 plants were randomly selected for each treatment and immediately transferred to the controlled environments. In all cases, only the third leaf was used in photosynthetic and growth analysis. The third leaf was held horizontal to the light sources by white string.

The plastic film filters were routinely replaced every two or three days to reduce photodegradation and maintain the desired spectral irradiance.

Results

Ontogeny and photosynthesis of *Rumex patientia* L. leaves exposed to 4 levels of UV irradiance

Mean net photosynthesis rates of the third leaf of *R. patientia* L. exposed to 4 levels of UV irradiance (see Figure 14) are presented in Figure 15. Except for day 9, plants of treatment 4 (curve D, Figure 14) maintained the highest photosynthetic rates throughout the study. Mean net photosynthetic rates on day 9 for treatments 3 and 4 were almost identical (8.49 and 8.43 $mgCO_2 \cdot dm^{-2} \cdot hr^{-1}$ for treatments 3 and 4, respectively). After day 9, mean net photosynthetic rates were depressed as a function of the amount of biologically effective UV irradiation of each treatment. That is, treatment 4 (no biologically effective irradiation above 1.0×10^{-3} $W \cdot m^{-2} \cdot nm^{-1}$ by equation 2) resulted in the highest mean net photosynthetic rates throughout the study followed by treatment 3 (0.0087 $W \cdot m^{-2}$), treatment 2 (0.0296 $W \cdot m^{-2}$), respectively. Longevity of the third leaf was similarly decreased with increased biologically effective UV irradiance. This effect was most pronounced in treatment 1 where leaf death occurred prior to 39 days. A leaf was considered dead when at least 90 percent of the leaf was brown and dry. In contrast, leaf death for treatment 3 and 4 occurred after 53 days and prior to 49 days in treatment 2. Although the UV irradiance of treatment 3 resulted in a reduction of mean net photosynthetic rates after 9 days exposure relative to treatment 4, leaf longevity of these two treatments did not differ.

Figure 15. Mean net photosynthesis of the third leaf of Rumex patientia L. exposed to four levels of UV irradiance (Figure 14) (A) simulating a 0.18 atm·cm ozone column when the sun is at 30° from the zenith, (B) simulating a 0.22 atm·cm ozone column when the sun is at 30° from the zenith, (C) simulating a 0.29 atm·cm ozone column when the sun is at 15° from the zenith and (D) with no biologically effective UV irradiation as defined by equation 2 above 1.0×10^{-3} $W \cdot m^{-2} \cdot nm^{-1}$. This controlled-environment study was conducted at 800 $\mu einsteins \cdot m^{-2} \cdot s^{-1}$ during the middle 8 hr of an 11-hr photoperiod with the remaining 3 hr irradiance at 680 $\mu einsteins \cdot m^{-2} \cdot s^{-1}$. The vertical bars represent ± one standard deviation and each point represents the mean of 4 to 6 replicates.

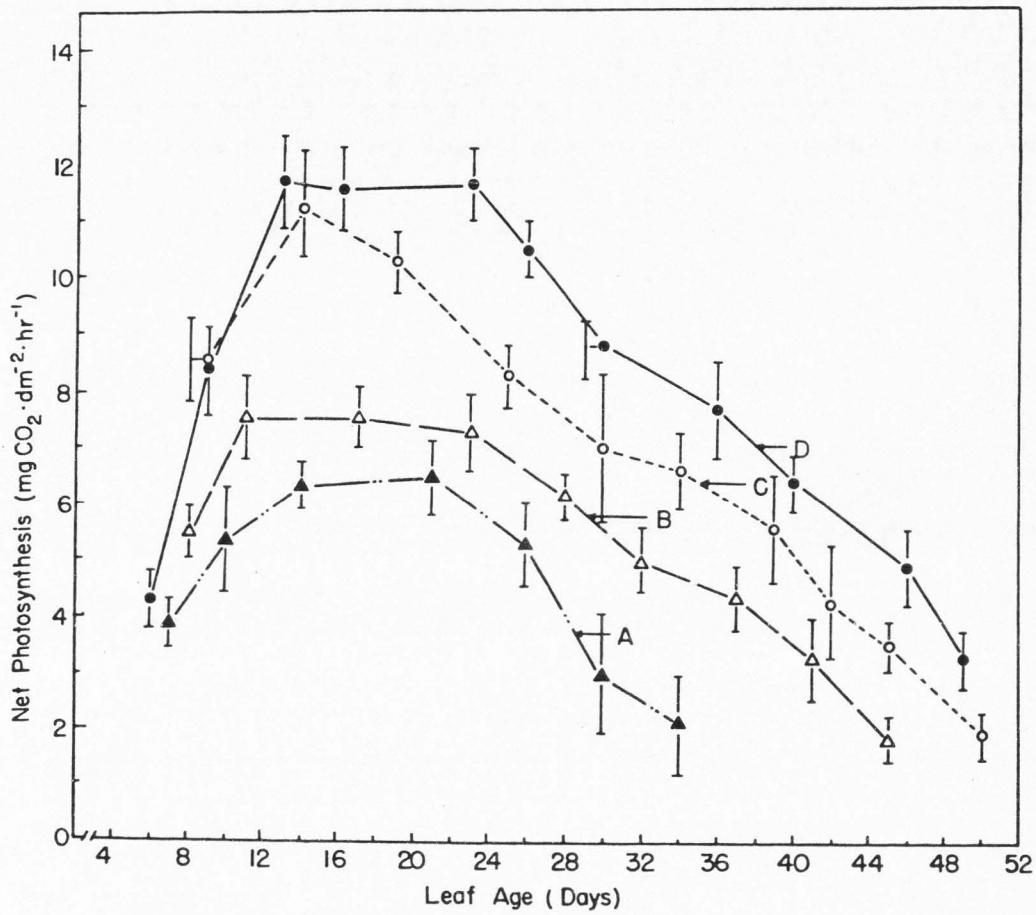
Net Photosynthesis (mg $CO_2 \cdot dm^{-2} \cdot hr^{-1}$)
Leaf Age (Days)
A
B
C
D

Leaf area measurements determined concomitantly with net photosynthetic rate determinations for the four UV irradiation treatments are shown in Figure 16. As similarly determined for mean net photosynthetic rates exposed to the four UV irradiation treatments, the degree of leaf area suppression was a function of the amount of biologically effective UV irradiation. That is, mean leaf area of those plants in treatment 1 displayed the greatest reduction relative to treatment 4 followed by treatment 2 and 3, respectively. Although the third leaf in treatment 1 and 2 underwent leaf senescence and death prior to treatments 3 and 4, whole-plant senescence and death was not observed in any treatment during the study.

The reciprocity relationship for depression of photosynthesis and leaf growth of *Rumex patientia* L. exposed to UV irradiation

The photosynthetic data of treatments 1 through 4 (Figure 15) were fitted by least squares techniques with the results shown in Figure 17. In this form, the photosynthetic data from treatments 1, 2 and 3 were compared to treatment 4 to determine the percent reduction in net photosynthetic rates. These values are graphically represented in Figure 18 with the abscissa representing accumulated biologically effective UV irradiation. Thus, each point represents the percent reduction in photosynthesis that occurred relative to treatment 4 and the accumulated biologically effective UV irradiation to that day. The data shown in Figure 18 represent a comparison of photosynthetic rates of the plants of treatments 1

Figure 16. Leaf area measurements of the third leaf of Rumex patientia L. exposed to four UV spectral irradiance (Figure 14) (A) simulating a 0.18 atm·cm ozone column when the sun is at 30° from the zenith, (B) simulating a 0.22 atm·cm ozone column when the sun is at 30° from the zenith, (C) simulating a 0.29 atm·cm ozone column when the sun is 15° from the zenith and (D) with no biologically effective UV radiation as defined by equation 2 above 1 x 10^{-3} $W \cdot m^{-2} \cdot nm^{-1}$. The controlled-environment study was conducted at 800 $\mu einsteins \cdot m^{-2} \cdot s^{-1}$ during the middle 8 hr of an 11 hr photoperiod with the remaining 3 hr irradiance at 680 $\mu einsteins \cdot m^{-2} \cdot s^{-1}$. The vertical bars represent ± one standard deviation and each point is the mean of 4 to 6 replicates.

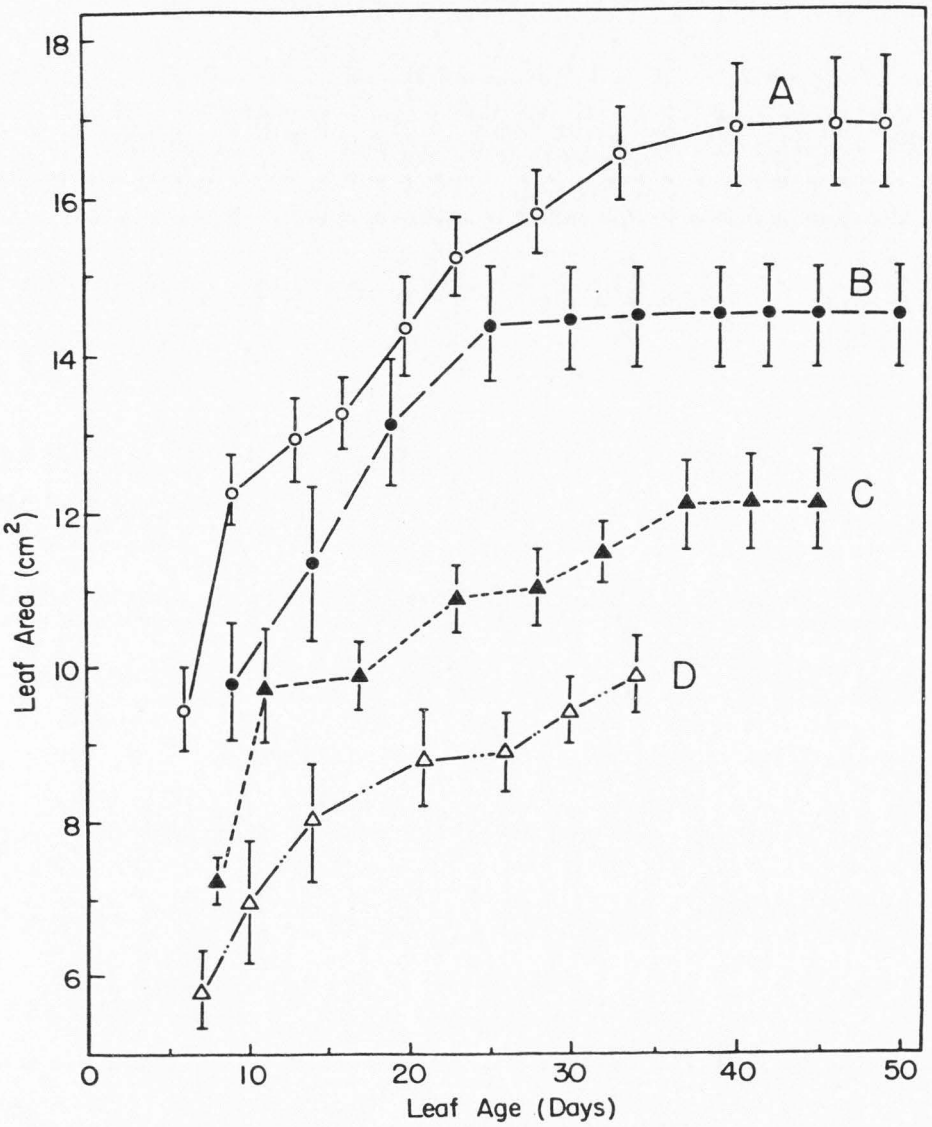
18
16
14
12
10
8
6
Leaf Area (cm²)
0
10
20
30
40
50
Leaf Age (Days)
A
B
C
D

Figure 17. Least squares fit to the net photosynthesis data determined for the third leaf of Rumex patientia L. exposed to four levels of UV irradiance (treatment 1 ▲——··——▲; treatment 2 △—— ——△; treatment 3 o----o; treatment 4 ●——●). Each point represents the mean of 4 to 6 replicates.

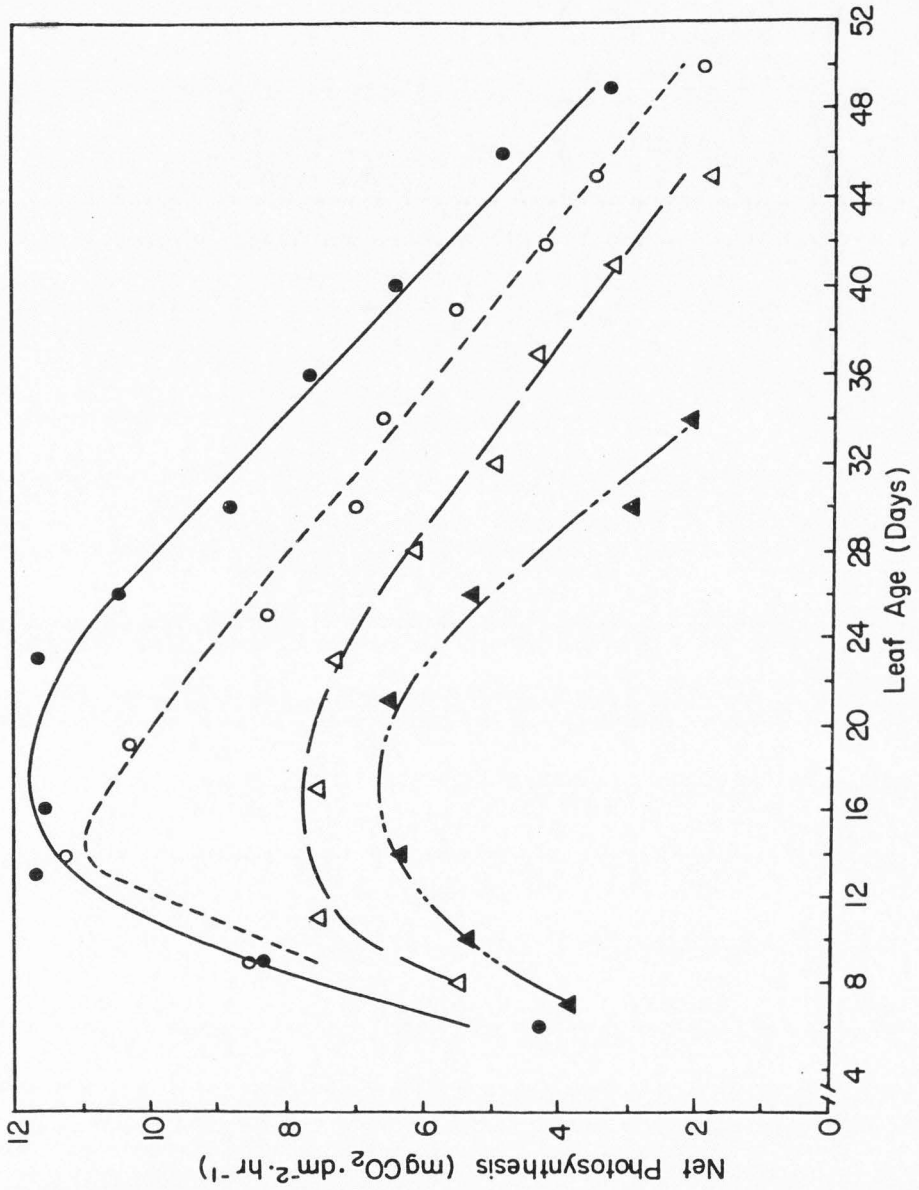
Net Photosynthesis ($mgCO_2 . dm^{-2} . hr^{-1}$)
0
2
4
6
8
10
12
4
8
12
16
20
24
28
32
36
40
44
48
52
Leaf Age (Days)

Figure 18. Plot of the percent reduction in net photosynthesis determined for treatments 1 (▲), 2 (Δ) and 3 (o) relative to treatment 4 as a function of biologically effective UV irradiance as defined by equation 2. The curve represents a least squares fit to the data.

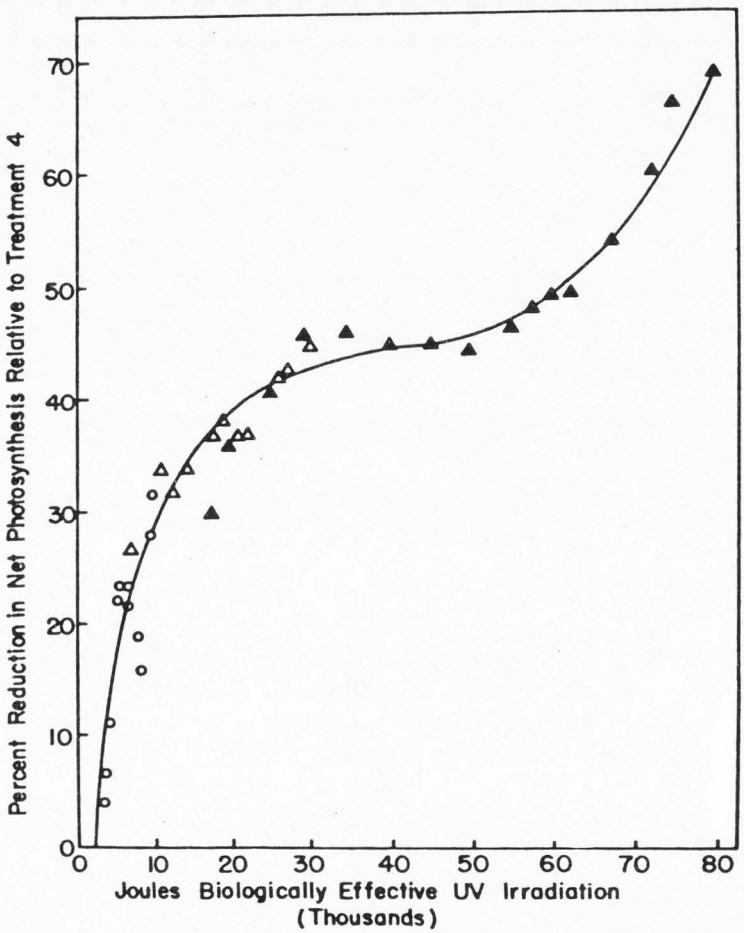
Percent Reduction in Net Photosynthesis Relative to Treatment 4
0
10
20
30
40
50
60
70
0
10
20
30
40
50
60
70
80
Joules Biologically Effective UV Irradiation
(Thousands)

through 3 compared to treatment 4 only between the initial and final day of actual measurements of photosynthesis. Since the shape of the curves beyond the measurements are not known, extrapolation of the data to the point where photosynthesis was totally inhibited or prior to the measurements was not made.

If the inhibition of photosynthesis by biologically effective UV irradiation exhibits reciprocity, the same degree of reductions in photosynthesis must occur when the sum of daily biologically effective UV irradiation is the same. Representative comparisons between treatments where the accumulated biologically effective UV irradiation values were nearly identical is presented in Table 4. For those comparisons shown in Table 4, 1 through 5 were essentially equivalent in the accumulated biologically effective UV irradiation and the reduction in photosynthesis relative to treatment 4. However, comparison 6 deviated somewhat in that the biologically effective UV irradiation of treatments 1 and 3 were identical, but a 7 percent difference in the percent reduction in photosynthesis occurred.

Figure 19 is a plot of the logarithm of photosynthetic reduction as a function of biologically effective UV irradiation. Data for this plot were taken from Figure 18 to illustrate reciprocity, i.e. that short periods of higher intensity UV irradiation were equally effective in repressing photosynthesis as were longer periods of lower intensity irradiance. Thus, reciprocity is indicated between 6350 and 31750 J biologically effective UV irradiance. Data above and below 6350 and 31750 J biologically effective UV

Table 4. Percent reduction in photosynthesis of UV irradiance treatments 1, 2 and 3 relative to treatment 4 and their associated biologically effective UV irradiance.

Treatment number		Days of treatment	Percent reduction in photosynthesis relative to treatment 4	Biologically effective UV irradiance (Joules)
(1)	2	9	27.3	6714
	3	42	28.0	9198
(2)	2	16	31.9	11936
	3	45	32.0	9855
(3)	1	8	36.3	19872
	2	27	37.0	20142
(4)	1	10	40.1	24840
	2	35	42.0	26110
(5)	1	12	46.0	29808
	2	40	44.8	29840
(6)	1	7	30.0	17388
	2	23	37.0	17158

Figure 19. Plot of the logarithm of net photosynthetic reduction of treatments 1 (▲), 2 (o) and 3 (Δ) relative to treatment 4 (no biologically effective UV radiation above 1.0×10^{-3} $W \cdot m^{-2} \cdot nm^{-1}$ as defined by equation 2) as a function of biologically effective UV irradiation. The line represents a least squares fit to the data.

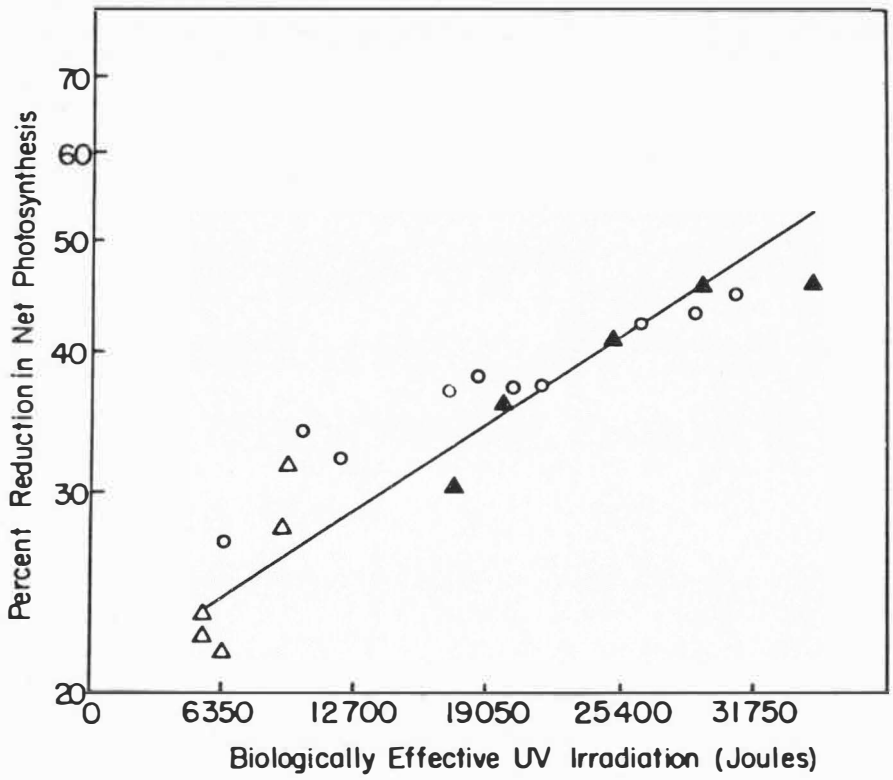
Percent Reduction in Net Photosynthesis
70
60
50
40
30
20
0
6350
12700
19050
25400
31750
Biologically Effective UV Irradiation (Joules)

irradiation (Figure 18) could not be tested in terms of reciprocity since the total biologically effective UV irradiation as defined by equation 2 were not comparable between treatments.

Area of the third leaf of R. patientia L. for treatments 1 through 4 (Figure 16) determined concomitantly with net photosynthetic rates and fitted by least squares analysis are shown in Figure 20. Leaf area expansion rates ($cm^2 \cdot day^{-1}$) computed from a least squares fit to these data are shown in Figure 21 for treatments 1 through 4. As shown previously for leaf elongation rates, the depressive action of UV irradiation on leaf expansion was most effective during the initial few days of exposure. Thereafter, leaf expansion rates were much less affected by UV irradiation. This type of response does not support a reciprocal mode of action by UV irradiation on leaf expansion rates. Rather, depression of leaf expansion took place during the first few days of leaf expansion and was dependent upon the level of biologically effective UV irradiance rather than the accumulated irradiation.

Simulation model of photosynthesis and leaf growth of Rumex patientia L. exposed to solar UV radiation corresponding to reduced atmospheric ozone concentrations

A simulation model was developed on the basis of biologically effective UV irradiation as defined by equation 5 and its relationship to net photosynthesis and leaf growth of R. patientia L. The analytic equations of Green et al. (1974) were used to predict hourly global UV radiation between 280 and 315 nm for the

Figure 20. Leaf area of the third leaf of Rumex patientia L. exposed to four levels of UV irradiance in a controlled-environment study. The curves represent least squares fits to the data (treatment 1 (▲), 2 (△), 3 (o) and 4 (●)). Each point represents the mean of 4 to 6 replicates.

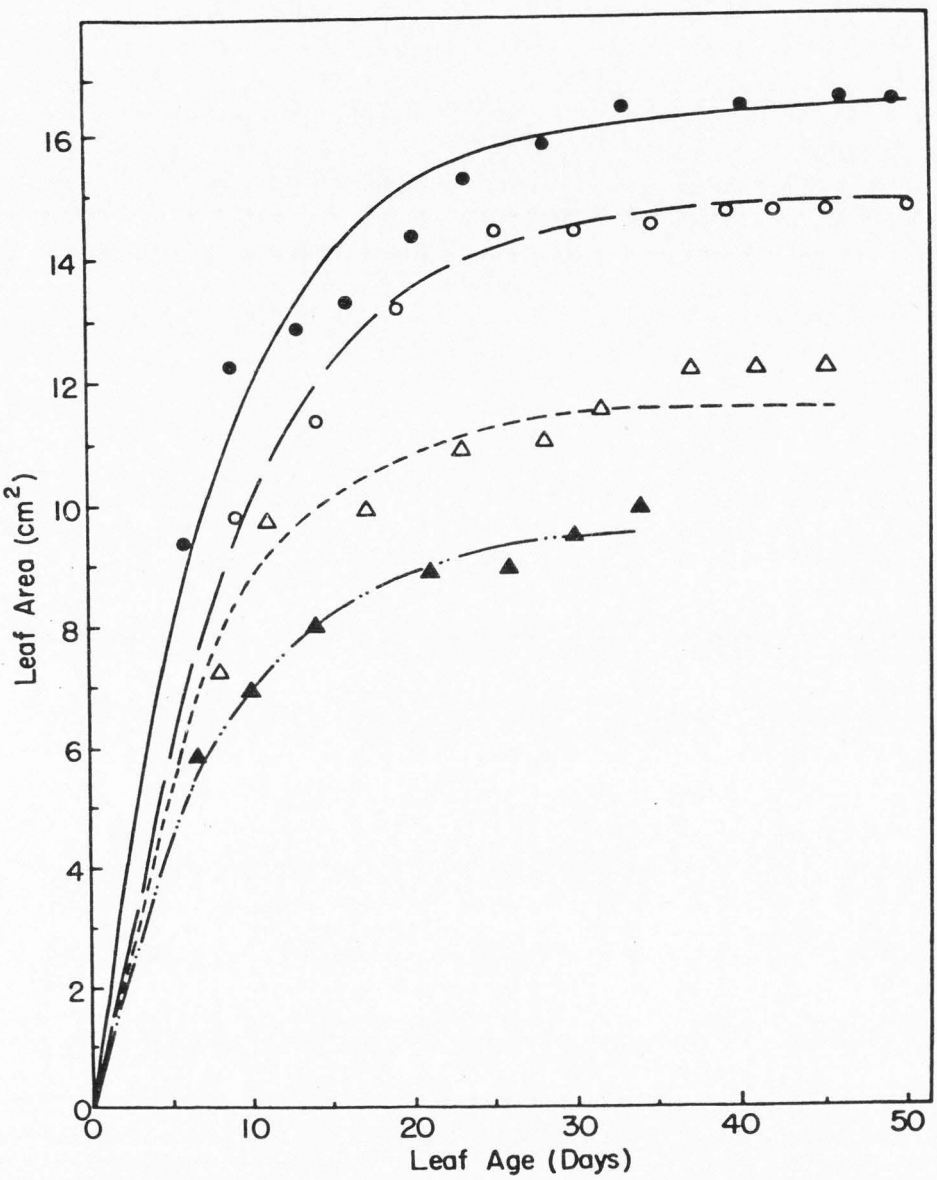
Leaf Area (cm^2)
0
2
4
6
8
10
12
14
16
0
10
20
30
40
50
Leaf Age (Days)

Figure 21. Leaf expansion rates of the third leaf of Rumex patientia L. exposed to four levels of UV irradiance determined from the least squares fits to the data of Figure 20 (treatment 1 (——··——), 2 (----), 3 (—— ——) and 4 (————)).

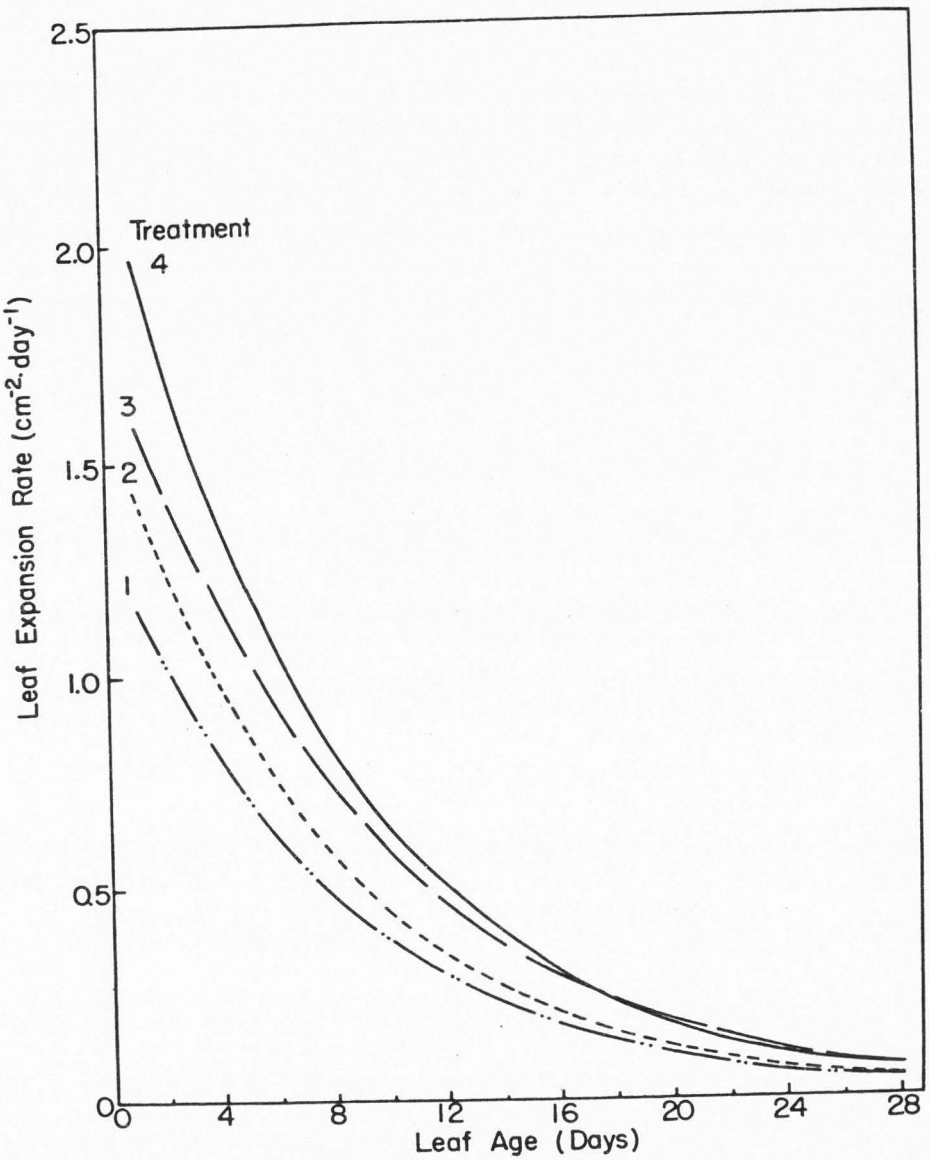
2.5
2.0
1.5
1.0
0.5
0
Treatment
4
3
2
1
Leaf Expansion Rate (cm-2·day-1)
0
4
8
12
16
20
24
28
Leaf Age (Days)

determination of hourly biologically effective UV irradiation by equation 5. The prediction of UV radiation within the 280 to 315 nm waveband by these equations are dependent on hourly angle of the sun from the zenith and daily concentrations of ozone (atm·cm). Hourly angle from zenith (θ) is calculated by:

$$\theta = \cos \phi \cos \delta \cos \zeta + \sin \phi \sin \delta \quad (6)$$

where the latitude, ϕ, is 42°N and the hour angles (ζ) are -90° (6 AM) to 90° (6 PM) (List, 1971). Daily declination (δ) values are predicted by the equation:

$$\delta = 23.27 \sin (0.9918A - 0.3016) \quad (7)$$

where A is the day number between 1 (March 21) and 185 (September 21). This equation was derived by a least squares fit to the data of List (1971).

For the determination of global UV-B radiation under normal ozone conditions, a least squares fit to the ozone data of Hering and Borden (1967) was used to predict an ozone concentration for those days between March 21 and September 21. The least squares fit to these data is shown in Figure 22 and can be represented by the equation:

$$\text{Ozone (atm·cm)} = 0.3728 + B\ (-0.5028 \times 10^{-3}) \quad (8)$$

where B represents the day number between March 1 (day 1) and September 21 (day 185). A reduced ozone concentration is determined by simply reducing the predicted ozone concentration by a given percent. Daily biologically effective UV irradiation for both the normal and reduced ozone concentrations are determined by averaging the total hourly values between 0600 and 1800. The difference

Figure 22. A least squares fit to the ozone concentration data (•) of Hering and Borden (1967) from March 1 to September 21, 1965.

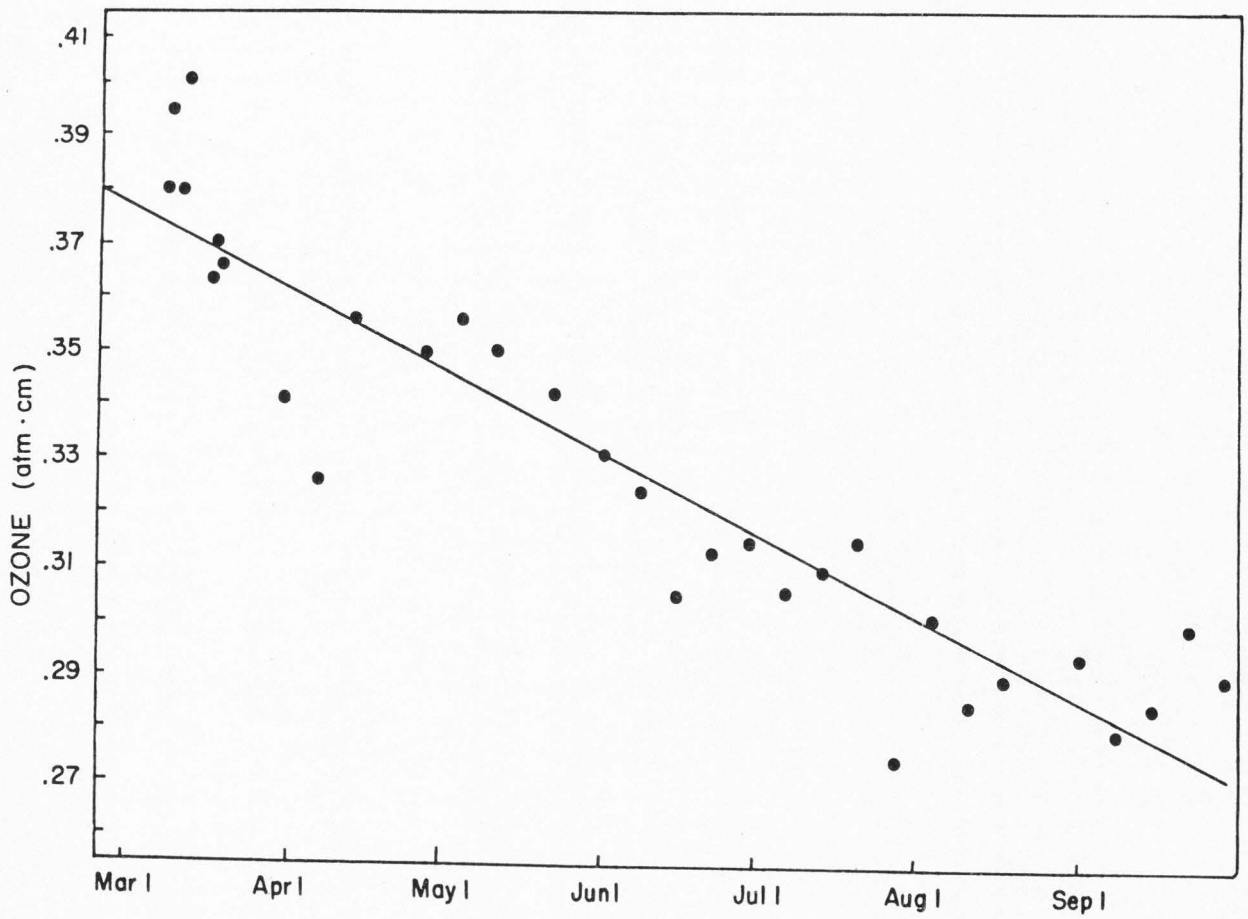
.41
.39
.37
.35
.33
.31
.29
.27
OZONE (atm·cm)
Mar 1
Apr 1
May 1
Jun 1
Jul 1
Aug 1
Sep 1

between the daily biologically effective UV irradiation for the normal and reduced ozone concentrations is the quantitative measure of the additional biologically effective UV irradiation occurring due to ozone reduction as defined by equation 5.

Daily biologically effective UV irradiation values determined for normal ozone concentrations and reductions of 5, 15 and 40 percent for April 1 to September 10 are shown in Figure 23. Biologically effective UV irradiation as used in this study and defined by equation 5 is represented in this graph as the difference between those values given for the normal ozone condition and the reductions. Data presented in this graph represent maximum values since cloud cover is not considered. The largest biologically effective UV irradiation values occur during mid-June since the solar angle from zenith is minimal during this period in northern Utah (42°N latitude) and relatively low concentrations of ozone are prevalent.

Net photosynthetic rates of R. patientia L. exposed to various levels of atmospheric ozone reduction and associated UV radiation are predicted by the relationship shown in Figure 18. That is, biologically effective UV irradiation accumulated over time results in a reduction in photosynthesis by:

$$y = -0.444 + (-0.4671C) + (0.23791C^2) + (0.01181\sqrt{C+0.5}) \quad (9)$$

where C is the accumulated biologically effective UV irradiation. This equation represents a least squares fit to the data shown in Figure 18. Absolute values of photosynthesis through the complete

Figure 23. Predicted daily biologically effective UV irradiation ($J \cdot m^{-2} \cdot day^{-1}$) for cloudless days between April 1 and September 21 for ozone concentration reductions of 5 (B), 15 (C) and 40 percent (D) from a least squares fit (Figure 22) to the ozone data of Hering and Borden (1967).

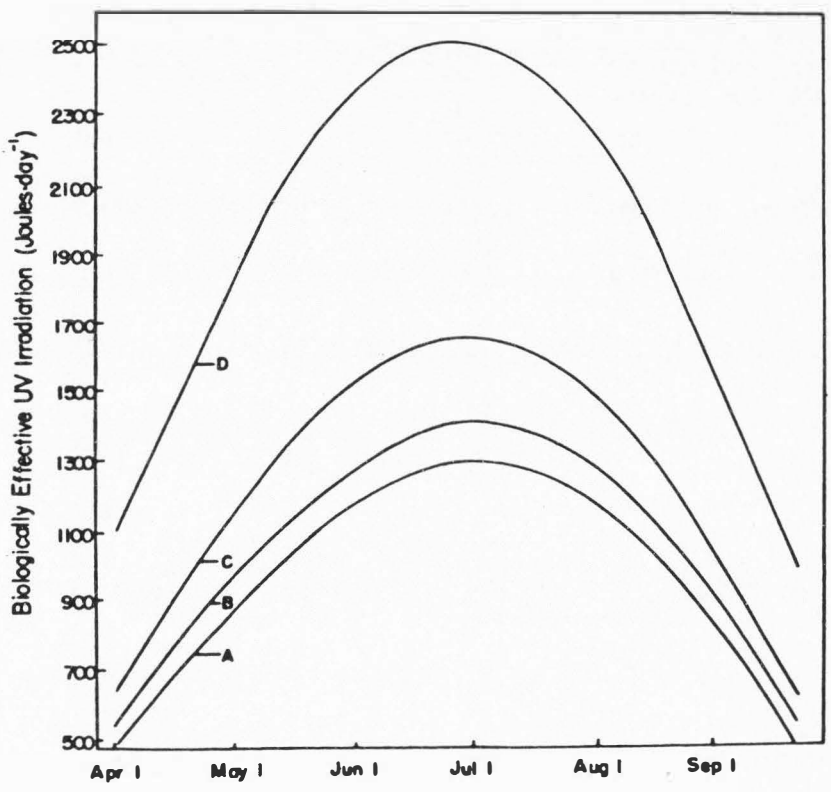
Biologically Effective UV Irradiation (Joules-day⁻¹)
2500
2300
2100
1900
1700
1500
1300
1100
900
700
500
D
C
B
A
Apr 1
May 1
Jun 1
Jul 1
Aug 1
Sep 1

ontogeny of all R. patientia L. leaves in a field situation under existing ozone conditions were not determined in this study. Thus, photosynthetic rate predictions by the simulation model are expressed by a percent reduction from the least squares fit to the photosynthetic rate data determined for treatment 4 with no biologically effective UV radiation (Figure 15).

Predicted net photosynthetic rates of the third leaf of Rumex patientia L. exposed to UV-B radiation simulating a 5 percent ozone reduction with 800 μeinsteins$\cdot m^{-2} \cdot s^{-1}$ (400-700 nm) is shown in Figure 24 for both the April 1 to May 5 and June 1 to July 5 periods. A detectable reduction in net photosynthetic rates per unit leaf area of this leaf did not occur until 21 days exposure or when the accumulated biologically UV irradiation was 2095 J for the June 1 to July 5 period. After 35 days simulation, a reduction of 6 percent in the photosynthetic rate of this leaf occurred. For a 5 percent ozone reduction between April 1 and May 5, a decrease in photosynthetic rate was not detected until 31 days. This increased exposure period before photosynthetic rates were reduced for the April 1 to May 5 period is due to higher ozone concentrations and greater prevailing angles from the zenith. These two factors in combination result in a reduction of UV-B radiation. As shown in Figure 18 and defined by equation 9, biologically effective UV irradiation of about 2095 J must be accumulated prior to a detectable reduction in photosynthetic rates per unit leaf area.

Figure 24. Predicted net photosynthetic rates of the third leaf of Rumex patientia L. exposed to UV-B radiation simulating a 5 percent atmospheric ozone reduction for the April 1 to May 5 (----) and June 1 to July 5 (—— ——) periods. Predicted photosynthetic rates are expressed as a reduction from a least squares fit (———) to the photosynthetic data of treatment 4.

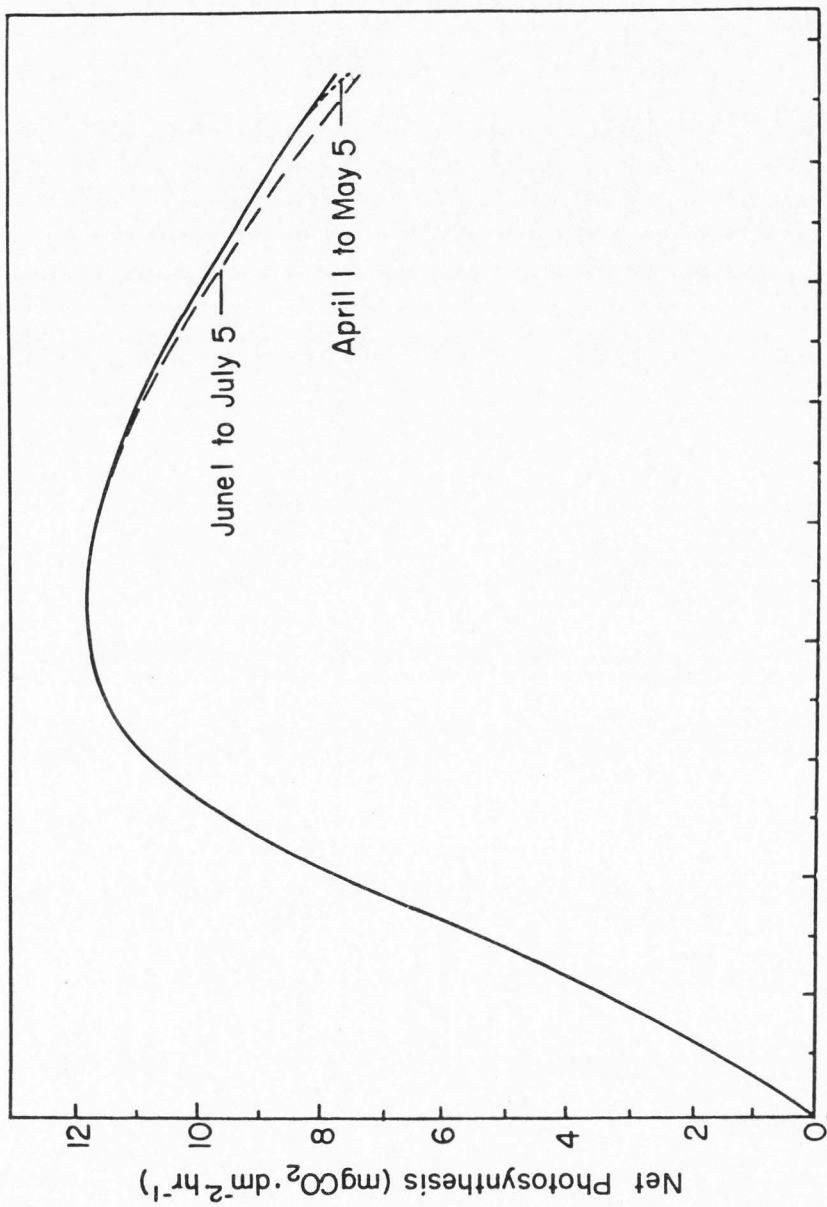
Net Photosynthesis ($mgCO_2 \cdot dm^{-2} hr^{-1}$)
0
2
4
6
8
10
12
0
4
8
12
16
20
24
28
32
36
Leaf Age (Days)
June 1 to July 5
April 1 to May 5

Photosynthetic rates predicted under a simulated 15 percent ozone reduction for the third leaf of R. patientia L. for both April 1 to May 5 and June 1 to July 5 are shown in Figure 25. Under these conditions, the photosynthetic rate of leaf 3 is reduced after 7 days simulated exposure during the June 1 to July 5 period and after 12 days during the April 1 to May 5 period. When the leaf is 35 days old, a photosynthetic rate reduction of 13 percent occurred during the April 1 to May 5 period and 21 percent for this same leaf during the June 1 to July 5 period.

Under a simulated 40 percent stratospheric ozone reduction, 4 days were required to reduce photosynthetic rates when the third leaf was initiated on April 1 and 2 days when initiated on June 1 (Figure 26). A reduction of 42 percent occurred after 35 days for this leaf when initiated on June 1 and a 36 percent reduction after this same time period when initiated on April 1.

Least squares fits to the leaf area expansion rates ($cm^2 \cdot day^{-1}$) determined for the third leaf of R. patientia L. exposed to the four UV irradiance treatments (Figure 21) were used in the prediction of leaf expansion rates in the simulation model. The computation of daily leaf expansion was based on the predicted daily biologically effective UV irradiation. Thus, depending on the predicted leaf age and biologically effective UV irradiation, reduction of expansion rates was determined by linear interpolation between the nearest applicable functions in Figure 21. For example, for a predicted daily biologically effective UV irradiation of 1200 $J \cdot day^{-1}$, a linear interpolation was made between the leaf expansion rate of

Figure 25. Predicted net photosynthetic rates of the third leaf of Rumex patientia L. exposed to UV-B radiation simulating a 15 percent atmospheric ozone reduction for the April 1 to May 5 (----) and June 1 to July 5 (—— ——) periods. Predicted photosynthetic rates are expressed as a reduction from a least squares fit (———) to the photosynthetic data of treatment 4.

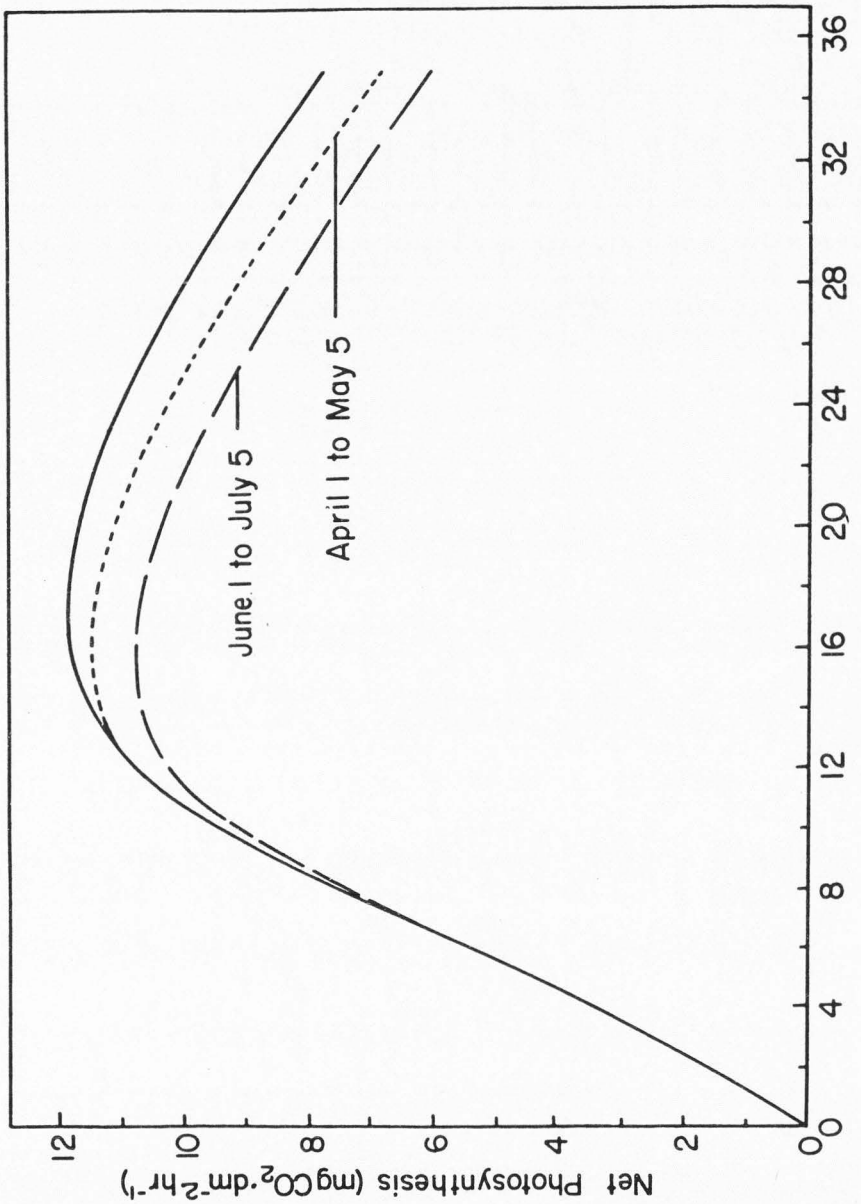
Net Photosynthesis ($mgCO_2 \cdot dm^{-2} hr^{-1}$)
0
2
4
6
8
10
12
0
4
8
12
16
20
24
28
32
36
Leaf Age (Days)
June 1 to July 5
April 1 to May 5

Figure 26. Predicted net photosynthetic rates of the third leaf of Rumex patientia L. exposed to UV-B radiation simulating a 40 percent atmospheric ozone reduction for the April 1 to May 5 (----) and June 1 to July 5 (—— ——) periods. Predicted photosynthetic rates are expressed as a reduction from a least squares fit (———) to the photosynthetic data of treatment 4.

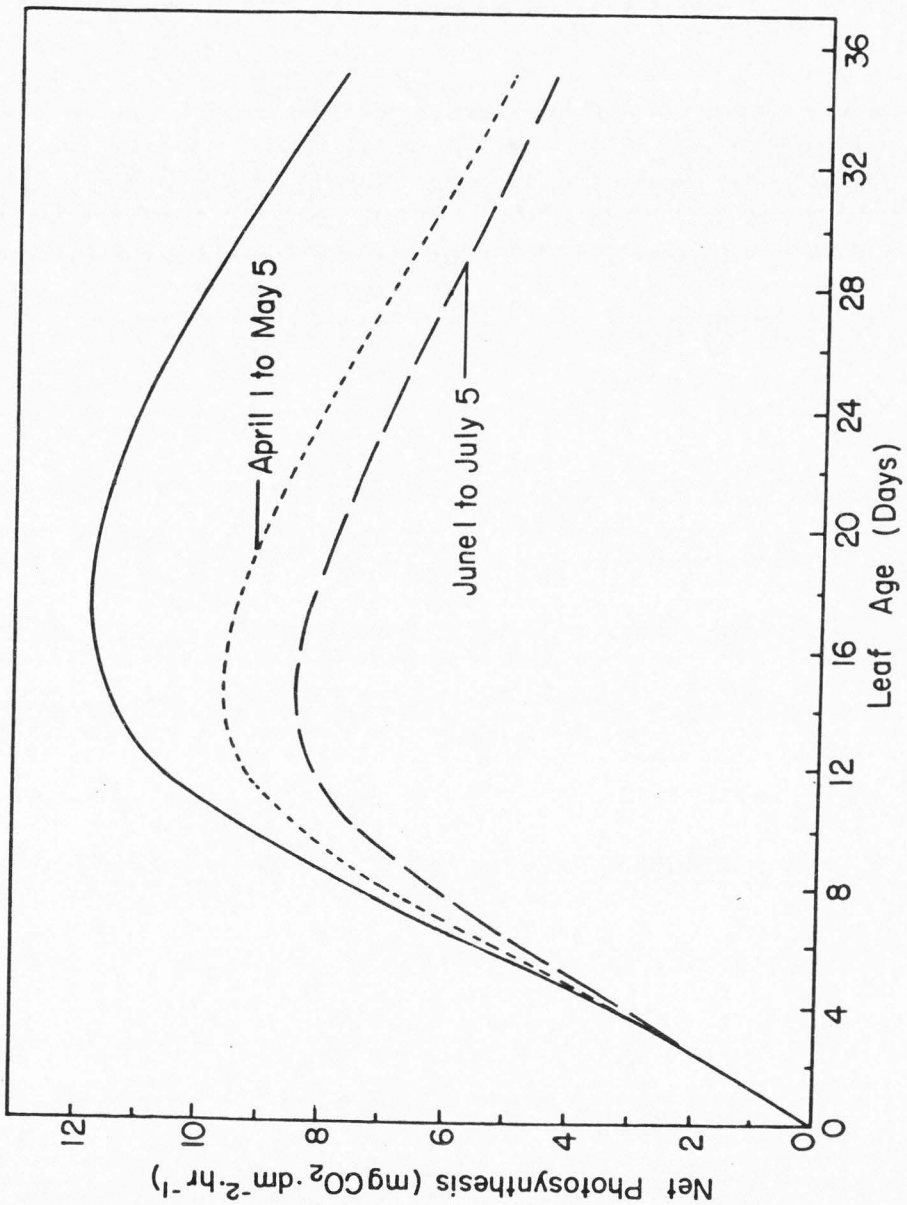
Net Photosynthesis (mgCO_2·dm^{-2}·hr^{-1})
0
2
4
6
8
10
12
0
4
8
12
16
20
24
28
32
36
Leaf Age (Days)
April 1 to May 5
June 1 to July 5

treatment 2 (746 $J \cdot day^{-1}$) and 1 (2484 $J \cdot day^{-1}$) at day 5. Since the predicted growth rates are based on the third leaf, and leaf areas of leaves number 1 and 2 are approximately 40 and 70 percent of subsequent leaves (see Figure 11), respectively, leaf area expansion rates of the first two leaves were adjusted accordingly. An interval of 7 days between newly initiated leaves was used for these simulations.

Figures 27 and 28 represent predicted total leaf area of R. patientia L. exposed to UV-B radiation simulating normal ozone concentrations (Hering and Borden, 1967; Figure 22) and reductions of 5, 15 and 40 percent for respective periods of April 1 to May 5 and June 1 to July 5. After 35 days, leaf area reductions of 2, 7 and 20 percent occurred under 95, 85 and 60 percent of the normal ozone concentration during the April 1 to May 5 period when compared to leaf area predicted under normal ozone concentrations. For this same comparison, reductions of 3, 11 and 26 percent occurred under 95, 85 and 60 percent of the normal ozone concentration, respectively. As occurred with predicted net photosynthetic rates, leaf expansion reductions are more severe during the June 1 to July 5 period due to higher biologically effective UV irradiation prevalent during this period.

Predicted total plant carbon dioxide uptake ($mgCO_2 \cdot hr^{-1}$) for the entire plant occurring from April 1 to May 5 and June 1 to July 5 under simulated ozone reductions of 5, 15 and 40 percent from normal (Figure 22) is shown in Figures 29 and 30, respectively.

Figure 27. Predicted total leaf area of Rumex patientia L. exposed to UV-B radiation corresponding to normal ozone concentrations (A), and reductions of 5 (B), 15 (C) and 40 percent (D) during the period April 1 to May 5. For these simulations, a new leaf is initiated every 7 days.

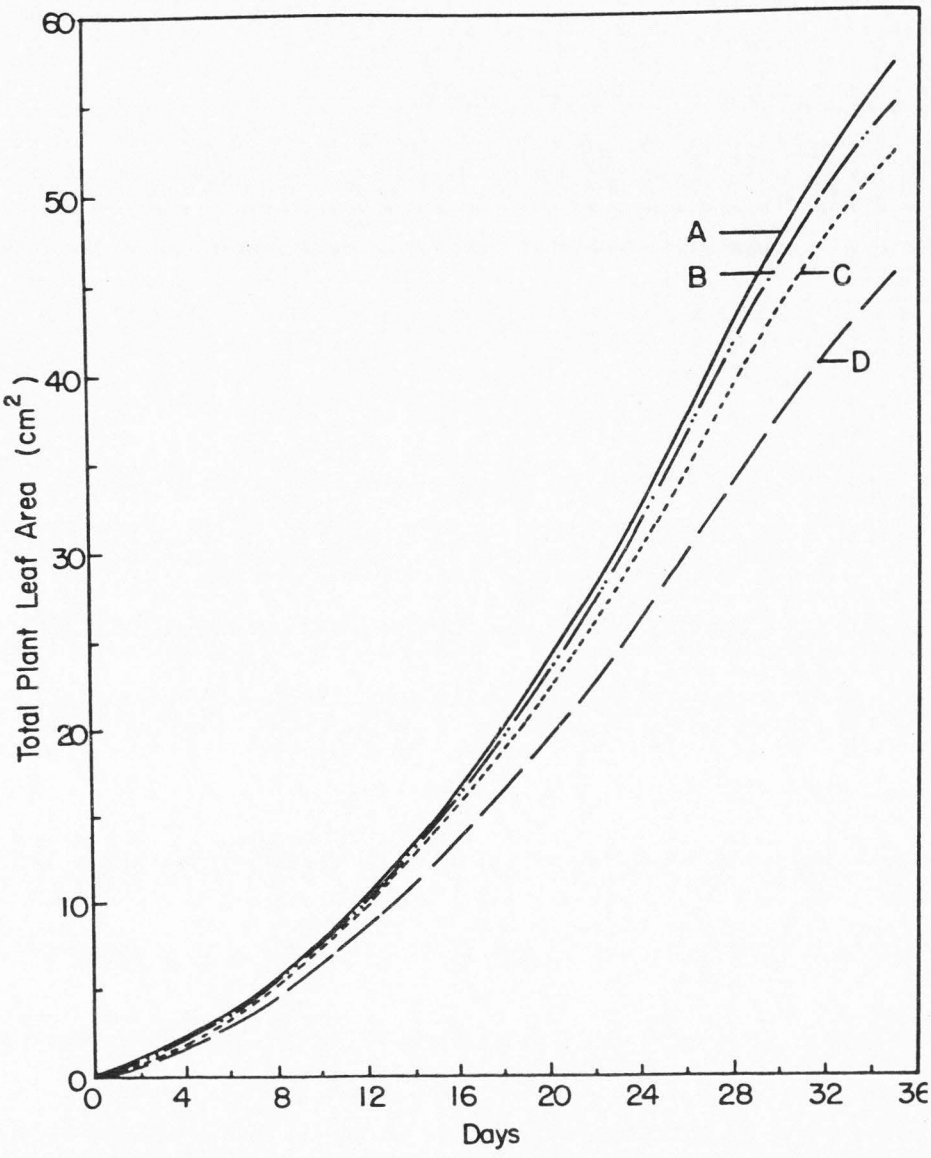
60
50
40
30
20
10
0
Total Plant Leaf Area (cm²)
0
4
8
12
16
20
24
28
32
36
Days
A
B
C
D

Figure 28. Predicted total leaf area of Rumex patientia L. exposed to UV-B radiation corresponding to normal ozone concentrations (A), and reductions of 5 (B), 15 (C) and 40 percent (D) during the period June 1 to July 5. For these simulations, a new leaf is initiated every 7 days.

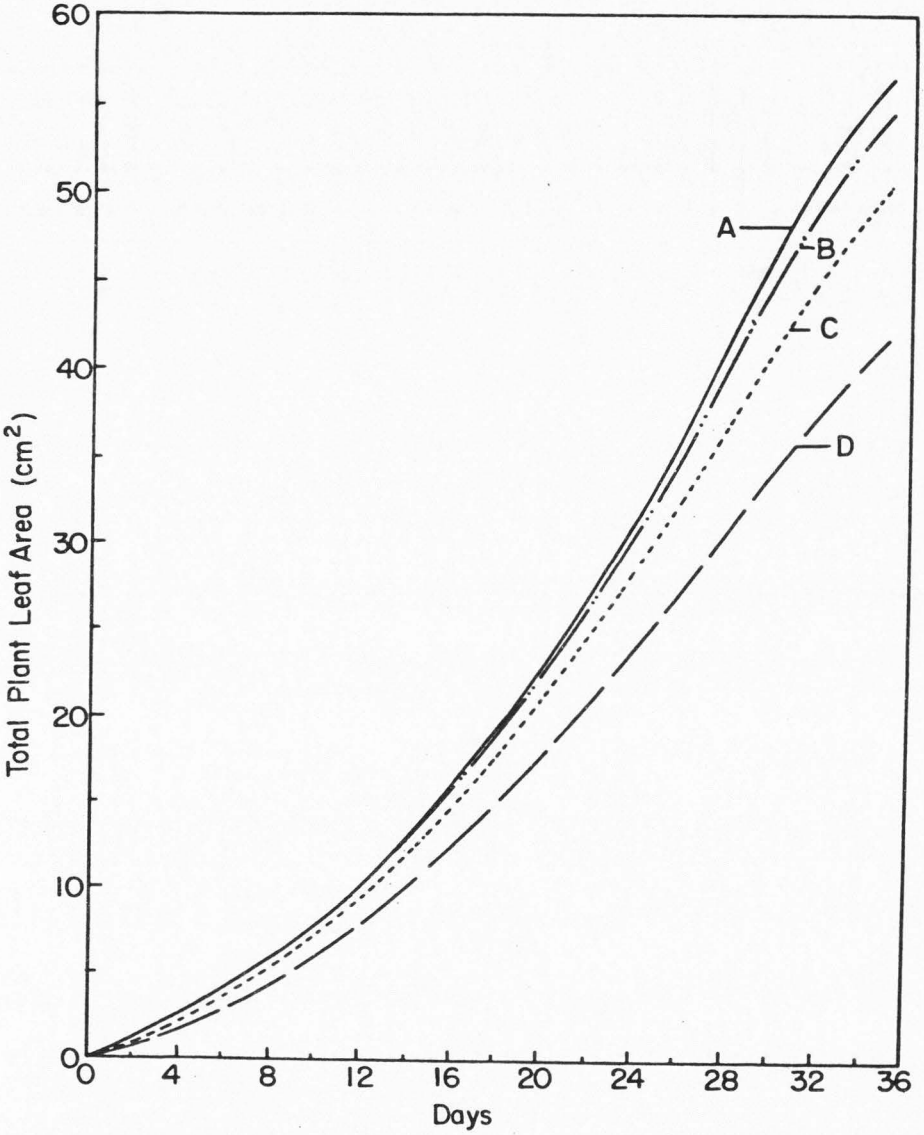
60
50
40
30
20
10
0
0
4
8
12
16
20
24
28
32
36
Days
Total Plant Leaf Area (cm²)
A
B
C
D

Figure 29. Predicted total carbon dioxide uptake ($mgCO_2 \cdot hr^{-1}$) for Rumex patientia L. exposed to UV-B radiation corresponding to normal ozone concentrations (A), and reductions of 5 (B), 15 (C) and 40 percent (D) during the period April 1 to May 5. For these simulations, a new leaf was initiated every 7 days and irradiance within the 400 to 700 nm waveband was 800 $\mu einsteins \cdot m^{-2} \cdot s^{-1}$.

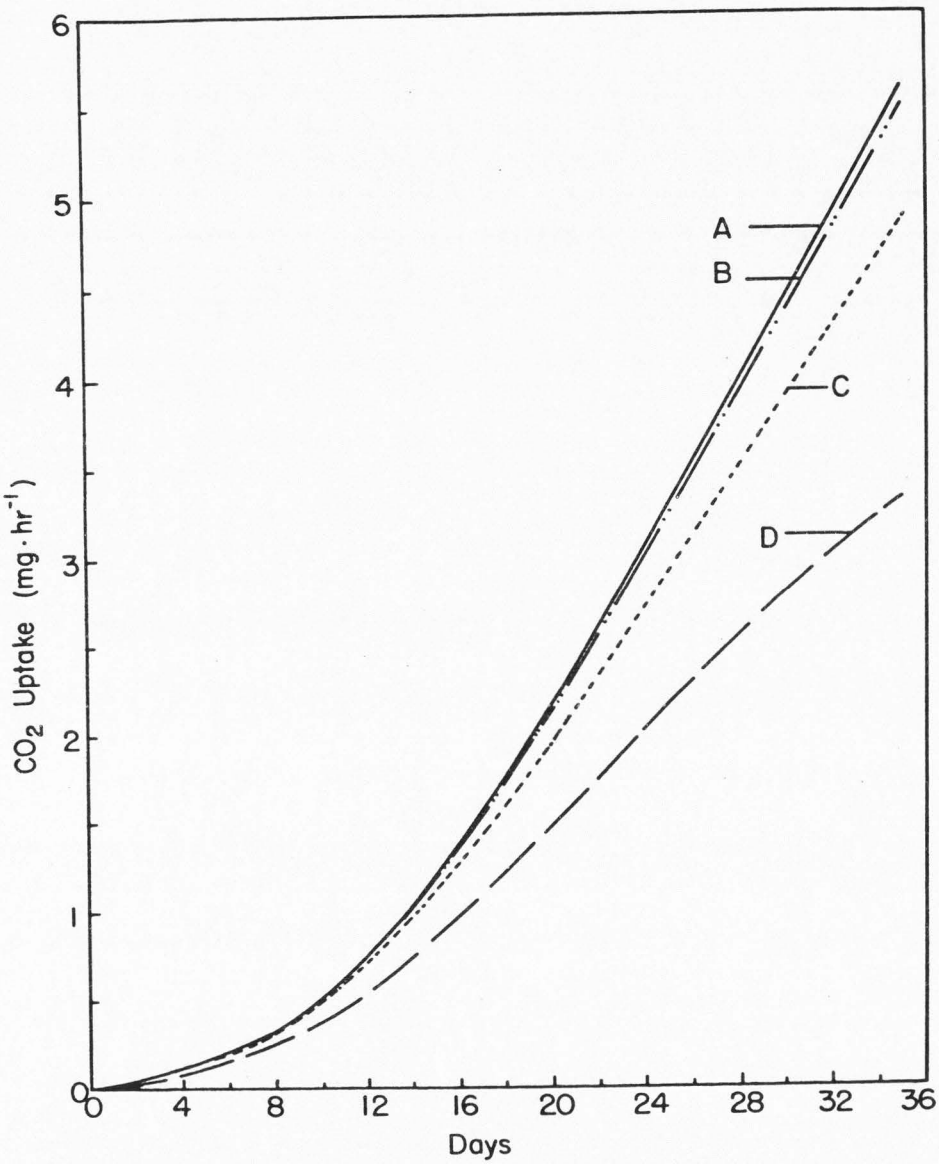
6
5
4
3
2
1
0
0
4
8
12
16
20
24
28
32
36
Days
CO_2 Uptake ($mg \cdot hr^{-1}$)
A
B
C
D

Figure 30. Predicted total carbon dioxide uptake ($mgCO_2 \cdot hr^{-1}$) for Rumex patientia L. exposed to UV-B radiation corresponding to normal ozone concentrations (A), and the reductions of 5 (B), 15 (C) and 40 percent (D) during the period June 1 to July 5. For these simulations, a new leaf was initiated every 7 days and irradiance within the 400 to 700 nm waveband was 800 $\mu einsteins \cdot m^{-2} \cdot s^{-1}$.

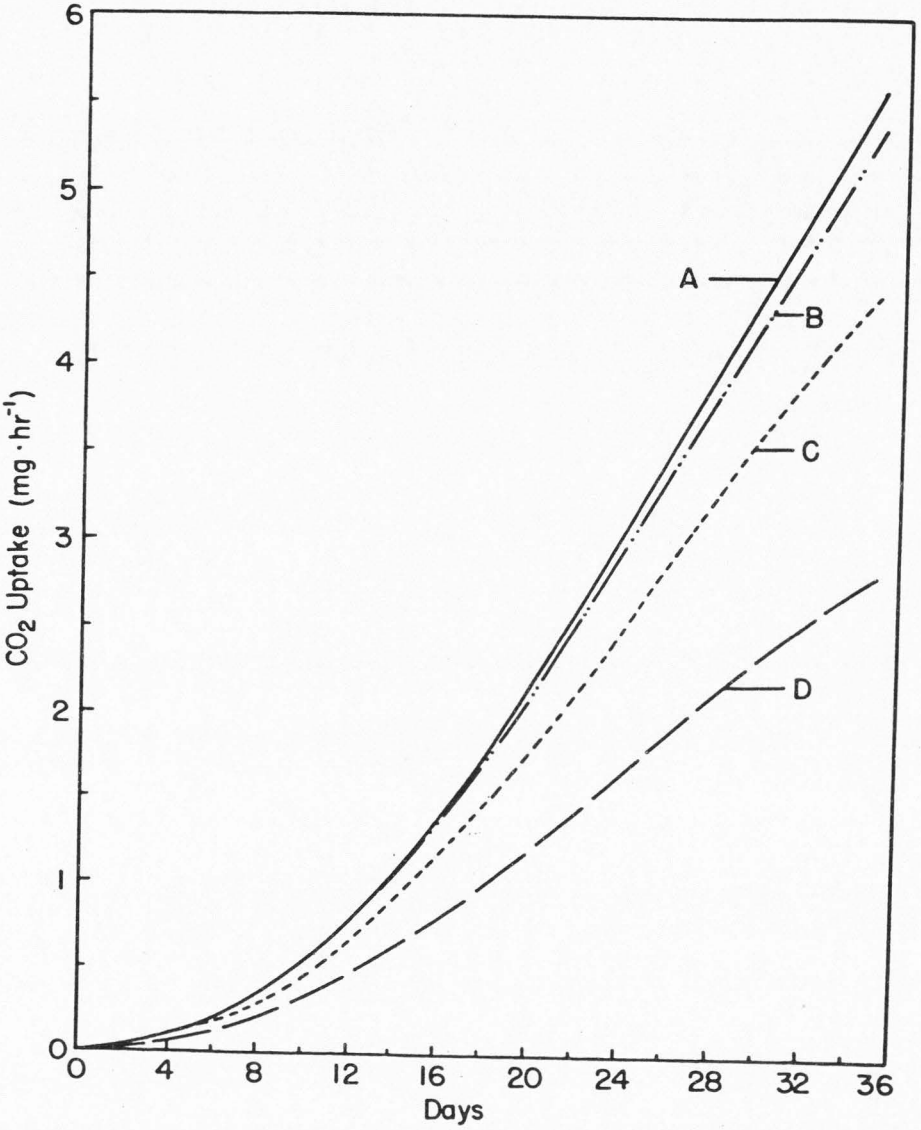
6
5
4
3
2
1
0
CO_2 Uptake ($mg \cdot hr^{-1}$)
0
4
8
12
16
20
24
28
32
36
Days
A
B
C
D

These values represent photosynthesis occurring under visible irradiation (400-700 nm) of 800 μeinsteins$\cdot m^{-2} \cdot s^{-1}$ and with a new leaf being initiated every seven days.

A validation test of the simulation model was made utilizing measured photosynthetic rates of R. patientia L. exposed to UV radiation simulating a 0.18 atm·cm ozone column (when the sun's angle is 30° from the zenith) in a field experiment. Hourly ozone values used to predict photosynthetic rates as a function of biologically effective UV irradiation were taken from Figure 6. The photosynthetic rates in the simulation model were set at the measured photosynthetic rate (18.04 $mgCO_2 \cdot dm^{-2} \cdot hr^{-1}$) on day zero of the field experiment. Thereafter, predicted photosynthetic rates were reduced from the measured control-treatment photosynthetic rates as a function of biologically effective UV irradiation accumulated through the eight-day experiment.

Predicted photosynthetic rates under these ozone concentrations were within one standard error of the measured photosynthetic rates on days 4 and 6 (Figure 31). However, in general, the predicted photosynthetic rates were greater than those actually measured. These results were not surprising since cloud cover was not considered in the simulation model. Total global irradiation data ($cal \cdot cm^{-2} \cdot min^{-1}$) obtained during the July 10 to July 17, 1974, field experiment period showed that only 4 of the 8 days were cloudless (July 10, 11, 12 and 14) (Figure 32) (I. Dirmhirn, personal communication). During periods of cloudiness, the proportional increment of biologically effective UV irradiation would

Figure 31. Net photosynthesis of the third leaf of Rumex patientia L. during 8 days of UV irradiance (Δ——Δ) (simulating a 0.18 atm·cm stratospheric ozone level at an angle of 30° from the zenith) and control (o——o) treatment in field studies, and those predicted (□——□). Irradiance between 400 and 700 nm for both the measured and predicted rates was 800 μeinsteins·m^{-2}·s^{-1}.

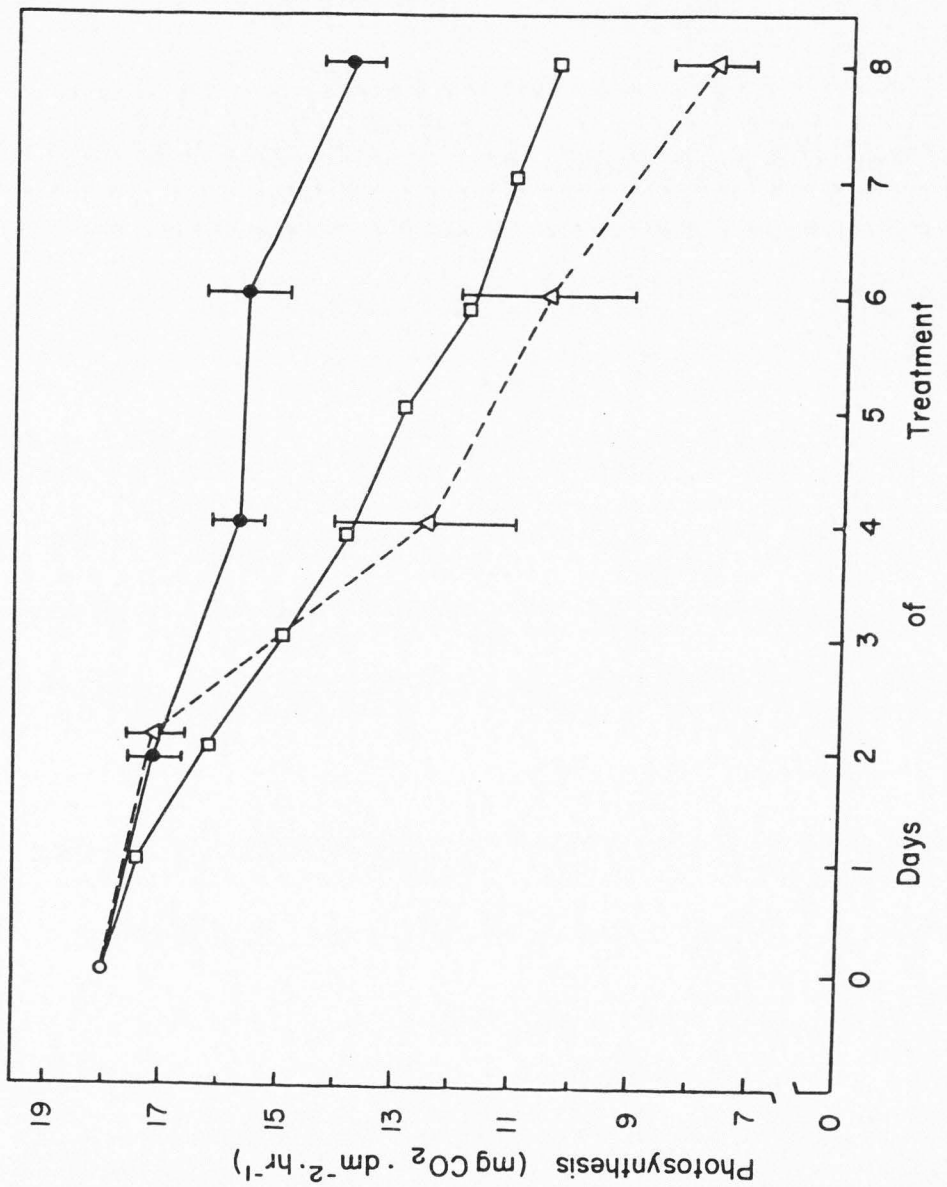
Photosynthesis (mg CO_2 . dm^{-2}. hr^{-1})
19
17
15
13
11
9
7
0
0
1
2
3
4
5
6
7
8
Days of Treatment

Figure 32. Total global irradiation ($cal \cdot cm^{-2} \cdot min^{-1}$) for July 12, 13, 15, 16 and 17, 1974. Total global irradiation for July 10, 11 and 14 were cloudless days and the same as shown for July 12 (I. Dirmhirn, personal communication).

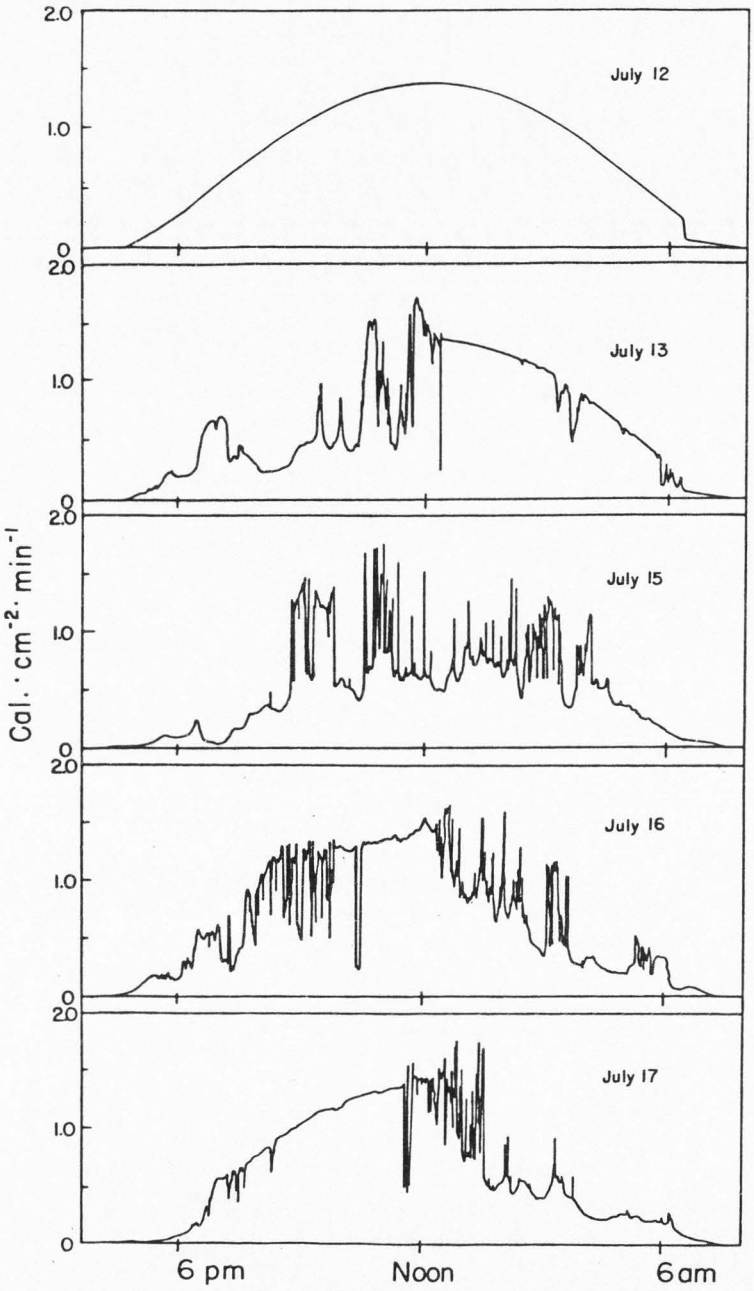
2.0
1.0
0
July 12
July 13
July 15
July 16
July 17
Cal. · cm⁻² · min⁻¹
6 pm
Noon
6am

increase considerably since supplemented UV radiation from the lamps remained constant while the normal ambient solar UV radiation fluctuated with cloud cover. Computations for the prediction of photosynthetic rates of the UV-treated plants do not include these periods of proportionately increased biologically effective UV irradiation resulting from cloud cover and are thus too high. If the ambient cloud cover were incorporated into the simulation model, the resulting predicted photosynthetic rates would more closely correspond to those measured.

As shown by this validation test, the simulation model predicts reasonable decreases of photosynthesis when used for field conditions. Thus, the basis of the simulation model, biologically effective UV irradiation as defined by equation 5, appears to provide a reasonable quantitative measure of additional UV radiation load under reduced ozone concentrations in the production of these deleterious physiological effects.

Discussion

Although the UV-B radiation waveband (280 to 315 nm) comprises but a small portion of the global irradiance, the ability of this waveband to suppress plant physiological processes makes it a significant part of the total spectrum. Exposure of R. patientia L. to four levels of biologically effective UV irradiation showed that relatively small increases in biologically effective UV irradiation depressed photosynthesis. In addition, leaves exhibited

the tendency to accumulate damage even when exposed to low-intensity biologically effective UV irradiance. In these experiments, reciprocity was shown to occur between 6350 and 31750 J. This tendency of the plants to accumulate damage when exposed to UV-B irradation could be important in terms of carbon dioxide uptake even under subtle ozone reductions. For sensitive plants with long-lived leaves exposed to full global irradiance over long periods of time, this would be particularly significant.

The function represented in Figure 18 suggests a minimum or threshold of accumulated biologically effective UV irradiation of approximately 2095 J prior to a repressive effect on photosynthesis. However, this apparent threshold is a result of extrapolation from a least squares fit to the photosynthetic data of treatments 1, 2 and 3 relative to treatment 4. Since the data from which this function was derived do not include values less than 3066 J, the extrapolation of this function to the point of no biological effect is uncertain and may pass through the origin. If this is the case and reciprocity applies below 6350 J, then the repressive effect on photosynthesis would begin upon initial exposure and be dependent upon the level of biologically effective UV irradiation to which a leaf is exposed.

Leaf expansion, unlike photosynthesis, was repressed as a function of the level of biologically effective UV irradiance and primarily during the initial few days of UV-B radiation exposure. However, it is during this initial period of leaf ontogeny that

leaf expansion rates are the highest. Thus, a reduction of leaf expansion during this initial period of leaf ontogeny substantially reduced subsequent total plant leaf area and the potential for carbon gain. In addition to reducing leaf expansion, leaf longevity decreased with increased UV irradiation. Longevity of R. patientia L. leaves exposed to 2484 $J \cdot day^{-1}$ (treatment 1) were reduced 14 days when compared to leaves exposed to no biologically effective UV irradiation. Although leaf longevity was decreased, an acceleration of whole-plant senescence and death was not observed at any time during these short-term studies.

In its present form, the simulation model should be viewed as a first approximation in the quantification of photosynthesis and growth of R. patientia L. exposed to various levels of atmospheric ozone decrease. Although the validation test of the model showed a reasonable correlation to the results of a field study, additional parameters should be incorporated. This is especially true of differing cloud conditions and their effects on UV-B radiation. In addition, the interactive effects of plant stress such as water deficits and temperature would improve the models' applicability as it pertains to R. patientia L. Expansion of the model to include plant species from both natural ecosystems and agricultural crops representing a range of tolerance to UV radiation would considerably enhance the scope of the model.

The principle driving variable of the model, biologically effective UV irradiation as defined by equation 5, appears to provide a reasonable quantitative measure of additional UV-B

radiation under reduced atmospheric ozone concentations for the prediction of photosynthetic reduction of R. patientia L. This measure of UV-B radiation is based on a host of action spectra determined for a variety of plants. These include the photoinhibition of spinach chloroplasts (Jones and Kok, 1966), the inhibition of photosynthesis in Chlorella pyrenoidosa (Bell and Merinova, 1961), epidermal cell damage on Oxyria digyna leaves (Caldwell, 1968), induction of chromosomal aberrations in Tradescantia paludosa pollen (Kirby-Smith and Craig, 1957) and the cessation of cytoplasmic streaming in epidermal cells of Allium cepa (Glubrecht, 1953). Nucleic acids and proteins, of universial occurrence in higher plants, are believed to be the principal chromatophores in these studies (Caldwell, 1971). Although higher plants might be expected to respond similarly to UV-B radiation on the basis of nucleic acid and protein sensitivity, Cline and Salisbury (1966) have shown that plants range from sensitive to very tolerant when exposed to UV-C radiation. Thus, differential sensitivity of plants to UV radiation is probably based on the protection of nucleic acids and proteins by tissues or compounds which filter the radiation such as flavonoids and cuticles. The capacity of different species to repair radiation damage to different degrees may also play a role in the differential sensitivity of nucleic acids and proteins. Therefore, the response displayed by R. patientia L. to biologically effective UV radiation, as represented by Figure 18, may not reflect that of more tolerant plant species. Although plant species sensitive to small increases in global UV radiation would be those

initially affected under reduced ozone conditions, species more tolerant would also be adversely affected if they are shown to possess the capacity to accumulate damage in a manner similar to *R. patientia* L.

CHAPTER V

CONCLUSIONS

Results of this study show that UV-B radiation corresponding to a 0.18 atm·cm ozone column when the sun is at 30° from the zenith is detrimental to plant physiological processes in Rumex patientia. In addition, data of this study also suggest that levels of ambient UV-B radiation presently occurring in global irradiance could repress plant processes.

Damage resulting from the absorption of UV radiation is not completely irreversible. Photorepair processes are well documented phenomena (Jagger, 1960) and dark repair has been shown to occur in higher plants (Howland, 1975). Dark repair efficiency appears dependent upon the total damage. That is, an approximate 100 percent repair was shown to occur when few dimers are produced under low intensities of UV radiation (14 $J \cdot m^{-2}$; 254 nm radiation). With higher intensities of UV radiation, dark repair becomes a highly inefficient process of repair. For example, Howland found 27 percent of the damage repaired when carrot protoplasts were exposed to 105 $J \cdot m^{-2}$ UV radiation and only 1.6 percent repair after exposure to 420 $J \cdot m^{-2}$ UV radiation (254 nm). Photorepair processes were shown to be 100 percent efficient when these same protoplasts were exposed to 42 $J \cdot m^{-2}$ UV radiation and then exposed to radiation of longer wavelengths, whereas only 56 percent of the damage was repaired by dark repair processes.

Photorepair has been shown to occur in a number of higher plants. Typically, the measure of UV radiation damage used in these studies was the development of leaf bronzing, browning, or the development of other visible lesions (Bawden and Kleczkowski, 1952; Caldwell, 1968; Chessin, 1958; Cline, Conner and Salisbury, 1969; Cline and Salisbury, 1966; Gurskij, Ostapovic and Sokolov, 1961; Tanada and Hendricks, 1953). The majority of these studies utilized 254 nm radiation with artificial lamps providing the longer wavelength radiation for photoreactivation. Gurskij et al. (1961), however, supplemented global irradiance with intense UV-B and UV-C (<280 nm) radiation and did not observe visible leaf damage. The absence of leaf damage was attributed to photoreactivation. The potential efficiency of photoreactivation when plants are exposed to global irradiance was similarly indicated by the study of Caldwell (1968). In this study, leaves of alpine plants were exposed to UV radiation at 296.7 nm and 302.3 nm without other wavelengths. Irradiance closely simulated UV radiation during a summer day in the alpine where the test species were collected. Although this level of UV radiation resulted in severe leaf damage, similar damage was not observed under comparable ambient UV radiation in the field. Thus, photorepair processes are apparently capable of repairing considerable damage and appear more efficient under global irradiance than when supplemented with artificial irradiation.

The only visible evidence of apparent leaf damage to R. patientia exposed to UV radiation occurred in the controlled environment studies reported in Chapter III and only under a simulated 0.18

atm·cm ozone column. This damage appeared as one to several pale bands extending the length of the leaf paralleling the midvein. This damage was pronounced in the 400 μeinsteins·m^{-2}·s^{-1} (400-700 nm) UV radiation experiment and less so in the experiment at higher visible irradiance (800 μeinsteins·m^{-2}·s^{-1}, 400-700 nm). Damage was initially observed in the UV-irradiated plants in the 400 μeinsteins·m^{-2}·s^{-1} (400-700 nm) experiment after six days exposure when the second leaf was eight days old. In addition, prominent leaf wrinkling occurred when plants were exposed to 400 μeinsteins·m^{-2}·s^{-1} under this same UV irradiance. Comparable visible damage was not observed in the field study at any time during 19 days exposure to identical supplemented UV-B radiation wavelengths and intensities as used in the controlled-environment studies. Thus, results of studies reported in Chapter III are in agreement with those of Caldwell (1968) and Gurskij et al. (1961). That is, photoreactivation is apparently an efficient process for repairing visible leaf damage resulting from UV radiation when simultaneously exposed to global irradiance.

Damage within the photosynthetic processes resulting from UV radiation has not been conclusively shown to be photoreactivable. Photoreactivation of damage to the photosynthetic processes was not indicated to occur in R. patientia exposed to UV radiation in either controlled-environment (see Figures 8, 9, 10 and 15) or field studies (see Figure 12). Rather, the repression of photosynthesis was indicated to be a cumulative response and dependent upon the level of UV irradiation to which a leaf is exposed (Figure 18).

Further evidence of an apparent lack of photorepair occurring within damaged photosynthetic processes was the reciprocal mode of action by UV radiation (Figure 19). The lowest intensity of biologically effective UV irradiation evaluated in the experiment designed to test for reciprocity was 219 $J \cdot day^{-1}$ (treatment 2; Chapter IV). This level of UV radiation is less than that received during a cloudless day in April (Figure 23). A detectable difference in photosynthetic rates between this level of UV radiation (219 $J \cdot day^{-1}$; treatment 2) and a treatment with no biologically effective UV irradiation (treatment 4) occurred after 14 days, or when the UV radiation to which that leaf was exposed had accumulated to approximately 3060 J. This level of UV radiation is equivalent to global irradiance of three cloudless, mid-June days (see Figure 23) and resulted in a reduction of about 4 percent in photosynthetic rates relative to treatment 4 (Figure 18).

If photoreactivation were implicated in the repair of damage to photosynthetic processes resulting from exposure to UV radiation, these processes would be expected to be more efficient under global irradiance than would occur under controlled-environment conditions. This was shown for leaf damage in the present studies with R. patientia and indicated in other studies (Caldwell, 1971; Gurskij et al., 1961). However, photosynthetic repression by accumulated UV radiation was comparable between controlled-environment and field studies as shown by the validation test of the simulation model (Figure 31). In addition, comparable depressions of photo-

synthesis resulted in experiments at both 400 and 800 μeinsteins·m^{-2}·s^{-1} (400–700 nm) after seven days of UV radiation treatment (see Figures 9 and 10). Irradiance within the photorepair waveband (313 to 500 nm) (Jagger, 1960) was considerably higher in the 800 μeinsteins·m^{-2}·s^{-1} irradiance experiment and might be expected to drive photorepair processes more effectively than would occur under lower visible irradiance. This would result if photorepair processes do not saturate at very low intensities. A saturation of these photorepair processes is not indicated by the observations made during this study since more severe leaf damage occurred in the lower visible irradiance experiment (400 μeinsteins·m^{-2}·s^{-1}; 400–700 nm) as discussed earlier.

The lowest intensity of UV radiation evaluated in this study (approximately 219 J·day^{-1}) was less than that predicted during cloudless April days (Figure 23) using the atmospheric ozone concentrations of Hering and Borden (1967) (Figure 22) and the analytic equations of Green et al. (1974). This level of UV radiation was shown to detectably depress photosynthesis (Figure 18) after 14 days and repress leaf expansion (Figure 20). If ambient UV radiation levels are indeed detrimental, the repressive effect would increase from April (approximately 500 J·day^{-1}) to mid-June (1300 J·day^{-1}). Plants may respond to this period of increased ambient UV radiation, or increased UV radiation occurring under natural atmospheric ozone concentration reduction, by producing higher concentrations of UV-radiation-absorbing compounds such as flavonoids. This phenomena has indeed been

shown to occur and as rapidly as half a day (Caldwell, 1968; Lautenschlager-Fleury, 1955). This ability to rapidly respond to fluctuating levels of UV radiation would be of considerable value to plants such as R. patientia which continuously initiate, and thus expose new leaves. However, sufficient levels of flavonoids or other UV-radiation-absorbing compounds were apparently not produced in R. patientia to protect physiological targets of photosynthetic (see Figures 8, 9, 10, 12 and 15) or leaf growth (Figures 11, 13 and 16) processes under the levels of supplemented UV radiation tested.

The efficiency of plant processes such as photosynthesis appears quite vulnerable to UV radiation. This is a result of their being damaged according to the level of accumulated UV radiation (Figures 8, 9, 10, 12, 15 and 18), and the apparent inability to completely repair damage or to produce sufficient protective UV-radiation-screening compounds such as flavonoids. However, ambient levels of UV radiation are reasonably low and substantial depressions of photosynthesis, or other plant processes responding to UV radiation similarly, would not be expected. Even under a simulated five percent ozone reduction from the ozone data of Hering and Borden (1967), predicted photosynthetic rates (Figure 24) and total-plant, CO_2 uptake (Figure 29 and 30) were only slightly reduced. In addition, predicted rates were only reduced in the late phase of leaf ontogeny when the contribution by that leaf to CO_2 uptake of the entire plant would be diminishing. With more substantial depletion in atmospheric ozone (ie. 15 and 40

percent), a considerable reduction in CO_2 uptake could result (Figure 29 and 30).

Dütsch (1973) has shown that year-to-year fluctuations in atmospheric ozone concentrations occur and are as great as 10 percent. The largest fluctuations reported were a high of about 0.36 atm·cm in 1940-1941 and a low of about 0.325 atm·cm in 1964-1965. However, mean fluctuations were considerably lower, usually less than 5 percent. The compounding effects of both normally-occurring low mean ozone concentrations plus small man-induced ozone reductions (ie., less than 10 percent) could result in substantial increases in UV radiation levels. For example, a reduction of 5 to 10 percent ozone from a mean yearly ozone level of 0.32 atm·cm would be more detrimental than this same reduction from a mean level of 0.36 atm·cm ozone. This effect would be more significant to those plant processes that are not photo-reactivable, such as appears for photosynthesis. In addition, this would be compounded with seasonal variations (Figure 23).

With the available lamp/filter systems it is not presently possible to simulate a certain level of atmospheric ozone reduction over an entire day (see Figure 6). Since field verification of controlled-environment studies are necessary, biologically effective UV radiation as defined by equation 5, could be used as the criterion upon which field and controlled-environment studies could be corroborated. In terms of photobiological action, UV-B radiation is highly wavelength-specific (Caldwell, 1971; Giese, 1964). Thus,

in order to facilitate a correlation of results to any specific atmospheric ozone reduction, or to compare field and controlled-environment studies, the added UV-B radiation wavelengths must be comparable. This can be achieved with a reasonably high degree of accuracy and repeatability with the lamp/filter systems described in Chapters II, III, and IV.

As noted in Chapter IV, R. patientia is probably representative of species which are sensitive to UV radiation. Cline and Salisbury (1966) showed in their survey of 67 plant species that plants sensitive to UV radiation tended to have thin, horizontal leaves similar to R. patientia. Of the sensitive species they examined anatomically, most had thin cuticles and thin epidermal layers although a few of the more resistant species also possessed these characteristics. Usually, the more resistant species possessed such characteristics as vertical leaves (e.g., grasses), several layers of thick-walled, sub-epidermal cells (e.g., conifers), tightly-packed globular crystals in the epidermis (e.g., cactus) and thick-walled hypodermal cells (e.g., Agave sp. and conifers).

If terrestrial UV radiation levels were increased due to atmospheric ozone reduction, plants sensitive to UV radiation and perhaps even species which are moderately resistant with long-lived plant parts would probably be affected. This could be especially true of those plants incapable of reflecting or attenuating UV radiation prior to absorption by physiological targets. This would be particularly critical for damage which is not efficiently repaired such as is apparently true of photosynthesis. In addition,

temperature has been shown to be important in the severity of damage sustained by plants exposed to UV radiation. El-Mansey and Salisbury (1971) showed that the deleterious effects of UV radiation increased with higher temperature. This temperature interaction could increase the potential effects of enhanced UV radiation resulting from reduced atmospheric ozone. Additional interactive factors that could increase the severity of damage to plants under increased terrestrial UV radiation are those involving water stress and natural competition. In land ecosystems, a subtle increase in UV radiation could repress certain species and result in a shift in species composition to those more tolerant of UV radiation. In the context of ecosystems, those plant species generally shaded or completing most of their growth prior to June when biologically effective UV radiation levels are highest (Figure 23), would probably not be considered as vulnerable.

LITERATURE CITED

Arnold, W. 1933. The effect of ultraviolet light on photosynthesis. J. Gen. Physiol. 17:135-143.

Arnon, D. I. 1949. Copper enzymes in isolated chloroplasts: polyphenol oxidase in Beta vulgaris. Plant Physiol. 24:1-15.

Bawden, F. C., and A. Kleczkowski. 1952. Ultra-violet injury to higher plants counteracted by visible light. Nature 169:90-91.

Bell, L. N., and G. L. Merinova. 1961. Effect of dosage and wavelength of ultraviolet radiation on photosynthesis of Chlorella. Biofizika (Trans.) 6:21-26.

Bener, P. 1972. Approximate values of intensity of natural ultraviolet radiation for different amounts of atmospheric ozone. Tech. Report, European Research Office, U.S. Army, London. Contract No. DAJA 37-58-C-1017. 59 p.

Biggs, W. W., A. R. Edison, J. D. Eastin, K. W. Brown, J. W. Maranville, and M. D. Clegg. 1971. Photosynthesis light sensor and meter. Ecology 52:125-131.

Black, C. C. 1973. Photosynthetic carbon fixation in relation to net CO_2 uptake. Ann. Rev. Plant Physiol. 24:253-286.

Bucholtz, A. F. 1931. The effect of monochromatic light of measured intensities on behavior of plant cells. Ann. Mo. Bot. Gard. 18:489-508.

Caldwell, M. M. 1968. Solar ultraviolet radiation as an ecological factor for alpine plants. Ecol. Monogr. 38:243-268.

Caldwell, M. M. 1971. Solar UV irradiation and the growth and development of higher plants, p. 131-177. In A. C. Giese (ed.) Photophysiology. Academic Press, New York.

Chessin, M. 1958. Light quality and photoreactivation of plants and viruses. Ann. Appl. Biol. 46:388-392.

Cicerone, R. J., R. S. Stolarski and S. Walters. 1974. Stratospheric ozone destruction by man-made chlorofluoromethanes. Science 185:1165-1167.

Cline, M. G., and F. B. Salisbury. 1966. Effects of ultraviolet radiation on the leaves of higher plants. Radiat. Bot. 6:151-163.

Dütsch, H. U. 1974. The ozone distribution in the atmosphere. Can. J. Chem. 52:1491-1504.

El-Mansey, H. I., and F. B. Salisbury. 1971. Biochemical responses of Xanthium leaves to ultraviolet radiation. Radiat. Bot. 11:325-328.

Erixon, K., and W. L. Butler. 1972. Destruction of C-550 by ultraviolet radiation. Biochem. Biophys. Acta. 253: 483-486.

Gaastra, P. 1959. Photosynthesis of crop plants as influenced by light, carbon dioxide, temperature and stomatal diffusion resistance. Med. Landb. Wageningen 59:1-68.

Giese, A. C. 1964. Studies on ultraviolet radiation action upon animal cells. p. 203-245. In A. C. Giese (ed.) Photophysiology. Academic Press, New York.

Gifford, R. M., and R. B. Musgrave. 1972. Activation energy analysis and limiting factors in photosynthesis. Australian J. Biol. Sci. 25:419-423.

Glubrecht, H. von. 1953. Über die Wirkung von UV-Strahlen in somatischen Zellen. Z. Naturforsch. 86:17-27.

Green, A. E. S., T. Sawada and E. P. Shettle. 1974. The middle ultraviolet reaching the ground. Photochem. Photobio. 19:251-259.

Grobecker, A. J., S. C. Coroniti and R. H. Cannon, Jr. 1974. The effects of stratospheric pollution by aircraft. Climatic Assessment Program, U.S. Dept. Transportation, Report No. DOT-TST-75-50, Nat. Tech. Info. Serv., Springfield, Va.

Gurskij, A. V., L. F. Ostapovic and Ju. L. Sokolov. 1961. V lijanie UF radiacii na vyssie rastenija. (The effects of UV radiation on higher plants). Izd. In-ta atomnoj energii im. I.V. Kurcatova AB SSSR, M.

Haldall, P. 1964. Ultraviolet action spectra of photosynthesis and photosynthetic inhibition in a green and red alga. Physiol. Plant. 17:414-421.

Hammond, A. L. 1975. Ozone destruction: Problem's scope grows, its urgency recedes. Science 187:1181-1183.

Hering, W. S., and T. R. Borden. 1967. Ozonesonde observations over North America. Vol. IV, U.S. Air Force, Environ. Res. Papers, No. 279. (Air Force Cambridge Research Laboratories, Bedford, Mass.)

Hollaender, A., and C. W. Emmons. 1941. Wavelength dependence of mutation production in the ultraviolet with special emphasis on fungi. Cold Spring Harbor Symp. Quant. Biol. 9:179-186.

Howland, G. P. 1975. Dark-repair of ultraviolet-induced pyrimidine dimers in the DNA of wild carrot protoplasts. Nature 254:160-161.

Jagger, J. 1960. Photoreactivation, p. 352-377. In A. Hollaender (ed.). Radiation protection and recovery. Pergamon Press, Long Island City, N.Y.

Johnston, H. 1971. Reduction of stratospheric ozone by nitrogen oxide catalysts from supersonic transport exhaust. Science 173:517-522.

Jones, L. W., and B. Kok. 1966. Photoinhibition of chloroplast reactions. Multiple effects. Plant Physiol. 41:1044-1049.

Kirby-Smith, J. S., and D. L. Craig. 1957. The induction of chromosome aberrations in Tradescantia by ultraviolet radiation. Genetics 42:176-187.

Klein, R. M., and P. C. Edsall. 1967. Interference by near UV and green light with growth of animal and plant cell cultures. Photochem. Photobio. 6:841-850.

Klein, R. M., P. C. Edsall and A. C. Gentile. 1965. Effects of near ultraviolet and green radiations on plant growth. Plant Physiol. 40:903-906.

Knapp, E., A. Ruess, O. Risse and H. Schreiber. 1939. Quantitative Analysis der mutalionsauslösenden Wirkung monochromatischen UV-Lichtes. Naturwiss. 27:304.

Koch, W., O. L. Lange and E. D. Schulze. 1971. Ecophysiological investigations on wild and cultivated plants in the Negev Desert. I. Methods: A mobile laboratory for measuring carbon dioxide and water vapor exchange. Oecologia 8:296-309.

Lautenschlager-Fleury, D. 1955. Uber die Ültraviolettduchlässigkeit von Blattepidermen. Ber. Schweiz. Bot. Ges. 65:343-386.

List, R. J. 1971. Smithsonian meteorological tables. Revised ed. Smithsonian Institution Press, Washington, D.C. 527 p.

Lockhart, J. A., and Ursula Brodfuhrere Franzgrote. 1961. The effects of UV radiation on plants. p. 532-554. In W. Rikland (ed.) Encyclopedia of Plant Physiology, Vol. 16, Springer-Verlag, Berlin.

Mantai, K. E., and N. I. Bishop. 1967. Studies on the effects of ultraviolet irradiation on photosynthesis and on the 520 nm light-dark difference spectra in green algae and isolated chloroplasts. Biochem. Biophys. Acta. 131:350-356.

McPherson, H. G., and R. O. Slatyer. 1973. Mechanisms regulating photosynthesis in Pennisetum typhoides. Aust. J. Biol. 26:329-339.

Meyer, A. D. H., and E. O. Seitz. 1942. Ultraviolette Strahlen ihre Erzeugung, Messung und Anwendung in Medizin, Biologie und Technik. Walter De Gruyter & Co., Berlin. 308 p.

Molina, M. J., and F. S. Rowland. 1974. Stratospheric sink for chlorofluoromethanes: chlorine atom-catalysed destruction of ozone. Nature 249:810-812.

Nachtwey, D. S. 1975. Linking photobiological studies at 254 nm with UV-B. In D. S. Nachtwey, M. M. Caldwell and R. H. Biggs, eds., Impacts of Climatic Change on the Biosphere, Part 1. Effects of Ultraviolet Radiation, Monog. V. Climatic Assessment Program, U.S. Dept. Transportation, Report No. DOT-TST-75-55, Nat. Tech. Info. Serv., Springfield, Va., pp. 3-50 to 3-84.

Owen, P. C. 1957. Effect of ultra-violet radiation on the respiration-rates of tobacco leaves, and its reversal by visible light. Nature 180:610-611.

Reynolds, E. S. 1935. The reactions of plants to ultra-violet. Ann. Mo. Bot. Gard. 22:759-769.

Shavit, N., and M. Avron. 1963. The effect of ultraviolet light on photophosphorylation and the Hill reaction. Biochem. Biophys. Acta. 66:187-195.

Sisson, W. B., and M. M. Caldwell. 1975. Lamp/filter systems for simulation of solar UV irradiance under reduced atmospheric ozone. Photochem. Photobio. 21:453-456.

Tanada, T., and S. B. Hendricks. 1953. Photoreversal of ultraviolet effects in soybean leaves. Amer. J. Bot. 40:634-637.

Trebst, A. 1974. Energy conservation in photosynthetic electron transport of chloroplasts. Ann. Rev. Plant Physiol. 25:423-458.

Van Baalen, C. 1968. The effects of ultraviolet irradiation on a Coccoid blue-green alga: Survival, photosynthesis and photoreactivation. Plant Physiol. 43:1689-1695.

Van Baalen, C., and R. O'Donnell. 1972. Action spectra for ultraviolet killing and photoreactivation in the blue-green alga Agmenellum quadruplicatum. Photochem. Photobio. 15:269-274.

Verhoff, F. H., and L. Bell. 1916. The pathological effect of radiant energy upon the eye. Am. Acad. Arts and Sci. Proc. 51:629-810.

Zill, L. P., and N. E. Tolbert. 1958. The effect of ionizing and ultraviolet radiations on photosynthesis. Arch. Biochem. Biophys. 76:196-203.